Septal coding and non-coding RNAs regulated in social fear
─ The role of lncRNA Meg3 in social fear extinction

Das Promotionsgesuch wurde eingereicht am: 30.04.2020

Die Arbeit wurde angeleitet von: Prof. Dr. Gunter Meister

Unterschrift:

……………………………………………..
(Melanie Royer)

TABLE OF CONTENTS

Table of Contents

ABSTRACT

Abstract

Social anxiety disorder (SAD) is characterized by fear and avoidance of social situations and displays the third most common anxiety disorder in society. However, even today, there is only sparse knowledge about the underlying mechanisms of SAD available. So far, applied therapies, which include cognitive-behavioural therapies combined with pharmacological intervention, show indeed partial achievements, but still with a high rate of non-responders and relapse. For the development of specific and more efficient treatment options, a better understanding of especially molecular mechanisms is urgently required. Here, RNA molecules are promising to provide insights on a regulatory as well as subsequently translational level during the state of SAD. In general, coding and non-coding RNAs are dynamically regulated as response to certain stimuli and their dysregulation lead to tremendous effects. Disorders are usually linked to pre- and post-transcriptional alterations and approaching these in context of SAD will help to identify disorder-causing signalling pathways and networks.

Thus, the thesis presented here aimed to characterize RNA profiles that are regulated in context of social fear acquisition and its extinction with a total RNA-Sequencing (RNA-Seq) approach. Therefore, I mimicked social fear in male mice by inducing social avoidance – the core symptom of social fear – using the social fear conditioning paradigm (SFC). SFC allows us to induce social fear during social fear acquisition, whereas during social fear extinction training, which is comparable to exposure therapy in humans, animals re-learn to investigate presented conspecifics again. For total RNA-Seq, samples were collected 90 min after the last behavioural assessment during the SFC protocol, with a specific focus on conditioned (SFC$^+$) animals that showed different extinction-success. Here, the septum was chosen as the brain region of interest as it is proven as an important regulator of social fear expression. RNA-Seq revealed many different RNAs regulated on a gene-based and a transcript-based level and after validation of interesting RNA candidates e.g. Sgk1 and Crfr2 among others, with qPCR, I focused mainly on the long non-coding RNA (lncRNA) Meg3, which was regulated in a Meg3 transcript- and extinction success-dependent manner. In more detail, the Meg3 variants containing an alternatively spliced long exon 10 were downregulated in SFC$^+$ animals 24 h after social fear acquisition and levels were restored in case mice could successfully overcome their social fear during the extinction training. In contrast, animals that stayed fearful after the extinction training still displayed reduced Meg3 level even 3 h after extinction training. Control experiments revealed that learning processes, and not social contact *per se*, are necessary for Meg3 regulation within the septum. Additionally, unique septal Meg3 expression patterns were found compared to hippocampal regions. *In vivo* Meg3 knockdown within the septum was achieved by the local

application of antisense LNA GapmeRs that induce RNaseH-dependent cleavage of specific Meg3 variants. Meg3 knockdown before acquisition and before extinction training revealed that social fear acquisition was not affected, whereas the extinction and the subsequent memory consolidation seemed to be slightly impaired. Furthermore, I investigated the activation of the PI3K/AKT signalling pathway as it was shown to regulate plasticity and long-term potentiation in neurons, and to be modulated by Meg3. Interestingly, I found increased phosphorylation levels of the regulatory subunit P85 of the PI3K and AKT at Ser473 in SFC$^+$ animals 3 h after unsuccessful extinction training, indicating an activation of this signalling pathway. Activation in successfully extinguishing animals is conceivable to happen at earlier time points and therefore deserves further investigation. In Meg3 knockdown experiments, I observed an activation of PI3K in SFC$^+$ control mice. In contrast, SFC$^+$ knockdown mice showed no increased activation compared to unconditioned (SFC$^-$) knockdown mice, which might be due to high basal PI3K activation in SFC$^-$ knockdown mice. Taken together, the presented data provide first, but strong indications on a regulatory link between Meg3 and PI3K/AKT signalling after social fear extinction training. Interestingly, many lncRNAs function as transcription regulators of target genes by altering chromatin structures. To assess changes in chromatin accessibility and histones modifications after social fear extinction on a general level, but also with a direct link to Meg3 for the identification of nuclear Meg3 action sites, I performed ATAC-Seq and CUT&RUN for H3K27me3.

In a second part, I further strengthened the role of the septum in social fear extinction processes. Based on originally planned microdialysis experiments for monitoring released neurotransmitter during social fear extinction, I observed that the implantation of the microdialysis probe into the lateral septum itself is sufficient to completely impair social fear extinction in male mice. The unilaterally caused damage still inhibited extinction even if an increased number of social stimuli was presented.

In summary, I was able to generate new data on altered transcriptomics, chromatin accessibility and histone modification H3K27me3 alterations in the context of social fear. Altogether, these data provide a solid background for the further investigation of molecular mechanisms involved in social fear and its extinction. Moreover, I could show for the first time that a lncRNAis dynamically regulated in social fear. Control experiments revealed the importance of learning and memory processes for Meg3 regulation. Moreover, region-specific Meg3 regulation during SFC as well as impaired social fear extinction after septal implantation of a microdialysis probe strengthened the role of the septum in social fear regulation.

ZUSAMMENFASSUNG

Zusammenfassung

Soziale Angst ist durch Angst und Vermeidungsverhalten von sozialen Situationen charakterisiert und stellt die dritthäufigste Angsterkrankung in unserer Gesellschaft dar. Trotz alledem ist auch heute noch wenig über die zugrundeliegenden Mechanismen bekannt. Aktuell zeigen angewandte Therapieansätze, die meist kognitive Verhaltenstherapien mit Medikationen kombinieren, erste Teilerfolge. Jedoch gibt es weiterhin viele Patienten, die nicht darauf ansprechen oder schnell rückfällig werden. Um spezifische und effizientere Behandlungsmöglichkeiten entwickeln zu können, ist vor allem ein besseres Verständnis über die zugrundeliegenden molekularen Mechanismen von Nöten. Hierbei sind RNA-Moleküle besonders vielversprechend, Einblicke in die molekularen Gegebenheiten, sowohl auf regulatorischer als auch auf nachfolgend translationaler Ebene, bei sozialer Angst zu geben. Generell sind kodierende und nicht-kodierende RNAs als Reaktion auf bestimmte Stimuli sehr dynamisch reguliert und ihre Fehlregulation hat meist schwerwiegende Auswirkungen zur Folge. Da Krankheiten oftmals mit spezifischen prä- und posttranskriptionellen Modifikationen verbunden sind, kann deren genauere Untersuchung im Kontext von sozialer Angst Aufschluss auf krankheitsrelevante Signalwege und deren Netzwerke geben.

Aus diesem Grund wurde die vorgelegte Doktorarbeit mit dem Ziel verfasst, RNAs, die durch soziale Angstkonditionierung und deren Löschung reguliert werden, mittels RNA-Sequenzierung zu identifizieren und zu charakterisieren. Hierzu habe ich mit Hilfe sozialer Angstkonditionierung soziales Vermeidungsverhalten, die Kernkomponente von sozialer Angst, in männlichen Mäusen induziert. Die soziale Angstkonditionierung ermöglicht die Etablierung von sozialer Angst, wohingegen bei der Angstlöschung, welche vergleichbar zur Konfrontationstherapie beim Menschen ist, die Mäuse lernen, wieder ungestraften Kontakt zu Artgenossen aufzunehmen. Für die RNA-Sequenzierung wurde 90 min nach der letzten Verhaltenstestung der sozialen Angstkonditionierung oder Angstlöschung RNA aus dem Septum der Mäuse isoliert. Hierbei lag ein spezielles Augenmerk auf konditionierten (SFC$^+$) Mäusen, die die Angstlöschung mit unterschiedlichem Erfolg abgeschlossen haben. Das Septum wurde als Zielregion gewählt, da dessen wichtige Funktion für die Regulation von sozialer Angst bereits mehrfach gezeigt wurde. Durch die RNA-Sequenzierung wurden viele RNAs identifiziert, die sowohl auf Gen- als auch auf Transkript-basierter Ebene reguliert waren. Nach anschließender Validierung mittels qPCR von auserwählten RNA-Kandidaten wie beispielsweise Sgk1, Crfr2 und weiteren, habe ich mich hauptsächlich auf die lange nicht-kodierende RNA Meg3 fokussiert, welche transkriptspezifisch und in Abhängigkeit von einer erfolgreichen Angstlöschung reguliert war. Genauer betrachtet waren jene Meg3-Varianten, die

ein langes alternativ gespleißtes Exon 10 enthielten, 24 h nach der Angstkonditionierung in SFC⁺ Mäusen herunterreguliert. Mäuse, die ihre soziale Angst während des Trainings zur sozialen Angstlöschung überwunden hatten, konnten die Expressionslevel zu unkonditionierten (SFC⁻) Tieren wieder angleichen. Tiere, die nach dem Training zur Angstlöschung noch immer sozial verängstigt waren, wiesen jedoch sogar noch 3 h nach dem Training niedrige Meg3-Levels auf. Kontrollversuche zeigten, dass Lernprozesse, und nicht soziale Interaktion alleine, für die Regulation von Meg3 nötig sind. Außerdem wurde Meg3 speziell im Septum, und nicht im Hippocampus reguliert vorgefunden. Um *in vivo* einen Meg3 Knockdown im Septum zu erzielen, wurden antisense LNA GapmeRs, die einen RNase H-abhängigen Abbau von spezifischen Meg3-Varianten induzieren, lokal verabreicht. Meg3 Knockdown-Versuche vor der Angstkonditionierung und vor dem Training zur Angstlöschung zeigten keine Auswirkungen auf die Angstkonditionierung, wohingegen die Angstlöschung und die anschließende Gedächtnisbildung und -festigung etwas beeinträchtigt zu sein schienen. Des Weiteren habe ich die Aktivierung des PI3K/AKT Signalweges untersucht, da diese bewiesenermaßen neuronale Plastizität und Langzeitpotenzierung reguliert und selbst von Meg3 moduliert wird. Interessanterweise konnte ich zeigen, dass die Phosphorylierungslevels von P85, der regulatorischen Untereinheit von PI3K, und AKT Ser473 3 h nach dem Training zur Angstlöschung in Tieren, die die Angst nicht erfolgreich löschen konnten, erhöht waren. Dies lässt auf eine Aktivierung des Signalweges schließen. Es ist denkbar, dass die Aktivierung in Tieren, die ein erfolgreiches Training zur Angstlöschung durchliefen, zu einem früheren Zeitpunkt stattfindet, was weitere Untersuchungen bedarf. In Meg3 Knockdown-Experimenten habe ich eine Aktivierung von PI3K in SFC⁺ Kontrolltieren beobachtet. Dieser Effekt blieb jedoch in SFC⁺ Knockdown-Tieren aus, was an den basal erhöhten Aktivierungslevels, die in SFC⁻ Knockdown-Tieren aufzufinden waren, begründet sein könnte. Insgesamt stellen die hier präsentierten Ergebnisse erste, aber bedeutende Hinweise über einen regulatorischen Zusammenhang von Meg3 und dem PI3K/AKT Signalweg nach dem Training zur sozialen Angstlöschung dar, welche noch weiter untersucht werden sollten. Interessanterweise regulieren viele lange nicht-kodierende RNAs die Transkription, indem sie Chromatinstrukturen beeinflussen. Deshalb habe ich ATAC-Seq und CUT&RUN durchgeführt, um Veränderungen auf Chromatinebene und der Histonmodifikation H3K27me3 zu charakterisieren. Hierbei wurden Veränderungen nach der sozialen Angstlöschung im allgemeinem, aber auch mit einem direkten Link zu Meg3 untersucht, um nukleare Interaktionsstellen von Meg3 für Zukunftsexperimente zu identifizieren.

In einem zweiten Teil der Dissertation, habe ich die Rolle des lateralen Septums für Prozesse der sozialen Angstlöschung weiter bestärkt. Basierend auf anfänglich geplanten Mikrodialyse-Experimente, die die Freisetzung von Neurotransmittern detektieren sollten, musste ich feststellen, dass die alleinige Implantation der Mikrodialyse-Sonde in das LS ausreichend war, die soziale Angstlöschung in männlichen Mäusen stark zu beeinträchtigen. Der unilateral verursachte Gewebsschaden verhinderte die Angstlöschung weiterhin, auch bei einer Erhöhung der Anzahl an präsentierten sozialen Stimuli.

Zusammenfassend konnte ich neue Daten über Veränderungen des Transkriptoms, der Chromatinzugänglichkeit und der Histonmodifikation H3K27me3 im Kontext von sozialer Angst generieren. All dies stellt ein solides Grundgerüst für die weitere Untersuchung von molekularen Mechanismen, die bei sozialer Angst und deren Löschung involviert sind, dar. Außerdem konnte ich erstmals zeigen, dass eine lange nicht-kodierende RNA dynamisch in sozialer Angst reguliert ist. Kontrollexperimente zeigten, dass Lern- und Gedächtnisprozesse für die Regulation von Meg3 notwendig sind. Zusätzlich bestärkten die regionsspezifische Meg3-Regulation und die eingeschränkte Angstlöschung bei septaler Implantation einer Mikrodialyse-Sonde die Rolle des LS in der Regulation von sozialer Angst.

ABBREVIATIONS

Abbreviations

Abbreviations	Meaning
µ	micro
µl	microliter
µM	micromolar
AKT	protein kinase B
ANOVA	analysis of variance
ATAC-Seq	assay for transposase-accessible chromatin with high throughput sequencing
AD	Alzheimer disease
AMPAR	α-amino-3-hydroxy-5-methyl-4-isoxazolepropionic acid receptor
ASD	autism spectrum disorder
BC1	brain cytoplasmic non-coding RNA
bp	base pairs
BSA	bovine Serum Albumin
cDNA	complementary DNA
CRFR2	corticotropin-releasing factor receptor 2
CUT&RUN	cleavage under target & release using nuclease
Cwc22	Cwc22 associated protein
DAPI	4',6-Diamidin-2-phenylindol
Dclk3	doublecortin-like kinase 3
DMR	differentially methylated region
DNA	deoxyribonucleic acid
dNTP	deoxyribonucleosid triphosphate
ECL	enhanced chemiluminescence
Ext$^-$	acquisition
Ext$^+$	extinction (training)
FACS	fluorescence-activated cell sorting
FPKM	fragments per kilobase million
GABA	γ-aminobutyric acid
Gtl2	gene trap locus 2
h	hour
(d/v) HPC	(dorsal/ventral) hippocampus
HRP	horseradish peroxidase
IG-DMR	intergenic differentially methylated region

IHC	immunohistochemistry
InDA-C	insert dependent adaptor cleavage
kb	kilobase
KD	knockdown
kDa	kilodalton
LNA	locked nucleic acids
lncRNA	long non-coding RNA
LS	lateral septum
LTP	long-term potentiation
mAB	monoclonal antibody
MDM2	murine double minute2; E3 ubiquitin ligase
Meg3	maternally expressed gene 3
miRNA	microRNA
mM	millimolar
MM	mastermix
mRNA	messenger RNA; coding RNA
MS	medial septum
mTORC (1/2)	mammalian target of rapamycin complex (1/2); serine/threonine kinase
n	nano
ng	nanogram
nm	nanometer
nt	nucleotide
OFC	operant fear conditioning
OFC$^-$	unconditioned in context of OFC
OFC$^+$	conditioned in context of OFC
OXT	oxytocin
OXTR	oxytocin receptor
p	phospho
pAB	polyclonal antibody
PBS	phosphate buffered saline
PCA	principal component analysis
PCR	polymerase chain reaction
PDK1	phosphoinositide-dependent protein kinase 1
PFA	paraformaldehyde

PI3K	phosphoinositide-3-kinase
PIP2	phosphatidylinositol-4,5-bisphosphate
PIP3	phosphatidylinositol-3,4,5-triphosphate
PolII	(RNA) polymerase II
PRC2	polycomb repressive complex 2
qPCR	real-time quantitative PCR
REST	RE1 silencing transcription factor
RNA	ribonucleic acid
RNA-Seq	total RNA-sequencing
RT	room temperature
SAD	social anxiety disorder
sCRFR2	soluble corticotropin-releasing factor receptor 2
SDS	sodium dodecyl sulfate
SDS-PAGE	sodium dodecyl sulfate polyacrylamide gel electrophoresis
SEM	standard error of the mean
Ser	serine
SFC	social fear conditioning
SFC$^-$	unconditioned in context of SFC
SFC$^+$	conditioned in context of SFC
SFC$^-$/Ext$^+$	unconditioned animal that was subjected to extinction training
SFC$^+$/Ext$^+$ (suc)	conditioned animal showing successful extinction of social fear
SFC$^+$/Ext$^+$ (unsuc)	conditioned animal showing unsuccessful extinction of social fear
SGK1	serum and glucocorticoid inducible kinase 1
TBS	Tris-buffered saline
TEMED	tetramethylethylendiamin
Thr	threonine
Tris	tris(hydroxymethyl)-aminomethane
V	volt

INTRODUCTION

1 Introduction

1.1 World of RNAs

At the beginning of the 20th century, nucleic acids have already been discovered as the responsible genetic factors, which encode genetic information. In the 1950s, Erwin Chargaff and Rosalind Franklin imaged DNA crystal structures (Franklin & Gosling, 1953a; Franklin & Gosling, 1953b; Klug, 1968), and the chemistry of DNA, which is composed of deoxyribose, a phosphate group and one of the bases adenine, thymine, guanine or cytosine, was identified (Chargaff, 1950). In parallel, a second class of nucleic acids, containing ribose instead of deoxyribose and uridine instead of thymine, got into the focus of research and is now known as ribose nucleic acid - short RNA. The "Central Dogma of Molecular Biology", stated by Francis Crick in 1957/58, was considered as a milestone in molecular biology, as it suggested for the first time a direct link of the three macromolecules DNA, RNA and protein (Crick, 1958; Crick, 1970). With some limitations, this dogma and its basic principles remain valid until today. Briefly, it states that genetic information within the DNA finally encodes for proteins, which are translated from messenger RNAs (mRNAs), single-stranded molecules transcribed from DNA. Further research and advances in methodology in the last decades identified specific mechanisms and important factors responsible for gene expression. Another milestone in molecular biology was set with completion of the human genome project. Surprisingly, this project revealed that only ~ 2 % of the human genome encodes for proteins (Lander, 2001). The other ~ 98 % of DNA was considered as "junk DNA" for a long time. However, in the last 20 years, more and more evidence occurred that most of the non-coding "junk DNA" is of highest regulatory significance.

In the following sections, I want to highlight the differences between coding and non-coding RNAs and their important interplay as well as their interaction with DNA and proteins.

1.1.1 Messenger RNAs and the importance of alternative splicing events

mRNAs undergo many processing steps before they can be translated into proteins (Hocine et al., 2010; Montecucco & Biamonti, 2013). RNA polymerase II (PolII) transcribes the primary transcript (pre-mRNA) from DNA. During this transcription process, RNA molecules undergo 5' capping and specific signal sequences upstream and downstream of the polyadenylation site are recognized by enzyme complexes, which leads the recruitment of poly(A) polymerase that adds up to ~ 250 A residues. The poly(A) tail together with the m7G cap represent important features for the quality control before nuclear export.

In higher eukaryotes, pre-mRNAs are characterized by intronic and exonic sequences. During splicing, the last step of the maturation process, introns are removed by the spliceosome that recognizes boundaries of an intron and an exon (Hocine et al., 2010). By two transesterification reactions, introns are removed and the flanking exons are connected. Here, many transcript variants can be generated depending on the splice site that has been chosen by the spliceosome (Wang et al., 2015a). Weaker splicing signals at splice sites, shorter exons or higher sequence conservation surrounding orthologous exons shift the balance from constitutive to alternative splicing. Whole exon skipping is the most prevalent mechanism for alternative splicing; intron retention and alternative selection of 5' and 3' splice sites within exon sequences are also possible. In fact, ~ 95 % of all human genes undergo splicing. In this way, ~ 25,000 human coding genes result in much more transcript variants per gene that often lead to different structures and functions of resulting proteins, thereby increasing the diversity to more than 90,000 different proteins (Wang et al., 2015a). Overall, splicing events are highly tissue- and cell type-specific and strictly regulated in developmental processes (Baralle & Giudice, 2017; Furlanis et al., 2019).

<u>Splicing events and subcellular localization of RNAs within the central nervous system</u>

The brain as highly complex and structured organ is exceedingly affected by splicing events. Intense research in this field revealed exclusive expression patterns of splice factors within the brain, e. g. NOVA1 that is exclusively expressed in neurons, and PTBP2, which is only expressed in the brain and shown to regulate, amongst others, axonogenesis (Hakimah Ab Hakim et al., 2017; M. Zhang et al., 2019). Splicing events play a crucial role during brain development and neurogenesis including cell-fate decisions, neuronal migration, axon guidance, and synaptogenesis (Su et al., 2018). Moreover, they are associated with psychiatric disorders like Alzheimer disease (AD), schizophrenia and others (Chabot & Shkreta, 2016; Hakimah Ab Hakim et al., 2017; Latorre et al., 2019).

For instance, alternative splicing in the serotonergic system is often linked to psychiatric disorders. This system is composed of the neurotransmitter serotonin that is synthesized by the tryptophan hydroxylase and aromatic amino acid decarboxylase, serotonin transporters, the monoamine oxidases for degradation and seven classes of serotonin receptors. For most of these components, many splice variants are known like 33 splice variants just for the serotonin receptor 2C and three splice variants for the tryptophan hydroxylase. The number of transcript variants and linked differences in dynamics and affinities as well as their tissue-specific

expression already implicate a key role of splicing in regulating the activity of the system and increasing its complexity (Latorre et al., 2019).

Other studies link splicing of certain mRNAs to altered learning capacities and anxiety-like behaviours. Neurexins, e.g., are cell adhesion-proteins on the presynaptic membrane that regulate synapse formation. They are affected by extensive splice events, thereby regulating the specificity of neuronal connectivity. Hence, neurexin 3, containing the alternative splice site 4, modulates plasticity by reducing postsynaptic α-amino-3-hydroxy-5-methyl-4-isoxazolepropionic acid receptor (AMPAR) trafficking and repressing long-term plasticity (Aoto et al., 2013). Besides, inclusion of the splice site 4 in neurexin 1 is required for memory formation and preservation after contextual fear learning within the dentate gyrus (Ding et al., 2017). Likewise, calcium channels are also important regulators of neuronal connectivity. *Cacn1b* encodes for the α1-pore forming subunit of the presynaptic $Ca_v2.2$ channel, which controls Ca^{2+} influx that triggers neurotransmitter release. Many known splice variants are cell type-specifically expressed such as the variant including the alternative exon 37a that was recently found to be enriched in Ca^{2+}/calmodulin-dependent protein kinase II excitatory projections neurons (Bunda et al., 2019). The same study found evidence that this alternative variant contributes to transmitter release at cortico-hippocampal synapses, thereby inhibiting exploratory and novelty-induced anxiety-like behaviour.

Another outstanding example, how splicing influences behaviour, is the alternatively spliced corticotropin-releasing factor receptor 2 (Crfr2) mRNA that mediates the anxiogenic effects of chronic oxytocin (OXT) treatment. OXT is generally considered to be anxiolytic, however, some studies observed that chronic treatment exerts fear and anxiety-enhancing effects in rodents and humans (Grillon et al., 2013; Peters et al., 2014; Tabak et al., 2011; Winter et al., in preparation). Winter et al. found that chronic OXT treatment activates the transcription factor MEF2A that induces transcription of the *Crfr2* gene by binding to the exon 2. Besides, MEF2A also binds exon 6, promoting alternative splicing and resulting in the soluble form of the CRFR2 (sCRFR2). The shift from the membrane-bound to the soluble form mediates the anxiogenic effects of the OXT treatment as the sCRFR2 levels correlate positively with anxiety-like behaviour. sCRFR2 competes with membrane-bound CRFR2 for ligand binding, hence, it might reduce the usually anxiolytic effects of membrane-bound CRFR2 activation in this context (A. M. Chen et al., 2005; Winter et al., in preparation).

Overall, splicing represents a powerful mechanism to increase diversity and complexity of the RNA pool and the resulting proteins, thereby helping an organism or cell to react to physiological or environmental stimuli. However, the response to stimuli often needs to be

immediate, and therefore, beside *de novo* transcription and alternative splicing, it is important that RNAs are already stored in certain compartments like so-called cytosolic P-bodies to be released when fast translation is required (Standart & Weil, 2018). Subcellular localization of mRNAs and ribosomes contribute to local synthesis on demand without significant delay. For neurons, dendritic branches and long axons with pre-synaptic compartments exemplify functional domains of cytoplasm that are separated from the cell body by long distances. In this case, several studies showed a high density of ribosomes and mRNAs in dendritic spines close to synapses, which turned out to be important for synaptic plasticity (Willis & Twiss, 2010). Ribosomes could even be detected in axons of the peripheral nervous system (Jung et al., 2012).

1.1.2 Non-coding RNAs

The first types of non-coding RNAs have already been discovered in the 1950s, when transfer and ribosomal RNAs were identified to play an essential role in protein translation. In the last decades, researchers found many additional types of non-coding RNA like small nuclear and nucleolar RNAs, microRNAs (miRNA), PIWI-interacting RNAs, circular RNAs and long non-coding RNAs (lncRNA) that have been mostly well characterized and investigated in the recent past. Non-coding RNAs are transcribed from all over the genome and their abundance within the cell roughly correlates with their level of conservation (Palazzo & Lee, 2015). Comparing the types and classes of RNAs, ribosomal and transfer RNAs represent the most abundant RNA types within a mammalian cell (Figure 1, Palazzo and Lee 2015).

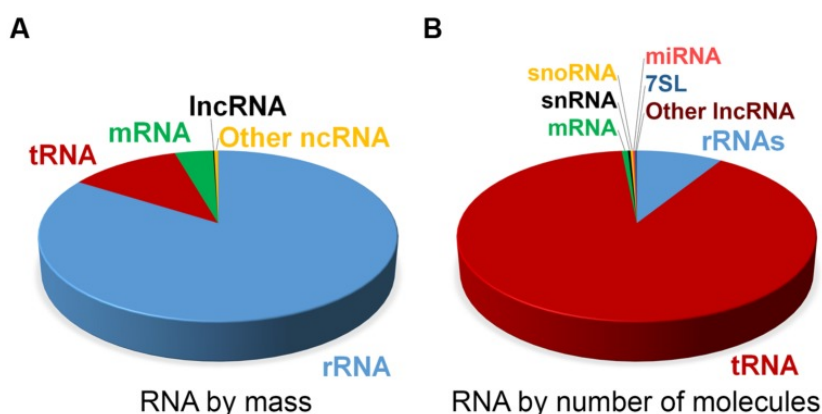Figure 1 Estimated abundance of different RNA classes in a typical mammalian cell.

Estimated proportions of various RNA classes in a mammalian somatic cell by (A) total mass and by (B) the absolute number of molecules. Non-coding (nc)RNAs shown here include small nuclear (snRNA), small nucleolar (snoRNA) and miRNAs, lncRNAs, 7SL RNA, ribosomal (rRNA) and transfer (tRNA) RNAs (adapted from Palazzo and Lee 2015).

Nevertheless, the role of less abundant non-coding RNA classes should not be neglected, as they often show cell- and tissue-specific expression and function (Quan et al., 2017). Also, their mode of action has been found to be quite varying, including the regulation of chromatin states, recognition and direct binding of various factors and regulatory elements, or the maturation and degradation of target molecules. As many lncRNAs are exclusively expressed in the brain (Derrien et al., 2012) and hold diverse functions due to their sequences and structures, I focus on this class of non-coding RNAs and their role in the regulation of behaviour in the following sections.

1.1.2.1 Long non-coding RNAs

LncRNAs are a fascinating class of RNAs, which are very diverse in their function, expression, localization, and even in their size. The length of lncRNAs varies between 200 nt and up to 100 kb and they are transcribed by RNA PolII. Various methodologies and the comparison of different lncRNA features are necessary to determine the conservation of lncRNAs across species, which might indicate their evolutionary functional importance. Multidimensional aspects like primary sequence conservation as well as the conservation of secondary structures, transcription status and splicing patterns have to be taken into account (Ulitsky, 2016).

Many lncRNAs are similar to mRNAs on the molecular level, as they are also capped, spliced and poly-adenylated. The striking difference is that the open reading frame is usually shorter than 300 nt, which is considered as an indication for the likelihood of non-coding properties. Therefore, lncRNAs are generally not, or only poorly, translated (Bhat et al., 2016; Cao, 2014; Frith et al., 2006). As originating from the sense or the antisense strand of the DNA, they can also be transcribed from intronic, intergenic, promoter or 3' UTR-associated regions (Wu et al. 2013). LncRNA promoters are as evolutionary conserved as the ones of mRNAs (Carninci et al., 2005; Derrien et al., 2012; Guttman et al., 2009). In line with this, expressed lncRNA promoters show similar active histone modifications, like enriched H3K4me3 or H3K27ac, as found for protein-coding promoters. Nevertheless, recent research revealed that there is also a global regulation of lncRNA expression (Zheng et al., 2014). Many promoters are bidirectional, meaning transcripts are produced as sense and antisense RNAs from the same promoter. In this way, sense and antisense transcripts can be simultaneously and coordinately expressed, resulting in similar expression levels (Core et al., 2008; Seila et al., 2008). However, differences in stability and elongation are remarkable, as sense transcripts are enriched for splice sites, whereas antisense transcripts show more polyadenylation signals ensuring the early termination of the

antisense transcript and fully elongation and maturation of the sense transcript (Quinn & Chang, 2016). Most of the lncRNAs belong to the group of these divergent transcripts and are thought to regulate their promoters and corresponding protein-coding genes in *cis,* meaning they regulate the expression or chromatin states of nearby genes (Guil & Esteller, 2012).

LncRNAs with *cis*-regulatory properties include lncRNAs from imprinted loci and dosage compensation lncRNAs like Xist (da Rocha et al., 2008; Sahakyan et al., 2018). Xist is transcribed from one of the X-chromosomes of female mammalian cells and subsequently inactivates the X-chromosome from which it is transcribed from (Sahakyan et al., 2018). Moreover, some enhancer RNAs belong to *cis*-regulatory RNAs as they are transcribed from enhancer regions and positively affect the expression of neighbouring genes (Lai & Shiekhattar, 2014; Li et al., 2016). *Trans*-acting lncRNAs leave their transcription site and operate at regions far away from their transcription site, even in the cytoplasm and other compartments of the cell (Kopp & Mendell, 2018).

LncRNAs are spatio-temporally regulated, especially within the brain in a cell-type specific manner and with functions in specific subcellular compartments (Cava et al., 2019; Mercer et al., 2008). Depending on their intracellular localization, lncRNAs can fulfil different functions (Figure 2). Due to the length of the RNA molecule, lncRNAs often form secondary structures, thereby providing an interaction and assembly platform for chromatin remodelers and transcription factors. Through sequence complementarity, they guide bound factors or complexes to particular regions of the genome thereby affecting e.g. chromatin remodelling or transcription. On the other hand, lncRNAs are also able to bind components and hence, titrating them away from their original action site. As post-transcriptional regulators, they influence mRNA processing, translation, modification and degradation by the similar mechanisms mentioned above (Wang & Chang, 2012).
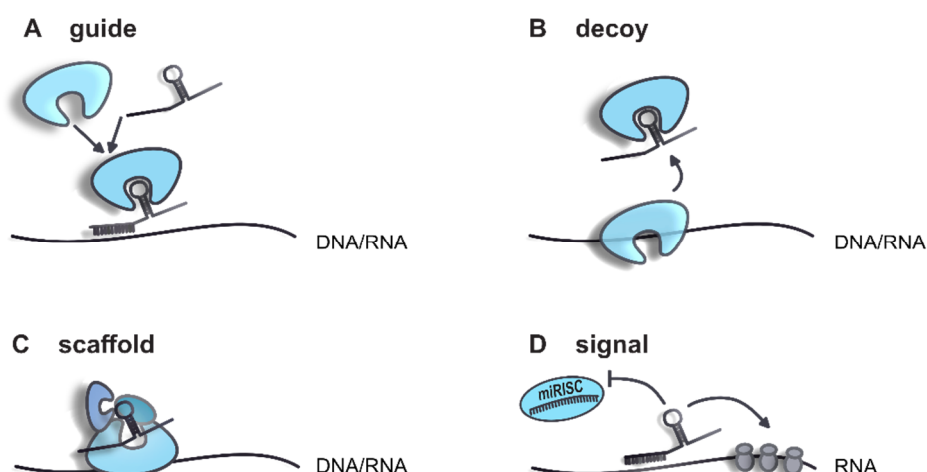
Figure 2 Schematic description of the main functions of lncRNAs.

(A) LncRNAs can guide complexes or factors to specific sequences on RNA or DNA molecules. (B) In the same way, factors can be bound by lncRNAs and be titrated away from their action site. (C) Secondary structures provide a platform for protein complex assembly. (D) LncRNA themselves can function as a signal and influence other mechanisms like miRNA-mediated cleavage or protein translation.

On average, lncRNAs have only a slightly shorter half-life than mRNAs. Nevertheless, there is a wide range of variability. Some lncRNAs have a half-life of less than 2 h; others show extreme stability with a half-life longer than 16 h. Intergenic origins or *cis*-antisense features support stability, whereas nuclear localization is usually linked to a short life span of lncRNAs (Clark et al., 2015). Due to structural similarities to mRNAs and weak open reading frames, a large fraction of lncRNAs is associated with ribosomes and consequently linked to nonsense-mediated decay (Niazi & Valadkhan, 2012; Zeng et al., 2018). Moreover, lncRNA turnover can be regulated by decapping and deadenylation events, miRNA-mediated decay and the binding of RNA binding proteins supporting or preventing degradation (Yoon et al., 2016).

1.1.2.2   The role of lncRNAs in neuropsychiatric disorders

An impressive number of about 40 % of lncRNAs being expressed specifically in the brain indicates a functional role of lncRNA in complex behaviours (Derrien et al., 2012). Their role during brain development is already well established and their involvement in glioma initiation and progression has been reported (Briggs et al., 2015; Nie et al., 2019). Apart from this, increasing evidence reveals lncRNAs as important regulatory players in social behaviour and neuropsychiatric diseases like Autism spectrum disorder (ASD) and schizophrenia.

ASD is a multifactorial and multisymptomal disorder mainly characterized by social and cognitive impairments and repetitive behaviours (Diagnostic and Statistical Manual of Mental Disorders; DSM-5, American Psychiatric Association, 2013). Wang et al. showed that lncRNA levels are strongly altered in blood of ASD patients and that these altered lncRNAs are associated with synaptic vesicle cycling as well as long-term depression and potentiation (Wang et al., 2015b). RNA Sequencing of *post mortem* frontal and temporal cortex samples from control and ASD subjects identified 60 differentially regulated lncRNAs (Parikshak et al., 2016). In a similar study with human cortical brain samples, Gudenas and colleagues used a computational pipeline combining differential gene expression patterns of ASD tissue in conjunction with gene co-expression networks of tissue-matched control samples to identify differentially expressed lncRNAs. During this analysis, they identified five lncRNAs, which are antisense to ASD risk genes like *Rapgef4, Dlx6, Stxbp5, Klc2* and *Dmxl2*. Furthermore, co-expression network analysis revealed that there is a correlation of regulated lncRNAs and ASD gene sets indicating that the identified lncRNAs are involved in biological processes dysregulated in ASD (Gudenas et al., 2017). Some other lncRNAs could also be linked to schizophrenia, which is characterized by abnormal social behaviour and impaired ability to understand reality. Animal models for schizophrenia were used to successfully identify even potential downstream targets of those lncRNAs. One example for a schizophrenia-linked lncRNA is the brain cytoplasmic non-coding RNA (BC1). BC1 usually forms ribonucleoprotein particles and regulates translation and glutamatergic transmission in neurons (Napoli et al., 2008; Zalfa et al., 2003). *BC1* knockout mice revealed deficits in sociability in the three-chamber-test, whereas social memory and social hierarchy were unaffected (Briz et al., 2017). Furthermore, BC1 increases the affinity of two regulatory proteins, FMRP and CYFIP1, in the brains. These proteins are both associated with schizophrenia, ASD and fragile X syndrome (Bardoni et al., 2001; Jansen et al., 2017; Pathania et al., 2014). FMRP, a RNA binding protein, binds the CYFIP1-eIF4E complex in the brain leading to repressed translation of FMRP targeted mRNAs (Napoli et al., 2008).

Another example is the lncRNA Gomafu, which is highly enriched in neurons. It is encoded in a schizophrenia-related locus and also dysregulated in schizophrenia patient brains. There is strong evidence for Gomafu being involved in alternative splicing as it binds QKI and SRSF1, RNA binding proteins that regulate pre-mRNA processing (Barry et al., 2014). In another study, Gomafu could be also linked to the schizophrenia-associated gene *Crybb1*. Here, Gomafu negatively regulates *Crybb1 via* the interaction with the polycomb repressive complex 1, thus increasing anxiety-like behaviour in mice (Spadaro et al., 2015).

NEAT1 is one of the most abundant lncRNAs and ubiquitously expressed in the human body, with the lowest expression in the central nervous system (Kukharsky et al., 2019). Downregulated NEAT1 levels in cerebrocortical regions were linked to schizophrenia and *Neat1* knockout mice display an altered socio-behavioural phenotype (Katsel et al., 2019; Kukharsky et al., 2019). Mice are naturally territorial and exhibit defensive behaviour when unknown conspecifics enter their territory. However, this defensive behaviour towards an intruder was nearly absent in *Neat1* knockout mice exposed as residents to the resident-intruder test. In these mice, physical social contact was also decreased, and a general lack of social interest was found in the Social Odor test (Kukharsky et al., 2019).

Contrary to the above-mentioned examples, only a few studies could implicate lncRNAs in the regulation of naturally occurring social behaviours. A recent study by Ma et al. identified the lncRNA AtLAS to regulate social hierarchy by controlling postsynaptic AMPAR trafficking in prefrontal cortical excitatory pyramidal neurons (Ma et al., 2020). They showed that in dominant mice, AtLAS is downregulated in the prefrontal cortex leading to hyperactivity of local neurons and the downregulation of synapsin 2b, which usually inhibits AMPAR insertion into the membrane.

All these above-mentioned examples highlight the regulatory relevance of lncRNA in the brain, especially in complex behaviour and psychiatric disorders. Nevertheless, we are far from a complete list of lncRNAs with specific functions in the central nervous system, their functions and potential interaction partners, or their role in diseases. Still intriguing is the role of lncRNAs in fine-tuning behaviours caused by different social factors or leading to socio-emotional perturbations. Therefore, high-throughput studies should help to provide potential candidates that might be involved in the regulation of socio-emotional behaviours.

1.2 Social anxiety disorders and related animal models

1.2.1 Social anxiety disorders and treatment options

"What will they think about me? They will laugh. I am not pretty and cool enough to be friends with them.

Why do they stare at me? I am not here… I am not here. I do not want to say anything wrong."

Some of these thoughts come up in one's mind when a person is worried about how other people think about or judge oneself. A balanced level of these kinds of thoughts usually helps people to work on themselves, perform better and endure particular, social and stressful situations, e.g. entering an occupied room, speaking in public, the first contact with new people at school, work or parties, or starting conversations with unfamiliar people (Ličen et al., 2016). These events are uncomfortable for many people, although most of the people can finally cope with them. However, if these negative thoughts and feelings become excessive, and if they are omnipresent although there is no concrete reason, stress generated by these social situations is overwhelming and – as consequence – affected people try to avoid such social situation (Morrison & Heimberg, 2013).

People chronically suffering from such states (longer than 6 months) are diagnosed with social anxiety disorder (SAD). SAD, or social phobia, shows an early onset during youth and an estimated lifetime prevalence of 10.7 % in the US, with a higher prevalence in females (Kessler et al., 2012). Next to major depressive disorders and specific phobias, this is the third most common anxiety disorder. According to the current definition (DSM-5), a SAD patient persistently fears one or more social or performance situations, in which he is exposed to unfamiliar people or possible scrutiny by others. A SAD patient fears embarrassment and humiliation. Exposure to such situations evokes anxiety and possibly situationally bound panic attacks. As a consequence, feared situations are avoided and together with the psychological state person's daily normal routine, occupational functioning and relationships are strongly restricted and quality of life is reduced (DSM-5, American Psychiatric Association, 2013). SAD is often comorbid with depression and other anxiety disorders such as generalized anxiety disorder, agoraphobia or obsessive-compulsive disorders (Fehm et al., 2005, 2008) and many studies found an increased risk for SAD patients to commit suicide (Fehm et al. 2005). This clearly indicates the necessity to find suitable and effective treatment options. To date, a combination of psychological and pharmacological treatment approaches are common. Psychotherapeutic interventions include mainly cognitive-behavioural exposure therapies and cognitive restructuring, which help SAD patients to understand that the situations are not

harmful but the patient's thoughts generate anxiety. In addition, at least for some clients, social skills training helps to better cope with social situations (Rodebaugh et al., 2004). Concerning pharmacotherapy, there are no specific chemical compounds available, which target specifically social anxiety. This might be also due to the limited knowledge about underlying molecular mechanisms. So far, serotine-reuptake inhibitors, benzodiazepines, serotonin-norepinephrine-reuptake inhibitors and monoamine-oxidase inhibitors, which are usually applied in context of depression, show positive, symptom-alleviative effects. Nevertheless, only 35-65 % of pharmacologically treated clients respond to medication (Davidson, 2003).

To understand underlying neurobiological mechanisms of SAD, a few fMRI studies were performed to identify brain regions that are differentially activated in patients suffering from SAD. One study investigated neuronal activity patterns in brains of SAD patients, when they were socially excluded during cyber games (Nishiyama et al., 2015). Here they found that social exclusion of socially anxious people led to increased activity of the anterior cingulate cortex, whereas social support through messages during social exclusion increased left dorsal prefrontal cortex activity, thereby positively correlating with social anxiety levels. This indicates that socially anxious individuals perceive social support but still are susceptible to negative evaluation. Another research group used the same cyber game with social exclusion and found that the inferior frontal gyrus plays an important role during re-inclusion (Heeren et al., 2017). They found that recovery from the negative event "exclusion" is much harder than the exclusion itself. Other studies revealed an amygdala hyperactivation in SAD patients in response to the social threat (Labuschagne et al., 2010; Minkova et al., 2017). Nevertheless, little is known about relevant brain regions involved in the onset and extinction of SAD, which is of importance for exposure therapies and medication.

In summary, it is obvious that the actual state of knowledge and treatment options for SAD are not sufficient. Detailed research for a better understanding of responsible brain regions, circuits and especially of underlying molecular mechanisms is not circumventive in order to help SAD patients and for the development of proper treatment options.

1.2.2 Social fear conditioning

Animal models are consulted to study molecular and underlying mechanisms and develop treatment options for complex psychiatric diseases. The development of animal models is based on the assumption that neuronal and hormonal systems are conserved and that homologous factors exist across various species (Neumann et al. 2011; Greek and Rice 2012). Regarding

social behaviours, there are several models available including models for chronic psychosocial stress, depression, PTSD and others (Langgartner et al., 2015; Neumann et al., 2011).

For studying social fear in rodents, a mouse model of "Social fear conditioning" (SFC) has been developed in 2012. It is based on operant fear conditioning principles and enables researchers to mimic social avoidance – the core symptom of SAD – in adult mice (Toth et al., 2012). During the social fear acquisition phase, mice associate an aversive event, i.e. a mild electric foot shock, with the contact of an unfamiliar conspecific, inducing a general social avoidance behaviour, which stays manifested up to several weeks (for protocol details see 2.3.1). Social fear extinction training by presenting several unknown conspecifics helps to overcome social fear, and is comparable to human exposure therapies. It results in similar effects, namely that it helps most, but still not all of the mice to extinguish their social fear so that they approach other mice again. The SFC paradigm is a unique model, as it does not induce other common comorbid behavioural changes like depressive-like or general anxiety-like behaviour (Toth et al., 2012), which is often the case in other models like social defeat or subordinate colony housing.

In the last years, pharmacological manipulations revealed that oxytocinergic, neuropeptide S and glutamatergic signalling can influence social fear. Neuropeptide S and OXT intracerebroventricularly infused completely reversed social fear expression during social fear extinction training (Zoicas et al., 2014, 2016), whereas Slattery et al. showed that, unlike non-social fear, blockage of the metabotropic glutamate receptor subtype 5 and activation of subtype 7 lead to impaired social fear extinction (Slattery et al., 2017). These studies provided first important key information, which neuropeptide systems might be involved in the regulation of social fear and its extinction. First hints for brain regions being specifically involved in social fear processes were obtained when Zoicas et al. used oxytocin receptor (OXTR) autoradiography and found differences in OXTR binding over the SFC paradigm especially in the dorsolateral septum (Zoicas et al., 2014).

1.2.3 The septum as a key region for social fear

Findings of Zoicas et al. highlighted the role of the septum in the regulation of social fear. With further experiments, they showed that infusion of OXT directly into the dorsolateral septum abolished social fear expression during social fear extinction training (Zoicas et al., 2014). Based on these findings, further research focused on the lateral septum (LS) in context of social fear. Menon and colleagues performed manipulations of the OXT system within the LS in virgin mice as well as in lactating mice that have a highly activated endogenous OXT system. Lactating

mice displayed no social fear at all, and blockage of the OXTR in the LS prevented this effect. The other way around, increasing OXT levels in the LS pharmacologically or genetically of virgin mice reversed SFC-induced social fear (Menon et al., 2018).

Obviously, the LS plays a role in social fear, so what kind of region is it? What makes it so important for social behaviour? The septum is a subcortical forebrain structure, which lies directly between the lateral ventricles in rodents. In humans, the septum pellucidum separates the lateral ventricles as a thin membrane, whereas the septum verum is composed of neuronal somata and runs next to the lateral ventricles. The rodent septum is composed of two main areas: the medial septum (MS) and the lateral septum (LS). The MS sends ascending projections mainly to the hippocampus (HPC), whereas the LS receives descending input from the HPC. These interconnections form together the septo-hippocampal formation, which is critical for learning and memory processes (Niewiadomska et al., 2009). In contrast to the mainly GABAergic and cholinergic neurons of the MS, the LS receives glutamatergic input from the HPC and sends GABAergic projections to hypothalamic areas and midbrain regions. Newest antero- and retrograde tracing methods confirmed primary projections from the LS also to the nucleus accumbens, Bed nucleus of the stria terminalis, amygdala and parts of the hypothalamus and thalamus (Deng et al., 2019).

With the central location and the high grade of interconnectivity, the LS represents an essential relay station for integrating cognitive information from cortex regions and the HPC with affective information from the amygdala, hypothalamus and bed nucleus. The converged information then is led to regions that directly trigger behavioural responses. Importantly, there is also an intraseptal feedback loop so that the LS inhibits its own activation and the activation of MS by GABAergic collaterals (De France et al., 1975; Stevens et al., 1987). This is in particular important for the septo-hippocampal pathway during learning and memory processes: the MS plays a key role in learning and memory as it stimulates synchronized firing of the HPC. Reciprocal downregulation of the MS activation can occur *via* direct GABAergic signalling from the HPC to the MS, or indirectly, *via* activation of LS, which then inhibits GABAergically the MS (Khakpai et al., 2013).

Functioning as a relay station, the septum is also involved in the regulation of different behaviours. It expresses receptors for various neurotransmitters that are released by input projections from different areas. Therefore, it is not surprising that the septum reacts to pharmacological interventions, which are applied for various psychiatric diseases in humans. Effective medication for schizophrenia and depression, for example, enhances LS activation

that is often confirmed by increased c-fos levels, a marker for cell activity (Sheehan et al., 2004). Interestingly, also structural changes of the septum pellucidum correlate with developing mental illnesses (Galarza et al., 2004; Wang et al., 2019). Regarding anxiety and fear-related behaviour, the LS shows higher activation during stressful and anxiety-provoking situations, indicating its role in controlling fear-related behaviour (Cullinan et al., 1995; Kollack-Walker et al., 1997; Mongeau et al., 2003). Septal lesion studies revealed a generalized disinhibition of fear, resulting in exaggerated defensive behaviour, enhanced startle reactions and freezing behaviour during contextual fear conditioning as well as increased intraspecific aggression (Brady & Nauta, 1955; Miczek & Grossman, 1972; Sparks & LeDoux, 1995; Vouimba et al., 1998). In summary, it is suggested by many researchers that an excited LS inhibits fear, whereas fear can be released and disinhibited following inhibition of the LS. This regulatory capacity enables adapted fear-related behaviours in response to particular situations. This idea is also supported by gain- and loss-of-function studies. Electric stimulation and optogenetic activation of the LS reduced fear and aggression in various contexts, consequently resulting in inactivation of the amygdala, the fear regulatory centre, again demonstrating an indirect regulation of fear by the LS (Thomas et al., 2013; Wong et al., 2016; Yadin et al., 1993).

The LS in context of social fear

So far it is known from studies using the SFC paradigm, that i) the neuropeptides OXT and neuropeptide S abolish the expression of SFC-induced social fear, ii) manipulation of metabotropic glutamate receptor subtype 5 and 7 impair social fear extinction and iii) local manipulation of the OXT system within the LS regulates social fear expression. Other studies further emphasize the role of the septum in social behaviours, but also in regulating anxiety and fear-related behaviours.

Consequently, the LS is strongly considered as a promising regulatory region in context of social fear and the SFC paradigm, which is worth to be studied in much more detail. In this line, it is indispensable to focus especially on molecular mechanisms within the LS, as so far nothing is known about signalling pathways, regulatory networks, the role of lncRNAs, chromatin states and interaction partners.

1.3 Technologies for detecting and manipulating RNAs and chromatin states

About forty years ago, the invention of Sanger-Sequencing revolutionized the field of biology. With this technology, it was for the first time possible to decipher the sequence of the genome. Over the last decades, many advances in sequencing technologies have been achieved, and nowadays it is possible to high-throughput the sequencing of DNA and RNA, thereby reducing time and costs. Novel sequencing approaches also allow us to investigate structures and interactions sites of RNA molecules, making these technologies a promising tool for investigating RNAs in a specific context of disease or normal physiology.

1.3.1 Total RNA-Sequencing

RNAs are important effector molecules, which are regulated as a consequence of certain stimuli or diseases. In order to understand, how a disease is manifested on a molecular level and how a particular behavioural or emotional phenotype is induced by stimuli, it is necessary to identify regulated RNAs in this context. In this regard, coding as well as non-coding RNAs are of interest as the latter are able to pre- and post-transcriptionally regulate transcription and translation levels. Total RNA-Sequencing (RNA-Seq) is a powerful tool to detect coding and multiple forms of non-coding RNAs. This technology belongs to the high throughput next generation sequencing technologies, which allows RNA analysis through cDNA sequencing at a massive scale. RNAs from a certain tissue or cell type can be isolated and during library preparation, they are reversely transcribed into cDNA, which is further fragmented and ligated to adaptor and barcode sequences. For sequencing, adaptor-ligated cDNA fragments are loaded on flow cells, which contain billions of nanowells. Within one nanowell, a cluster originated from only one cDNA fragment, is built. Afterwards, clusters are sequenced by the technology "sequencing by synthesis", meaning a fluorescent signal is detected when a fluorescently labelled nucleotide is incorporated during strand synthesis (Fuller et al., 2009). Depending on the scientific question, different read lengths are possible and it can be chosen, whether fragments are sequenced from only one or both ends (single or paired-end sequencing). In case there is no research focus on ribosomal RNA, it is recommended to deplete ribosomal RNA during library preparation as they are the most abundant RNA molecules and the coverage of less present RNA molecules would be greatly reduced. Through the ligated barcode sequence, each read can be assigned to the sample from which it originated. With complex bioinformatical analyses, reads are aligned to a reference genome and depending on the bioinformatics pipeline and workflow, transcript and gene-based alterations, as well as *de novo* transcripts, can be calculated.

1.3.2   ATAC-Sequencing

Sequencing approaches are also used to investigate chromatin states. On the one hand, there are open chromatin regions, where the DNA is accessible for binding of transcription factors or enzymes. On the other hand, there is closed chromatin characterized by tightly packed DNA, which is wrapped around histone octamers and therefore not accessible. Reactions and adaptations of cells or organisms to any type of stimuli are always linked to chromatin remodelling events leading to changes in chromatin state and accessibility and in this way, finally to transcription changes. In 2013, Buenrostro and colleagues established a protocol called "Assay for Transposase-Accessible Chromatin with high throughput sequencing" – short ATAC-Seq –, which enables us to identify open chromatin regions (Buenrostro et al., 2013), thereby needing much fewer cell numbers compared to other methods like MNase-Seq (Zaret, 1999), ChIP-Seq (Landt et al., 2012) or DNase-Seq (Song & Crawford, 2010). The protocol is based on a hyperactive Tn5 transposase that inserts adapter DNA in accessible DNA regions on a genome-wide level (Figure 3). For this, the Tn5 transposase is artificially loaded with known DNA sequence tags for later construction of a library for sequencing.
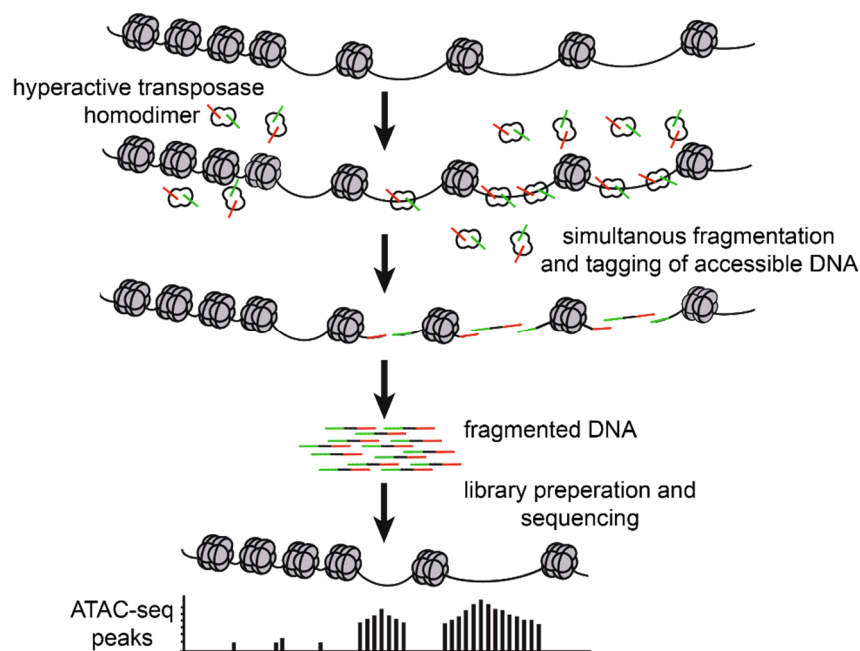
Figure 3 Principle and procedure of ATAC-Seq.

Transposases can bind to open chromatin regions where they cut the DNA and insert adaptors (green and red) to generate DNA fragments. Sequencing results in more peaks in originally open chromatin regions than compared to closed regions (adapted from Sun et al., 2019).

1.3.3 CUT&RUN

In order to detect chromatin binding sites of DNA-interacting proteins or the genome position of certain histone marks, Skene and Henikoff have previously described an alternative to chromatin immunoprecipitation (Skene & Henikoff, 2017). This *in situ* method called "Cleavage Under Targets & Release Using Nuclease" (CUT&RUN) marks transcription factors or histone modifications with an antibody, which is later recognized by a Protein A-Micrococcal Nuclease fusion protein (Protein A-MNase; Figure 4). Activation of the nuclease leads to the excision of the bound complex (DNA/target/antibody and nuclease) and the cleaved DNA can be extracted and sequenced. In CUT&RUN, unlike in chromatin immunoprecipitation, cells do not need to be broken up, which favours the natural protein-DNA interaction state. Moreover, as the antibody directly binds to the protein and only bound DNA excised, a more efficient isolation and sequencing readout with less background are achieved. There are several modified CUT&RUN protocols available making it possible to perform CUT&RUN on frozen or fresh tissues and cells, with a low or high starting number of permeabilized cells or isolated nuclei (Hainer et al., 2019; Skene & Henikoff, 2017).
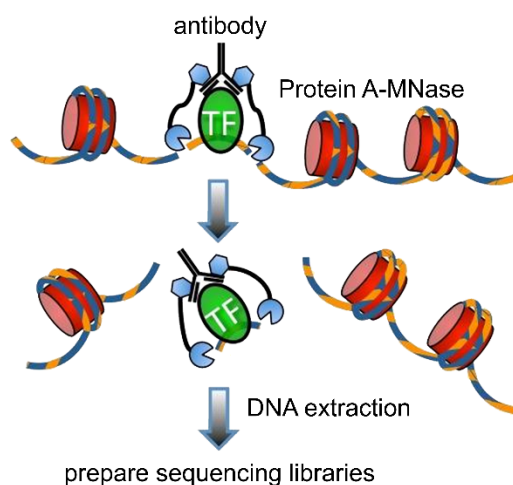
Figure 4 Schematic diagram of CUT&RUN mechanism.

Protein A-MNase diffuses into the cell nucleus and binds to an antibody. After activation, MNase cleaves the DNA and DNA fragments are released. Extracted DNA from the supernatant is used to prepare libraries for sequencing. TF = transcription factor.

1.3.4   LNA antisense GapmeRs

Studying the function of RNA molecules *in vivo* requires molecular tools, which are highly efficient without showing negative side effects on the animal. For studying the effect of knockdown of a particular RNA, the antisense technology has proven to be a valuable tool. Array of modifications in the backbone are now known to improve the stability and specificity of antisense oligonucleotides while making them stable and less toxic. Regarding the knockdown of lncRNAs *in vivo*, so-called LNA antisense GapmeRs have been widely used. LNA antisense GapmeRs (short GapmeRs) are single-stranded oligonucleotides with a central block of deoxyribonucleotide monomers. Pairing of this DNA-like sequence with RNA molecules induces the recruitment of and cleavage by RNase H1, which usually degrades the RNA primers from Okazaki fragments during DNA replication. The central sequence is flanked by locked nucleic acids (LNA) (Braasch & Corey, 2001), ribonucleotides with a methylene bridge between the 2'-oxygen of the ribose and the 4'-carbon. LNAs increase the binding affinity to complementary sequences and decrease degradation levels by exonucleases. The combination of all features in antisense LNA GapmeRs makes them a highly specific and efficient tool with high potency without the need for transfection reagents. In this way, they can be applied *in vivo* without toxic effects and through labelling, distribution of LNA antisense GapmeRs can even be monitored.

1.4   Potential RNA candidates

1.4.1   Maternally expressed gene 3

Maternally expressed gene 3 (Meg3) is a lncRNA that was discovered in imprinting studies in 2000 (Miyoshi et al., 2000). *Meg3* is an imprinted gene localized on the human chromosome 14q and the syntenic mouse distal chromosome 12, originally named as *Gtl2* (gene trap locus 2) (Schuster-Gossler et al., 1998). Imprinting studies revealed that Meg3 is exclusively expressed from the maternal chromosome. The human *Meg3* shows 67 % homology to the mouse *Meg3/Gtl2* and consist of 10 exons, which alternatively spliced results in at least 12 different isoforms in humans (Zhang et al., 2010b). Regarding the mouse Meg3 variants, it highly depends on the databases how differentially the variants are defined and how many variants are annotated (for an overview see Figure 5).

A

B

		RefSeq ID (NCBI)		
		NR_027652.1 (1924 bp)	NR_003633.3 (11488 bp)	NR_027651.2 (11476 bp)
U C S C I D		uc007pap.2 (1503 bp) uc007pat.2 (1762 bp) uc007pav.2 (870 bp) uc007par.3 (1913 bp) uc011ysb.1 (728 bp)	uc007pau.4 (11473 bp) uc029rxy.3 (12940 bp) similarly encoded by both variants	uc007paq.4 (11460)
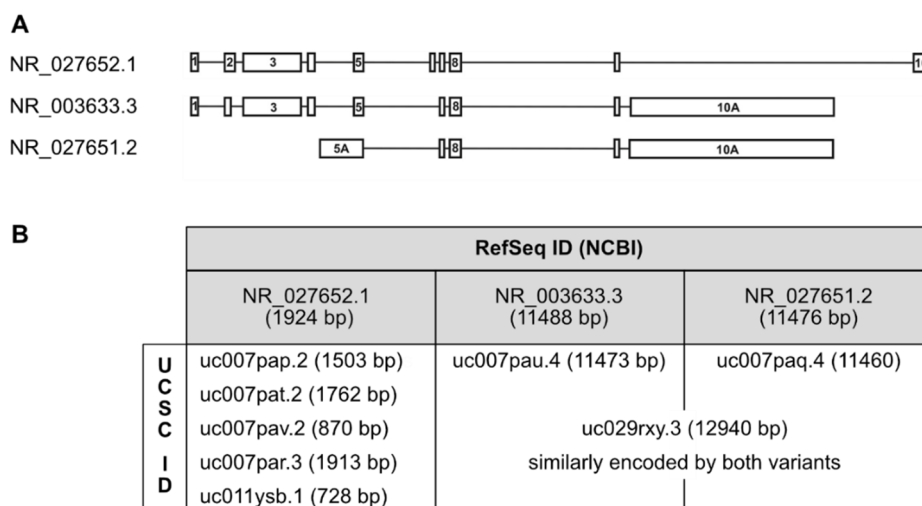
Figure 5 Overview of Meg3 variants.

(A) There are three mouse Meg3 variants annotated in RefSeq, the sequence database of NCBI. NR_027652.1 contains 10 exons. NR_003633.3 and NR_027651.2 contain a large alternative exon 10 (10A). NR_027651.2 has additionally an alternative exon 5 (5A) (adapted from (Zhu et al., 2019)). (B) There are eight annotations for Meg3 variants in the UCSC Genome Browser. Variants annotated in RefSeq include the sequences of the UCSC annotated variants.

In general, Meg3 is mainly reported to stay nuclear but there are some studies showing cytoplasmic localization where Meg3 functions for example as miRNA sponge (Cheng et al., 2020; R. Li et al., 2018; J. Zhang et al., 2019).

1.4.1.1 Imprinted locus of Meg3

Meg3 is encoded in the ~1 Mb polycistronic *Dlk1-Dio3* imprinted region, which comprises three paternally expressed protein-coding genes, *Dlk1*, *Rtl1* and *Dio3*, and the non-coding RNAs *Meg3*, *Rtl1-antisense RNA*, the snoRNA cluster *Rian* as well as the miRNA cluster *mirg*, which are expressed from the maternal chromosome (da Rocha et al. 2008, see Figure 6). *Meg3* contains a well-defined TATA-containing promoter, which is missing for any other maternally expressed genes downstream of *Meg3* and therefore indicating that all maternally transcribed genes are transcribed from the *Meg3* promoter as one long RNA transcript, which is further processed afterwards (Tierling et al., 2006). Genomic imprinting is controlled *via* differentially methylated regions (DMR). Deletion studies found imprinting of the *Dlk1-Dio3* locus to be regulated by an intergenic DMR (IG-DMR) and a Meg3-DMR (Figure 6). The Meg3-DMR starts about 1.5 kb upstream of the *Meg3* gene and overlaps with the first exon and partially with the first intron (Zhu et al., 2019). The IG-DMR is ~ 13 kb upstream of the *Meg3* gene (Paulsen et al., 2001).

Lou and colleagues found a proximal enhancer 10 kb upstream of *Meg3* locus. The transcription factor ZFP281 binds to the enhancer and recruits AFF3, a component of the RNA PolII elongation complex, which starts the transcription from the *Meg3* locus on the maternal chromosome. On the paternal chromosome, the AFF3 is arrested on the methylated IG-DMR, thereby inhibiting the genesis of an active enhancer (Luo et al., 2016).
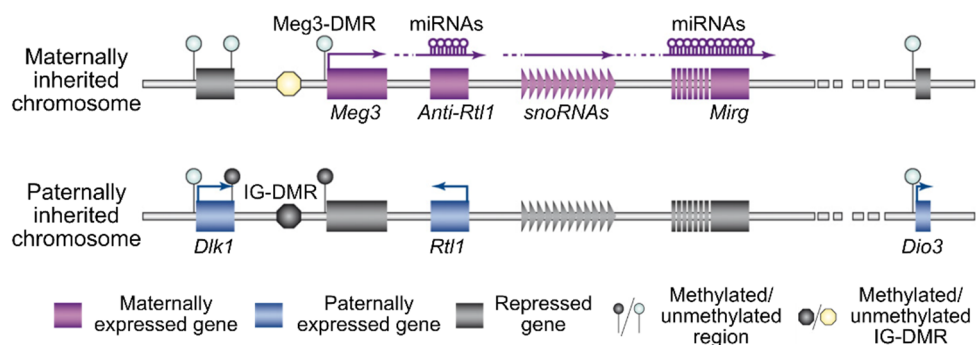
Figure 6 Schematic representation of the imprinted *Dlk1-Dio3* locus. Adapted from da Rocha et al. 2008.

Under normal or disease-related conditions, Meg3 expression is regulated by gene deletion, hypermethylation of its promoter or of the IG-DMR (He et al., 2017). Moreover, there is a cAMP responsive element in the proximal *Meg3* promoter region, which stimulates promoter activity (Zhao et al., 2006).

1.4.1.2 Knockout models for Meg3

In both, humans and mice, loss of imprinting in this locus causes severe diseases, developmental defects and premature death (Georgiades et al., 2000; Handley & McBlane, 1993; Ioannides et al., 2014; Ogata & Kagami, 2016). Several knockout mouse models were generated in order to determine the role of Meg3 during development. In a first study, mouse lines having both copies from either the paternal or maternal chromosome 12, showed detrimental abnormalities leading finally to non-viability. Embryos with the copies only from the paternal chromosome die late in gestation and show costal cartilage defects and skeletal muscle maturation defects. Embryos with the maternal chromosome die perinatally and are growth-retarded (Georgiades et al., 2000).

Other *Meg3* knockout mutants were generated by a 10 kb deletion including exon 1-5 and the Meg3-DMR (Takahashi et al., 2009). Heterozygous mutant mice with the deficiency inherited from the mother, show normal physiques after birth but die within 4 weeks. Their growth rate

is decreased and histological analysis identified symptoms of severe hypoplastic pulmonary alveoli and hepatocellular necrosis. Most of the pups with the paternally inherited *Meg3* deficiency died within a few days after birth and only about ~ 25 % survived and grow up to fertile adults. Nevertheless, the surviving pups weigh significantly less and exhibit microplasia during the growth period. Surprisingly, homozygous knockout of *Meg3* exon 1-5 was not lethal and mutants developed normally. The birth weight was less, but lung and liver defects were not present. Expression level analysis of surrounding non-coding RNAs and Dlk1 and Dio3 revealed a downregulation of Rian, Mirg and the miRNAs and snoRNAs derived from these non-coding RNAs in maternal knockout mice. For paternal knockout mice, Rtl1 and Dlk1 repression are suggested to be responsible for neonatal lethality. In homozygous knockout mice, miRNA and snoRNA levels are restored. Based on these findings, it is proposed that the deletion of *Meg3* and the Meg3-DMR affects the expression of neighbouring genes in *cis*, and this may affect their regulatory properties on the other parental allele in *trans*.

In a similar approach, Zhou and colleagues created a *Meg3* knockout mouse line deleting exon 1-5 and additionally ~ 300 bp of the adjacent upstream promoter sequence (Zhou et al., 2010). Here, all pups carrying the paternal *Meg3* gene deletion appeared and grew up healthy. By contrast, maternal depletion was lethal: pups had similar body weight compared to wild type but the stomachs were empty and lungs were filled with water. Homozygous knockout was also lethal. In order to examine the time point of death, embryos were examined at day 18.5 of pregnancy. Embryos with all genotypes (paternal or maternal knockout, homozygous knockout) were alive, with only paternal knockout embryos showing less weight. These data indicate that paternal transmission of the *Meg3* deletion leads to growth retardation, whereas maternal transmission leads to perinatal death. Histological examinations showed dramatical skeletal muscle defects and silencing of downstream maternally expressed genes, resulting in activation of paternally expressed genes in the embryos.

Presented *Meg3* knockout mouse lines revealed important insights into the role of Meg3 during development. Moreover, important aspects concerning the regulation of the *Dlk1-Dio3* locus could be investigated using these *Meg3* knockout lines. However, they cannot be used to study the role of Meg3 during adolescence and adulthood because of early lethality of the animals. Therefore, region- and time point-specific knockdown approaches have to be used for addressing the role and functions of Meg3 at later time points in a specific context.

1.4.1.3 Function and signalling pathways of Meg3

Meg3 is expressed ubiquitously including the adrenal gland, placenta, testes, ovary, pancreas, spleen, mammary glands, and liver, with especially high abundance in the brain and the pituitary (Zhang et al., 2003). In the brain, Meg3 expression was almost exclusively found in neurons where it shows mainly nuclear localization (Reddy et al., 2017; Zhang et al., 2014).

The most abundant Meg3 variant is the 1.9 kb variant containing all exons 1-10 (Zhu et al., 2019). Meg3 became quite prominent as tumour suppressor as it has been repeatedly shown to be downregulated in various types of human cancers, such as non-functioning pituitary adenomas, neuroblastoma, hepatocellular cancers, gliomas and meningiomas (Zhang et al., 2010a; Zhou et al., 2012). Tumour suppressors inhibit tumour initiation and cell proliferation. In many studies, epigenetic modifications in form of hypermethylation of the IG-DMR and the Meg3-DMR were shown to be responsible for the downregulation of Meg3 (Astuti et al., 2005; Gejman et al., 2008; Kagami et al., 2010; Zhang et al., 2010a). Moreover, Meg3 has due to its conserved structures and sequence the potential to interact through secondary structures with protein complexes and sequester miRNAs (Mondal et al., 2015; Sherpa et al., 2018; Uroda et al., 2019; Zhang et al., 2010b).

<u>**P53 signalling**</u>

The tumour suppressor P53 is one of the most studied downstream factor of Meg3. P53 is a transcription factor that regulates cell processes like DNA repair, cell cycle arrest, and apoptosis during stressful or harmful events. Under normal conditions, P53 protein is present at low cellular levels. The E3 ubiquitin ligase MDM2 (murine double minute 2) ubiquitinylates P53, which is consequently degraded *via* the ubiquitin-proteasome pathway. Inhibition of MDM2, therefore, stabilizes P53 (Wasylishen & Lozano, 2016). Meg3 functions also as tumour suppressor *via* the increase of P53 levels and enhancing the P53 binding to its target promoters (Zhou et al., 2012; Zhu et al., 2015). Uroda and colleagues identified conserved structured domains containing two distal motifs that form pseudoknot structures, which are crucial for P53 stimulation (Uroda et al., 2019). Some studies describe that Meg3 reduces MDM2 levels thereby preventing ubiquitination of P53 and elevating its levels (Ali et al., 2019; Lyu et al., 2017; Shi et al., 2018; Zhou et al., 2007). Consequently, in cancer and other diseases, decreased Meg3 goes along with higher MDM2 and less or no P53 levels. Next to this, P53-independent Meg3 effects were observed, which were mediated for example *via* the MDM2/retinoblastoma tumour suppressor signalling pathways (Lyu et al., 2017; Yap et al., 1999; Zhou et al., 2007). Interestingly

and based on newest microscopy techniques and computational analysis, a recent study claims that Meg3 does not disrupt P53/MDM2 binding, which challenges the long-lasting belief of the directly linked regulation of Meg3/MDM2/P53 and supports the idea of alternative ways mediating the effect of Meg3. Nevertheless, a co-regulation of Meg3/MDM2/P53 has been described in many types of diseases like osteosarcoma, leukemia, neuroglioma, breast adenocarcinoma, hepatoma and stroke mediated ischemic neuronal death (Ali et al., 2019; Lyu et al., 2017; Shi et al., 2018; Yan et al., 2016; Zhou et al., 2007).

PRC2

A subset of lncRNAs regulates gene expression by the interaction with chromatin and chromatin modifying enzymes in a *cis-* or *trans*-regulatory mode. Meg3 was found to bind the polycomb repressive complex 2 (PRC2) that mediates methylation of H3K27, an indicator for closed and inactive chromatin. EZH2 is the catalytic subunit of the multicomponent enzyme complex (Laugesen et al., 2019). Mondal and colleague found the Meg3 directly interacts with EZH2 and fine-mapped probable interaction points in the human Meg3 lncRNA. They further could show that Meg3/EZH2 targets genes of the TGF-ß pathway *via* GA-rich sequences and through the formation of RNA-DNA triplex structures in a breast cancer cell line (Mondal et al., 2015). In addition, Meg3 and other *Dlk1-Dio3* locus imprinted lncRNAs were shown to interact with JARID2, an accessory component of PRC2 that stimulates the activity of EZH2, and crosslink it to EZH2 *in vivo*. The lncRNAs support the interaction of JARID2 with EZH2 and orchestrate the distribution and activity of PRC2 (Kaneko et al., 2014). High-throughput studies also confirmed Meg3/EZH2 binding in various tissues, e.g. brain, liver, spleen, intestine, muscle, and blood (Wang et al., 2018). Structural analysis of human Meg3 revealed a highly structured molecule, forming 50 double-strand helices and ~ 61 % of nucleotides form Watson-Crick or wobble base-pairs as well as internal loops, junctions, and bulges. The first 5' ~ 900 nt are highly conserved in sequence, structures and functional motifs over various species like human, mouse, rat, pig and orangutan. Moreover, structural analysis could confirm regions found by Mondal et al. 2015 to be important for the interaction with EZH2 (Sherpa et al., 2018). The interaction of Meg3 with the PRC2 plays an important role not only in epigenetic regulation and diseases (Iyer et al., 2017; Terashima et al., 2017) but also during neural differentiation, where Meg3 regulates its own imprinted locus. *Dlk1*, a paternally transcribed gene of imprinted *Dlk1-Dio3* locus, becomes imprinted during neuronal differentiation that involves upregulated gene transcription from the paternal chromosome whereas the maternal *Dlk1* remains silenced.

Maternally expressed Meg3 stays in *cis* and prevents maternal *Dlk1* expression through recruitment of EZH2 (Sanli et al., 2018).

miRNAs

Besides interactions with enzymes, Meg3 has been demonstrated to be a competitive endogenous RNA for various miRNAs (Moradi et al., 2018). Competitive endogenous RNAs contain miRNA response elements and bind miRNAs, thereby facilitating the translation of originally targeted mRNA and preventing their degradation. In order to provide an example, miR-93 is directly targeted by Meg3 in context of gliomas. Meg3 is significantly downregulated, whereas miR-93 levels are increased in glioma tissue. Overexpression of Meg3 suppresses not only cell proliferation but also decreases miR-93 levels. These findings together with luciferase-reporter assay indicate that miR-93 is a direct target of Meg3. Further manipulation studies revealed that miR-93 promotes glioma cell growth *via* the activation of the PI3K/AKT pathway. Meg3 represses the activation by reducing the membrane translocation of AKT (Zhang et al., 2017).

Summing up the above-mentioned mechanisms and examples, Meg3 indirectly influences gene expression *via* recruitment of the histone modifying complex PRC2 and the interaction of miRNAs. Therefore, it can be, at least partially, considered as part of the epitranscriptome, which similarly to epigenetics, but based on RNA molecules, modifies expression levels without altering underlying DNA sequences (Royer et al., 2019). Epitranscriptomics caused increasing sensation in the last years as its role in mental disorders and psychopathologies became obvious. Meg3 expression within the brain has also been found to be dysregulated in psychopathologies, but compared to cancer research, there is little knowledge about mechanisms and downstream signalling available.

1.4.1.4   The involvement of Meg3 in psychopathologies

Huntington's disease is a neurodegenerative disorder characterized by chorea, psychiatric problems and dementia. Several transcription factors, including the RE1 silencing transcription factor (REST), mediate the effect of the mutated Huntingtin, which is responsible for the aetiology of the disease. Johnson et al. found that Meg3 is downregulated in the brain of Huntington's disease patients. Moreover, they detected binding sites of REST within the transcription start site of *Meg3*. Whether there is a causal link between Huntington's disease-

related REST signalling and alterations in Meg3 expression has to be determined (Johnson, 2012). In another study, a mouse model and different cell lines were used to study Meg3 in context of Huntington's disease. Here, they found increased Meg3 levels in the mouse cortex that modulates the aggregate formation of mutated Huntingtin. Furthermore, interaction partners of Meg3 were enriched in biological processes that are known to be involved in Huntington's disease (Chanda et al., 2018). The findings of the two studies indicate region-specific dysregulation and an involvement of Meg3 in Huntington's disease.

In schizophrenia, Meg3 and five other lncRNAs were suggested to function as diagnostic biomarkers. They were highly upregulated in the blood cells of female schizophrenia patients (Fallah et al., 2019). An interesting study applied a rat model for AD to study the involvement of Meg3 in AD (Yi & Chen, 2019). Meg3 was significantly downregulated in the HPC of AD rats. Upregulation of Meg3 within the HPC improved cognitive functions like spatial learning and memory capability. It further prevented apoptosis and deposition of the AD-typical amyloid-beta, and led to an activation of the PI3K/AKT signalling pathway within the HPC. In summary, the study highlights the potential role of Meg3 in improving cognitive capacities in context of AD and implies the potential of Meg3 to function as a biomarker and therapeutic target. Further, Meg3 was also shown to modulate memory formation *via* PI3K/AKT signalling way (Tan et al., 2017). Tan and colleagues found increased Meg3 levels after long-term potentiation in primary cortical neurons. *In vivo*, they could confirm the upregulation of Meg3 2 h after associative learning during auditory fear conditioning, whereas it was downregulated 24 h post-training. Collectively, the data imply a dynamic regulation of Meg3 by neuronal activity. Further *in vitro* studies showed that Meg3 regulates AMPAR expression and trafficking, which is important for the induction and maintenance of long-term potentiation (LTP), by controlling the PTEN/PI3K/AKT signalling pathway. In more detail, activation by phosphorylation of the PI3K regulatory subunit P85 as well as the phosphorylation of AKT, a direct downstream target of PI3K, was observed after induction of LTP. Moreover, PTEN, a counteracting factor of PI3K/AKT signalling, was decreased, supporting the activation of the signalling pathway.

1.4.1.5   PTEN/PI3K/AKT signalling pathway

A regulatory pathway affected by Meg3 and involved in various brain functions has been reported to be the PI3K/AKT signalling pathway (Tan et al., 2017; Yi & Chen, 2019; L. Zhang et al., 2017). But which components belong to this signalling pathway? As mentioned above, the main players are the PI3K, AKT and its negative regulator PTEN. PI3K is a heterodimer composed of a regulatory (P85) and a catalytic subunit (P110). Upon activation by external stimuli *via* receptor tyrosine kinases or G-protein coupled receptors, PI3K phosphorylates phosphatidylinositol-4,5-bisphosphate (PIP2), thereby producing phosphatidylinositol-3,4,5-triphosphate (PIP3). PIP3 recruits inactive AKT and phosphoinositide-dependent protein kinase 1 (PDK1) to localize into the membrane. AKT, also known as protein kinase B, has three isoforms. AKT becomes activated by PDK1 that phosphorylates threonine 308 (Thr308), whereas serine 473 (Ser473) is primarily phosphorylated by the mammalian target of rapamycin complex 2 (mTORC2). Phosphorylation of Ser473 stabilizes Thr308 phosphorylation and is important for full activation. The lifetime of phosphorylated AKT is relatively short, as it shows activity 2 h post-stimulation. Once activated, AKT phosphorylates many different downstream substrates, cytoplasmic as well as nuclear, which become inactivated or activated by phosphorylation. PI3K/PIP3 signalling is primarily terminated by the PIP3 phosphatase PTEN (Franke 2008; Manning and Toker 2017) and activated AKT becomes inactivated by dephosphorylation by phosphatases like PP2A (Liao & Hung, 2010).

1.4.2   Serum and glucocorticoid inducible kinase 1

The serum and glucocorticoid inducible kinase 1 (*Sgk1*) is an immediate early gene (von Hertzen, 2005) that encodes a serine threonine kinase (Amato et al., 2009; Lang et al., 2010). It is regulated by cell stress including osmotic or isotonic cell shrinkage, and elevated levels of glucocorticoids and mineralocorticoids (Lang et al., 2006). Insulin, vasopressin, steroids and interleukin 2 have been shown to activate the enzyme (Amato et al., 2009). Amongst others, glucocorticoids and corticotropin releasing hormone lead to an upregulation of cerebral SGK1 (Lang et al., 2006, 2010). SGK1 becomes activated by mTORC2-mediated phosphorylation of Ser422 (García-Martínez & Alessi, 2008), which subsequently leads to phosphorylation of Thr256 by PDK1 (Biondi et al., 2001; Collins et al., 2003). The half-life of the SGK1 protein is approximately 30 min due to ubiquitination and subsequent degradation by the proteasome (Brickley et al., 2002). Considering that *Sgk1* is an early gene, the short mRNA half-life of approximately 20 min is explainable (Di Cristofano, 2017; Firestone et al., 2003).

SGK1 is part of the PI3K signalling pathway, where it shares functions with AKT, another kinase involved in the PI3K pathway. SGK1 is able to take over AKT function in case of AKT-repression or inhibition, and *vice versa* (Di Cristofano, 2017). Even if PI3K is inhibited, SGK1 can phosphorylate AKT substrates, which leads to an activation of mTORC1 (Castel et al., 2016; Di Cristofano, 2017). Nonetheless, downstream of activated PI3K signalling, SGK1 itself is involved in cellular transformation processes thereby being independent of AKT (Di Cristofano, 2017). In the context of learning processes, contextual fear conditioning and re-exposure to the context were previously shown to increase Sgk1 mRNA expression in the HPC (Lang et al., 2006; von Hertzen, 2005). Learning and memory formation are biochemical processes, which lead to LTP, in which glutamate receptors such as AMPARs are supposed to play a key role (Kullmann et al., 1996). SGK1 was shown to act on such glutamate receptors like AMPARs and kainite receptors and is therefore expected to intensify the excitatory effects of glutamate (Lang et al., 2006), which is favourable to LTP. Similarly, an equal rise in SGK1 protein levels is considered to play an important role in long-term memory formation (Ma et al 2006). This is in line with a study, in which wild-type SGK1 rats showed enhanced learning abilities, while inactive Sgk1 transfection led to defects in learning abilities like spatial learning, fear conditioning learning and novel object recognition learning (Lang et al., 2006). Additionally, transient transfection of inactive Sgk1 in neurons impaired fear retention of contextual fear conditioning (Lee et al., 2007).

1.5   Aims and outlines of the present study

Even in today's modern and innovative research societies, we still lack specific and effective treatment options for SAD patients. So far, cognitive-behavioural therapies in combination with unspecific pharmacological intervention result only in partial remission of symptoms, with a high percentage of non-responders or relapse. The SFC paradigm is a mouse model that enables us to study social fear and social avoidance as core symptoms of SAD. Using this model, our lab could already reveal an important role of the LS in social fear, but underlying molecular mechanisms of social fear and its extinction still need to be investigated.

Here, the regulation of RNAs, coding as well as non-coding, is of particular interest as RNA molecules convert external stimuli into protein-coding information or undertake a regulatory role on a pre- and posttranscriptional level contributing to long-lasting effects. For above-mentioned facts, I pursued this thesis with the following overall aims in focus:

a)   Identification of the effects of SFC on RNA expression within the septum

b)   In-depth characterization of selected RNA candidates (especially Meg3) regarding their temporal expression dynamics during SFC in high-resolution, downstream signalling, and brain region specificity in the context of social fear

c)   Characterization of the role of Meg3 in the regulation of social fear by selective and specific Meg3 knockdown within the septum

d)   Strengthening the role of the LS in social fear extinction by monitoring the local release of neurotransmitters during social fear extinction training using microdialysis

MATERIALS AND METHODS

2 Materials and Methods

2.1 Materials

Buffers and solutions

Table 1 Composition of buffers and their applications.

Buffer	Composition	Application
Binding buffer	20 mM HEPES-KOH pH 7.9, 10 mM KCl, 1 mM $CaCl_2$, 1 mM $MnCl_2$	CUT&RUN
Blocking buffer	20 mM HEPES pH 7.5, 150 mM NaCl, 0.5 mM Spermidine, 0.1 % BSA, 2 mM EDTA, protease inhibitor cocktail 1x	CUT&RUN
1x PBS (0.01 M)	10 mM Na_2HPO_4, 1.8 mM KH_2PO_4, 137 mM NaCl, 2.7 mM KCl; pH 7.4	Perfusion, IHC
NE (nuclear extraction) buffer	20 mM HEPES-KOH pH 7.9, 10 mM KCl, 0.5 mM Spermidine, 0.1 % TritonX-100, 20 % glycerol, protease inhibitor 1x	CUT&RUN
NIB (nuclear isolation) buffer	10 mM Tris, 10 mM NaCl, 3 mM MgCl2, 0.1 % Igepal, 0.1 % Tween, protease inhibitor cocktail 1x	FACS (ATAC-Seq)
Staining buffer ATAC-Seq	0.5 % BSA in 1x PBS	FACS (ATAC-Seq)
Sort buffer ATAC-Seq	1 % BSA, 1 mM EDTA in 1x PBS	FACS (ATAC-Seq, CUT&RUN)
Storing buffer ATAC-Seq	5 % BSA in 1x PBS	ATAC-Seq
1x TBS-T	10 mM Tris, 150 mM NaCl, 0.01 % Tween-20, pH 8	Western blot
Wash buffer	20 mM HEPES pH 7.5, 150 mM NaCl, 0.5 mM Spermidine, 0.1 % BSA, 2 mM EDTA, protease inhibitor 1x	CUT&RUN
5x SSC (saline-sodium citrate) buffer	750 mM NaCl, 75 mM $Na_3C_6H_5O_7$	RNAscope
2x Stop buffer	200 mM NaCl, 20 mM EDTA, 4 mM EGTA, 50 µg/ml RNase A, 40 µg/ml Glycogen, 10 pg/ml yeast spike-in DNA	CUT&RUN

Kits and ready-made solutions

Table 2 Kits and Ready-mode solutions.

Name	Manufacturer
NucleoSpin Gel and PCR Clean-up #740609	Macherey-Nagel GmbH & Co KG
NucleoSpin miRNA #740971	Macherey-Nagel GmbH & Co KG
Ovation SoLo RNA-Seq System, Mouse #0501-32	NuGEN Technologies
Protein Quantification Assay #740967	Macherey-Nagel GmbH & Co KG)
Restore Western Blot Stripping Buffer #21059	Thermo Fisher Scientific
RNAscope Multiplex Fluorescent V2 Assay	Advanced Cell Diagnostics

2.2   Animals and husbandry

Male CD1 were kept group-housed mice (Universitätsklinikum Regensburg, Regensburg, Germany, 8-12 weeks of age at the start of experiments) under standard laboratory conditions (12/12 h light/dark cycle, lights on at 07:00, 21 - 23 °C, 55 % humidity, food, and water *ad libitum*) in polycarbonate cages (16 x 22 x 14 cm) until described otherwise. Age and sex-matched CD1 mice were used as social stimuli in the SFC paradigm. All experimental procedures were performed between 08:00 and 12:00 in accordance with the Guide for the Care and Use of Laboratory Animals of the Government of Oberpfalz and the guidelines of the NIH.

2.3   Behavioural testing

2.3.1   Social fear conditioning

The SFC paradigm was performed as previously described (Toth et al., 2012). Briefly, the paradigm consists of three phases: the social fear acquisition, the social fear extinction training and the social fear recall. Three days prior to social fear acquisition, mice are single-housed into observation cages (transparent walls, 30 x 25 x 35 cm) for monitoring and videotaping the behaviour.

<u>Phase 1: social fear acquisition</u>

During social fear acquisition, the experimental mouse is transferred into a fear conditioning chamber (45 x 23 x 36 cm; transparent Perspex box with a stainless-steel grid floor, TSE Multiconditioning Systems GmbH, Bad Homburg, Germany). After a habituation period of 30 s, an empty wire mesh cage (7 x 7 x 6 cm) is put into the corner of the conditioning box and the mouse is allowed to freely explore the area and the empty cage. After 3 min, the empty cage

is exchanged by an identical cage containing an age and sex-matched unknown conspecific. In case of a conditioned mouse (SFC$^+$), the mouse receives an electric foot shock (0.7 mA, pulsed) as soon as it shows direct contact (sniffing) with the conspecific. The electric foot shock is applied until the mouse reached the most possible distance (~ 1 s). 2 min after the last shock, the mouse is removed and put back into its home cage, where an empty cage was meanwhile positioned for overnight. If only one shock was necessary to punish the mouse, 6 min without any contact have to pass before finishing the acquisition procedure. In case of an unconditioned mouse (SFC$^-$), no punishment occurs when the mouse gets into contact with the conspecific. Free exploration is allowed for 3 min.

Phase 2: social fear extinction training

The social fear extinction training is usually performed 24 h after social fear acquisition (in case of knockdown experiments using antisense LNA GapmeRs: 72 h after microinfusion). The empty wire mesh cage, which was presented overnight, is removed 30 min before the start of the extinction training. At first, the known empty cage is presented three times, each 3 min, with an inter-stimulus break of 3 min as well. Next, six different unfamiliar conspecifics are consecutively presented for 3 min, with 3 min breaks between the presentations. The cages are placed on the short wall of the home cage to provide the most possible distance within the home cage for the animal and the social stimuli. In this way, conscious approaches by the mouse towards the stimuli are observable.

Phase 3: social fear recall

During social fear recall, mice are again exposed to six different conspecifics in different wire mesh cages to determine whether the fear extinction memory was consolidated. Therefore, each conspecific is presented for 3 min with a 3 min inter-stimulus interval in the home cage.

2.3.2   Scoring of behaviours

In order to quantify the social fear levels and investigation times, 3 min interaction phases with the empty cages or conspecifics are screened for following behaviours:

- Direct contact: the mouse has physical contact and sniffs on the empty cage/cage containing the stimulus conspecific
- Exploration: the mouse shows exploratory behaviour (which is the default option in case none of the other behaviours is being exhibited)
- Freezing: the mouse stays in one corner, without any movements for at least 2 s and freezing towards the presented stimulus
- On the cage: the mouse is on the cage without showing direct interest/sniffing towards the presented stimulus
- Burying: the mouse buries bedding towards the present stimulus

Behavioural parameters were manually scored by an observer blind for treatments and investigation time was calculated by dividing the seconds showing direct contact by the total time of stimulus presentation (3 min).

Animals showing less than 30 % investigation levels of the first social stimulus during social fear extinction training were considered as successfully conditioned and used for further analysis. For dividing the mice into groups of successful extinction and unsuccessful extinction of social fear after the extinction training, the mean of the investigations levels for the fifth and sixth social stimuli was calculated. The threshold for unsuccessful extinction (unsuc) was set to 45 % for this mean. Animals with means > 45 % for the fifth and sixth stimuli were assigned to the successful extinction group (suc).

2.4   Surgical procedures

Mice received a subcutaneous injection of the antibiotic Baytril (Baxter, 10 mg/kg Enrofloxacin) and an intraperitoneal injection of the analgetic Beprenovet (Bayer, 0.05 mg/kg Buprenorphine) 30 min before the start of the surgery. All stereotaxic procedures were performed under isoflurane anaesthesia and semi-sterile conditions. For additional local anaesthesia, Lidocaine (Lidocainhydrochlorid 2 %, Bela-pharm) was applied. All coordinates used are based on the mouse brain atlas (Paxinos & Franklin, 2001).

2.4.1 Intracerebral microinfusions

Antisense LNA GapmeRs (custom designed, Qiagen, Table 3) were bilaterally microinfused using a 5 µl calibrated micropipette (VWR, Darmstadt, Germany, inner diameter of 0.3 mm), which was pulled to create a long narrow shank. A 1-mm scale corresponds to a volume of ~ 70 nl. In total, 280 nl per animal were infused slowly by pressure infusion into the lateral septum. Two different dorsoventral positions were microinfused per hemisphere to guarantee the distribution of the antisense LNA GapmeRs exclusively, but within the total septum. Therefore, after the infusion at the first position (from Bregma +0.3 mm anteroposterior, ±0.5 mm mediolateral and –3.4 mm dorsoventral axis), the micropipette was kept in place for 30 s to ensure adequate diffusion. At position 2 (from Bregma +0.3 mm anteroposterior, ±0.5 mm mediolateral, and –3.0 mm dorsoventral axis), diffusion time was increased to 5 min to ensure that no antisense LNA GapmeRs are pulled to other regions while removing the micropipette. The wound was sutured with sterile nylon material. Animals were single-housed and allowed to recover at least for 2 days before behavioural testing.

Table 3 Sequences for GapmeR and scrambled control antisense oligonucleotides.

Name of antisense LNA GapmeR	Sequence
Negative Control A	36-FAM/AACACGTCTATACGC
NR_027651.2_1	CACACGCAGTCAACAT
NR_027651.2_2	TTCAATCACTCCATC
NR_027651.2_3	GGAAGACTAGAGCTAA
NR_027651.2_5	36-FAM/AGTTAAGTGGTCAGAT

36-FAM: 3' 6-carboxyfluorescein

2.4.2 Implantation of microdialysis probes

A U-shaped microdialysis probe with a molecular cut-off of 10 kDa was implanted unilaterally into the LS (from Bregma + 0.5 mm anterioposterior, – 0.4 mm mediolateral and – 3.8 mm dorsoventral axis). The implant was anchored to two stainless screws using dental cement. Following surgery, animals were single-housed and allowed to recover for 48 h. After the behavioral experiments, animals were sacrificed and brains were removed and snap-frozen in pre-chilled N-methylbutane on dry ice. The placement of microdialysis probes and cannulas was verified on 40 µm thick Nissl-stained coronal cryo-sections. Only animals with correctly positioned probes were included for statistical analyses.

2.5   Tissue collection, perfusion and brain slicing

Mice subjected to SFC were sacrificed at particular time points after the last behavioural assessment (0.5/1.5/3/24 h). The brains were rapidly removed, flash frozen in pre-chilled N-methylbutane on dry ice and stored at − 80 °C. Frozen brains were sliced in 200 μm cryo-sections (Bregma 0.98 mm – 0.02) to obtain tissue micropunches from the septum, paraventricular nucleus, amygdala, dorsal and ventral HPC. These micropunches were flash frozen in liquid nitrogen and stored at − 80 °C until RNA and protein isolation. For RNAscope, 10 μm coronal cryo-section were mounted on Superfrost Plus slides (#J1800AMNZ, Thermo Fisher Scientific, Schwerte, Germany).

For immunofluorescence staining, perfused brains were used. Animals were anaesthetized using a mixture of ketamine (10 %, 1 ml/kg, Medistar Arzneimittel GmbH, Ascheberg, Germany; company dosis) and xylazine (2 %, 0.5 ml/kg, Serumwerk Bernburg AG, Bernburg, Germany) intraperitoneally administered. Transcardial perfusion was then performed using ice-cold 0.01 M phosphate buffered saline (1x PBS) and 1x PBS supplemented with 4 % paraformaldehyde (PFA, Sigma Aldrich, Schnelldorf, Germany, pH 7.4) at a speed of 16.5 ml/min for 3 min. Afterwards, brains were removed and postfixed for 24 h at 4 °C in 4 % PFA solution, and cryo-protected in 30 % sucrose in 1x PBS for 48 h. Afterwards, brains were rapidly frozen in 2-methyl butane (Sigma Aldrich) cooled on dry ice and stored at − 80 °C. Mouse brains were cut in 40 μm coronal cryo-sections.

2.6   Sequencing

2.6.1   Total RNA-Seq

For the total RNA-Seq approach, male CD1 mice at the age of 9 – 10 weeks were subjected to the SFC paradigm as described in 2.3.1 and sacrificed 90 min after the last behavioural assessment (for an overview see Figure 7). Three replicates were used per group. Brains were processed and total RNA was isolated (see 2.7) from the septum. Before starting with the library preparation, RNA quality control was performed using the Agilent 4200 TapeStation System (Agilent High Sensitivity RNA Screen Assay, Agilent Technologies, Santa Clara, California, USA). For the library preparation for next generation sequencing, only RNAs with an RNA integrity number > 7.4 were used.
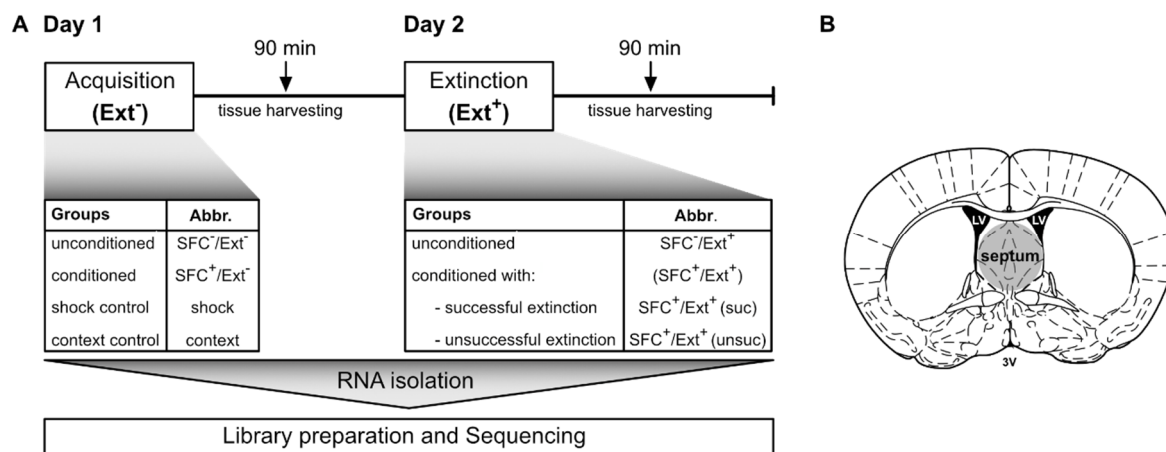
Figure 7 Schematic overview of samples used for Total RNA-Seq.

(A) Unconditioned (SFC⁻) and conditioned (SFC⁺) animals as well as animals of the shock and context control group (unpaired shocks; no shocks and social stimuli) were sacrificed 90 min after social fear acquisition training (Ext⁻). Another set of animal, which was subjected to social fear acquisition training (day 1) and the social fear extinction training (Ext⁺; day 2), were sacrificed 90 min after social fear extinction training. (B) RNA was isolated from tissue punches of the brain septum (grey). Abbr. = abbreviation; LV = lateral ventricle, 3V = third ventricle.

2.6.1.1 Library preparation

Libraries for next generation sequencing were prepared using the Ovation SoLo RNA-Seq System, Mouse (#0501-32, NuGEN Technologies, Leek, Netherlands). Libraries were prepared according to the manufacturer's protocol with an RNA starting concentration of 0.8 ng/µl.

Briefly, first strand primers were annealed to DNase-treated RNA and first strand cDNA synthesis was performed. Afterwards, cDNA was further processed including fragmentation and RNA degradation steps. Second strand synthesis was performed followed by end repair reactions, which ensure that the fragmented molecules are free of overhangs and contain 5' phosphate and 3' hydroxyl groups. In the next steps, the fragmented cDNA was ligated to barcoded adapters (Table 4). For adapter ligation purification Agentcourt RNAClean XP beads (#A63987, Beckman Coulter, Brea, USA) were used. Libraries were amplified by PCR reactions with 15 cycles. The optimal number of cycles was determined by qPCR in advance. After amplification and purification, the libraries were quantified with the Agilent 4200 TapeStation (High Sensitivity D1000 Screen Tape, #5067-5584, Agilent Technologies) before further processing. Here, the concentration of cDNA with a length between 180 -1000 bp was calculated. 10 ng of amplified cDNA was then used for insert dependent adaptor cleavage (InDA-C). InDA-C technology targets and depletes ribosomal RNA, which accounts ~ 80 % of total RNA. This step is necessary in order to ensure cost-effectiveness of sequencing and prevent off-target events that introduce bias. After InDA-C, the libraries were amplified and

purified. Final quantitative and qualitative assessment of the libraries using the Agilent 4200 TapeStation should reveal cDNA fragment peaks at a size between 300-350 bp (132 bp adaptors + X bp cDNA fragments). All libraries were pooled with equal concentrations (< 5 ng/µl).

Table 4 Sequences of barcodes used for total RNA-Seq.

Library name	Barcode sequence i7
LS1	CGCTACAT
LS2	AATCCAGC
LS3	CGTCTAAC
LS4	AACTCGGA
LS5	GTCGAGAA
LS6	ACAACAGC
LS7	ATGACAGG
LS8	GCACACAA
LS9	CTCCTAGT
LS10	TCTTCGAC
LS11	GACTACGA
LS12	ACTCCTAC
LS13	CTTCCTTC
LS14	ACCATCCT
LS15	CGTCCATT
LS16	AACTTGCC
LS17	GTACACCT
LS18	ACGAGAAC
LS19	CGACCTAA
LS20	TACATCGG

2.6.1.2   Sequencing with HiSeq3000

Total RNA-Seq was performed in the sequencer HiSeq3000 by the BSF, Vienna, Austria. Libraries were sequenced in a 150 bp paired-end mode. The first set, consisting of 16 libraries were pooled and distributed over three lanes (>310 million reads per lane), the second set with four libraries was sequenced in one lane. Custom R1 primers provided by the Ovation SoLo RNA-Seq system were used for sequencing.

2.6.1.3 Bioinformatical analysis

Bioinformatical analysis was performed by Dr Balagopal Pai and Mr Gerhard Lehmann from the Department of Biochemistry I, University of Regensburg, Germany.

After sequencing, raw data was downloaded from the server of the BSF facility. Fastq files were mapped to the Mus musculus genome (mm10 UCSC browser) using the HiSAT aligner (Kim et al., 2015). This step helps also to discover splice variants (Pertea et al., 2016). The assembler String Tie reconstructed and quantitated full-length transcripts for each gene locus (Pertea et al., 2015). The programme Ballgown was used to perform differential expression analysis based on FPKM (Fragments Per Kilobase Million) values.

Two other count-based strategies were performed since count-based differential expression analysis is more robust. For the first strategy, count data was calculated from the Ballgown data using an additional pipeline available, prepDE.PY. For the second strategy, the whole mapping was repeated using RNA STAR and the count data calculated using the HTseq pipeline. Both these count-based data were used to calculate differential expression of genes as well as transcripts. DESeq2 normalizes the raw read counts to the total size of each library and perform calculations on fold changes and significance based on p-value and adjusted p-value (giving the false discovery rates, FDR). Multiple comparisons were performed, especially with the focus on differences within the groups after social fear acquisition and after social fear extinction training.

2.6.2 FAC-sorting of neuronal nuclei

All steps of nuclei isolation for FACS were performed on ice or at 4 °C. Frozen micropunches from the mouse brain septum were thawed on ice and resuspended in 500 μl nuclear isolation buffer (NIB, for buffer see Table 1). Single cell separation was performed using a 21 G needle on a 1 ml syringe to shear the tissue through the needle 5 times and incubated for 10 min on ice. After centrifugation for 5 min at 500 g, supernatant was discarded and the pellet was resuspended in 500 μl staining buffer containing mouse anti-NeuN antibodies (1:1000, MAB377 EMB Millipore). The cells were incubated for 30 min at 4 °C, pelleted for 5 min at 500 g, and resuspended and incubated in 500 μl staining buffer with Alexa Fluor 488 goat anti-mouse antibodies (1:1000, #A11001, Thermo Fisher Scientific) overnight at 4 °C on a rotating platform. The next day, nuclei were pelleted and resuspended in 1 ml of sort buffer. 21 G needles were used for separating the cells and debris were removed by filtration using cell strainers (pore size 40, #93040, SPL lifesciences; Pocheon-si, Korea). Nuclei were transferred

into a FACS tube and stained with DAPI (1:1000). NeuN and DAPI positive cells were sorted using a BD FACSMelody cell sorter into 5 % BSA in PBS for ATAC-Seq and CUT&RUN.

2.6.3   ATAC-Seq and data analysis

FAC-sorted cells in 5 % BSA in PBS were pelleted for 20 min at 500 g at 4 °C. The pellet was resuspended in a mix of 12.5 µl illumina Tagmentation DNA buffer (#15027866, illumina, San Diego, USA), 1 µl illumina Tagmentation DNA enzyme 1 (transposase, #15027865, illumina) and 11.5 µl ddH$_2$O and incubated at 37 °C for 1 h. After the transposase reaction, DNA fragments were cleaned up. For proteinase digestion, 5 µl of Clean-up buffer, 2 µl of 5 % SDS and 2 µl of 20 mg/ml Protein kinase K (#3115828001, Roche, Mannheim, Germany) were added and incubated at 40 °C for 30 min. For 2x SPRI clean-up using Agentcourt AMPure XP beads (SPRI beads, Beckmann Coulter), 70 µl of room temperature (RT) pre-chilled SPRI beads were mixed with the sample and incubated at RT for 5 min. The mixture was transferred to a 96-well plate and put on a magnet for binding the beads and removing the supernatant. Still on the magnet, beads were three times washed with 100 µl freshly prepared 70 % ethanol. The plate was removed from the magnet and beads were dried at RT for 10 min. Beads were resuspended in 22 µl elution buffer and incubated at RT for 5 min. After binding beads for 5 min on the magnet, 21 µl of supernatant containing DNA fragments were transferred into a new well.

For library preparation, PCR1 was performed using a specific barcode for each sample (primer i5 and i7), which also has to be used for PCR2. PCR1 and PCR2 mixes are shown below (Table 5).

Table 5 Reaction mastermixes and cycler protocols for PCR1 and PCR2 for the library preparation for ATAC-Seq.

PCR1 reaction mix

DNA	18 µl
Primer1 i5	2 µl
Primer2 i7	2 µl
2x Kappa HiFi	22 µl
Total volume	44 µl

PCR1 Cycler protocol

98 °C	2 min	
98 °C	20 s	
63 °C	30 s	9 cycles
72 °C	1 min	
4 °C	∞	

PCR2 reaction mix

DNA	9 µl
Primer1 i5	1 µl
Primer2 i7	1 µl
2x Kappa HiFi	11 µl
Total volume	22 µl

PCR2 Cycler protocol

98 °C	2 min	
98 °C	20 s	
63 °C	30 s	6 cycles
72 °C	1 min	
4 °C	∞	

After PCR1 reaction, double size SPRI clean-up was performed. First, the volume was adjusted to 50 µl by adding 6 µl of elution buffer, then 0.5x SPRI beads (25 µl) were added and incubated for 5 min on RT. The supernatant was separated from beads by placing the tubes on a magnet for 4 min. The supernatant, containing smaller fragments was transferred to a new well. The plate was again placed on the magnet to ensure that there was no contamination with beads. After transferring the supernatant again to a new well, 1.8x SPRI beads were added (65 µl) and incubated for 4 min at RT. Placed on the magnet, beads were washed twice with freshly prepared 70 % ethanol. Beads were dried for 10 min at RT and resolved in 22 µl of elution buffer. After 4 min incubation at RT, the plate was placed on the magnet and 21 µl of supernatant was transferred into a new well. 9 µl of PCR1 eluate was used for PCR2 (Table 5). PCR2 product was mixed with 13 µl of elution buffer and 2x SPRI clean up was performed like mentioned above. The DNA concentration of the final libraries (eluted in 22 µl of elution buffer) was measured using Qubit. In order to ensure that open chromatin regions are enriched, qPCRs with primers against β-actin (forward primer: GCCATGTTAATGGGGTACT; reverse primer: CGGTGCTAAGAAGGCTGTTC) and α-crystalin A (forward primer: CTACCTCTCCCCACCTGTGA; reverse primer: GCCAAGGGACATCACTGTTT) were performed (sample was diluted 1:4). In case of enrichment, ΔC_T should be ≥3. Presence of cleaved fragments and size distribution were evaluated with the Agilent 4200 TapeStation. Ideally, profiles should look like the one shown in Figure 8.
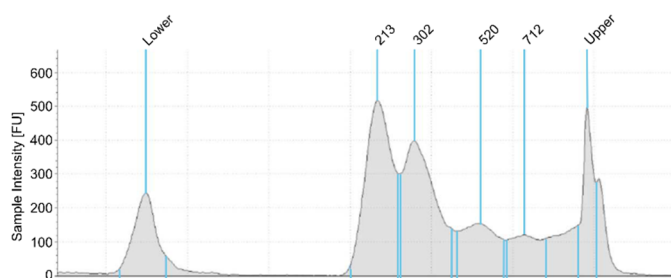

Figure 8 TapeStation profiles showing peaks for mono-, di- and tri-nucleosome prints.

For pooling the libraries, average DNA fragment size was calculated from fragment length varying from 180 to 800 bp. The final library pool had a concentration of 2 nM. Sequencing was performed using 50 bp paired-end mode and the NovaSeq (illumina). A sequencing depth of 20 million reads per sample was chosen.

ATAC-Seq data analysis was performed by Dr Igor Ulitsky, Weizmann Institute of Science, Rehovot, Israel. The analysis was performed as previously described in Rom et al., 2019. Three replicates were combined for all the analysis into five groups (SFC$^-$, SFC$^+$ (suc), SFC$^+$ (unsuc), SFC$^+$ control and SFC$^+$ Meg3 knockdown). Reads were aligned to the mouse genome assembly mm10. Each peak was calculated including signals from a surrounding region from −70 nt to +70 nt.

2.6.4   CUT&RUN

The CUT&RUN protocol was slightly modified from Hainer et al. 2019. Frozen brain tissue was resuspended in 1 ml nuclear extraction buffer (NE, buffers see Table 1) and mechanically sheared by pipetting up and down. In order to prepare single cells, a 21 G needle on a 1 ml syringe was used to shear the tissue through the needle 2 times. After an incubation time of 5 min on ice, extracted nuclei were pelleted for 3 min at 600 g. and the supernatant was discarded. Cells were resuspended in 700 µl of Sort buffer for FACS and filtered as described in 2.6.2. Nuclei were stained with DAPI (1:1000) and all DAPI positive cells were collected during FACS. In this case, FACS was necessary to remove debris, to ensure that enough nuclei are available and to adjust the amount of beads. Concanavalin A-coated beads (BP531, Bangs Laboratories, Fishers, Indiana, USA) were activated before adding nuclei. 150 µl of beads slurry per samples (50,000 collected cells) were transferred into 450 µl Binding buffer and the tube was placed on a magnetic stand to clear. The supernatant was discarded and beads were washed with 1 ml Binding buffer twice and finally resuspended in 300 µl Binding buffer. While gently vortexing the beads (< 1000 rpm), 600 µl suspension of nuclei were added and incubated for 10 min at RT on a 'nutator' (< 10 rpm). Tubes were placed on the magnetic stand and supernatant was discarded. The bead-bound nuclei were blocked with 1 ml cold Blocking buffer and incubated for 5 min at RT. After washing the beads with 1 ml Wash buffer, beads were dislodged from the wall by slowly adding 250 µl of the Wash buffer. Under gentle vortexing, further 250 µl of Wash buffer containing the antibody (rb α-H3K27me3 (C36B11) 1:100 in a total volume of 500 µl, mAB #9733, Cell Signaling Technologies, Danvers, USA; rb α-IgG 1:100, #2729, Cell Signaling Technologies) were added. Beads were incubated with primary antibody solution

overnight on a tube nutator at 4 °C. Afterwards, the beads solution was cleared on the magnetic stand and liquid was discarded.

The beads were washed twice with 1 ml Wash buffer and resuspended in a final volume of 250 µl. Under gentle vortexing, 1.25 µl of Protein A-MNase fusion protein (350 ng/ml in Wash buffer) were added to the beads. After an incubation time of 1 h at 4 °C on the tube nutator, beads were bound on a magnetic stand, supernatant was discarded and beads were washed twice with 1 ml cold Wash buffer. Finally, beads were resuspended in 150 µl Wash buffer while gently vortexing the tube. Tubes were placed on wet ice (ice mixed with NaCl and H_2O) to chill down to 0 °C for 5 min. Cleavage activity of the Protein A-MNase was activated by adding 3 µl 100 mM $CaCl_2$. After 5 min incubation at 0 °C wet ice, cleavage reaction was stopped by adding 150 µl 2x Stop buffer. The reaction mixture was incubated for 20 min at 37 °C to release CUT&RUN fragments from the insoluble nuclear chromatin. Samples were centrifuged at 16,000 g for 5 minutes. The supernatant containing digested chromatin was transferred into a new tube. DNA was extracted using the NucleoSpin Gel and PCR Clean-up kit (Macherey-Nagel GmbH & Co KG, Düren, Germany) according to the manufacturer's protocol. DNA was eluted with 20 µl elution buffer. Presence of cleaved fragments and size distribution were evaluated with the Agilent 4200 TapeStation.

Libraries were prepared following strictly the protocol from Janssens and Hernikoff, Version 3, 2019 (https://www.protocols.io/view/cut-amp-run-targeted-in-situ-genome-wide-profiling-zcpf2vn). For pooling the libraries, average DNA fragment size was calculated from fragment length varying from 180 to 800 bp. The final library pool had a concentration of 2 nM. Sequencing was performed using 50 bp paired-end mode and the NovaSeq (illumina). A sequencing depth of 15 million reads per sample was chosen.

CUT&RUN data analysis was performed by Dr Igor Ulitsky, Weizmann Institute of Science, Rehovot, Israel. Three replicates were combined for all the analysis into five groups (SFC⁻, SFC⁺ (suc), SFC⁺ (unsuc), SFC⁺ control and SFC⁺ Meg3 knockdown). Reads were aligned to the mouse genome assembly mm10 using Bowtie2 and peaks were called using MACS2. HOMER was used to quantify and compare the signals to gene bodies and across the ATAC-Seq peaks. P-values were computed using two-sided Wilcoxon-rank sum test.

2.7   Total RNA and protein extraction from one sample

Total RNA and protein were isolated from mouse septum using the NucleoSpin miRNA kit (#740971, Macherey-Nagel GmbH & Co KG) according to the manufacturer's protocol for animal tissues with minor adjustments.

Brain micropunches were homogenized in lysis buffer by pipetting and vortexing for 10 s. DNA was digested by rDNase for 20 min. RNA was eluted twice with 15 μl nuclease-free water. RNA concentrations were measured with the Nanodrop (NanoDrop Technologies Inc., Wilmington, Delaware, USA). If 260/280- and 260/230-quotients were 1.8 - 2, the sample was used for reverse transcription and PCR of cDNA.

Precipitated protein was flash frozen on dry ice and stored at – 20 °C. For further processing, the frozen protein pellet was slowly thawed on ice and washed with 500 μl 50 % ethanol for 1 min, 11,000 g. The protein pellet was dried on RT for > 15 min. 110 μl Protein Solving buffer with reducing agent (PSB-TCEP) was added and protein was resuspended by pipetting up and down and vortexing. Dissolved protein was incubated for 3 min at 95 °C for complete protein dissolving and denaturation. Once the sample was cooled down to RT, residual insolvable material was pelleted by centrifuging for 1 min, 11,000 g. Dissolved proteins were stored at – 20 °C.

2.8   Reverse transcription

500 ng of RNA was reversely transcribed into cDNA. The volume of reaction with the RNA was adjusted to a total volume of 13 μl with nuclease-free H_2O and mixed with 1 μl of Random Primers (Invitrogen, Lifetechnologies, Carlsbad, California, USA) and 1 mM of dNTP mix (Invitrogen). 13 μL ddH_2O were used as control to assure that there was no contamination of the mastermixes with genomic DNA. After primer annealing for 5 min at 65 °C, 4 μl of 5x Superscript IV buffer, 1 μl of 0.1 M dithiothreitol, and 1 μl of RNaseOUT (all from Invitrogen) were added and 2 μl of this mix were removed as a negative control to see whether there is DNA contamination. The rest of the mix was incubated with 1 μl of Superscript IV (Invitrogen) at 25 °C, 50 °C and 80 °C, each for 10 min. cDNA was stored at -20 °C.

2.9   PCR and electrophoretic separation on agarose gel

Polymerase chain reaction (PCR) was used to test self-designed primers for specificity. For the PCR, 12.5 μl of DreamTaq Green Mastermix (Thermo Fisher Scientific), 9.5 μl ddH_2O, 1 μl of

forward and 1 µl of reverse primer (2 µM/10 µM) were added to 1 µl of cDNA (1:10 diluted; or ddH$_2$O as negative control. PCR was performed using the ThermoCycler (Bio-Rad, München, Germany) using the following protocol (Table 6):

Table 6 Cycler program for PCR.

step1	95 °C	5 min		denaturation
	95 °C	30 s		
step2	60 °C	30 s	x40 cycles	amplification
	72 °C	1 min		
step3	72 °C	10 min		elongation
step4	4 °C	∞		cooling

Amplification products were electrophoretically separated on a 2.5 % agarose gel at 120 V for 1 h. Stained with RotiStain (Carl Roth GmbH + Co. KG, Karlsruhe, Germany), images were captured with ChemiDox XRS systems (Bio-Rad).

2.10   Quantitative real-time PCR

Real-time or quantitative PCR (qPCR) was carried out using the QuantiStudio 5 Real-time PCR System (Thermo Fisher Scientific) and the QuantiFast SYBR® Green PCR Kit (Qiagen, Hilden, Germany). SYBR Green intercalate in dsDNA and emits green light at 522 nm. A mastermix consisting of 5 µl of the SYBR Green, 2 µl of forward primer, 2 µl of reverse primer (2 µM) and 9 µl of ddH$_2$O per sample was prepared. 2 µl of 1:10 diluted cDNA was pipetted into one well of a 96-well plate and 18 µl of the prepared mastermix was added. In order to assure that there is no contamination of the mastermix, ddH2O was used instead of cDNA as a negative control. The 96-well plate was closed using a clear foil and centrifuged for at 1,000 g for 3 min. Samples were at least run in duplets using the protocol provided below (Table 7). Melt curves were generated by slowly heating up from 60 °C (20 s) to 95 °C (1 s), while constantly measuring the green fluorescence of the SYBR green. One single peak of the melting curve indicates primer specificity and amplification of one specific product. Gene expression was quantified relative to the expression of the housekeeping genes glyceraldehyde-3-phosphate dehydrogenase (GAPDH) or β-actin (Act). Primer efficiency for each primer pair was determined by serial dilution of cDNA using the Pfaffl method (Bustin et al., 2009; Pfaffl, 2001) (Table 8).

Table 7 Cycler program for qPCR.

step1	50 °C	2 min		UDG activation
step2	95 °C	2 min		Dual-look DNA Pol
step3	95 °C	3 s	x55 cycles	denaturation
	60 °C	30 s		annealing/extension

Table 8 Primer sequences for the detection and quantification of target genes *via* PCR or qPCR.

Name	Sequence 5'- 3'	Expected Length (bp)
m_AK133405_1F m_AK133405_1R	AGGAATCCCGCACCAAAGTT TACAACCAACCGTCCTGTGG	207
m_ATP5F1_1F m_ATP5F1_1R	CCTTGTGGCTTGAGAGATGGTA CAGCCCAAGACGCACTTTTC	115
m_ATP5F1_2F m_ATP5F1_2R	GGTTGTCATTCACCTTGTGGC TCCAAGCACATAAGGTCCTGT	193
ß-Act-F1 ß-Act-R1	CGTTGACATCCGTAAAGACC ATAGAGCCACCAATCCACAC	177
mouse crhr2 primer set 2 (metabion)	F: AGTCTGGGGACCTAGACCAC R: CTCTCCAACATCTCGTTGCT	220
m_sCRFR2_F m_sCRFR2_R	CGAAGAGCTGCTCCTGGAC CAGGCAGCGGATACTCCTTG	276
m_Efcc1_1F m_Efcc1_1R	TGTGTGAGTAGGTGTGACGAC AACCAAAGCTTGGTGCAAGG	486
m_EPS8_2F m_EPS8_2R	CAGCAGTGCAGGAAGAACAGAG ACCCACTGGAGCGGTTAGAC	70
GAPDH mmu fwd GAPDH mmu rev	AAGGGCTCATGACCACAGTC CAGGGATGATGTTCTGGGCA	111
m_Gm13157_1F m_Gm13157_1R	CGCCTAGTATTTGCGGAACC TCCAGGGTCTCTGTGGAGT	266
m_Gnas_1F m_Gnas_1R	CCTGCTGCTTCTAGGGAGAAAA TCTCACCATCGCTGTTGCTC	232
m_Hcrtr2_1F m_Hcrtr2_1R	TTGTGGCTCTCATCGGGAAC TTGGGTAAACTTCACCGCCC	465
m_Irak1_1F m_Irak1_1R	GAGACCCTTGCTGGTCAGAG GCTACACCCACCCACAGAGT	137
m_Lrrc14_1F m_Lrrc14_1R	GATCAACTGCTCAGCACCCT TGGCACTCAGTCAGCTCAAG	227

m_Map7_2F m_Map7_2R	GAGACACAGCATCTTGCAGC CTCTTGACAGGCCGGATGTT	382
m_Meg3_2F m_Meg3_2R	GTCGCGAAGGGATGAGAGAG GGCTGCTCTAGCCATTTCCA	289
Mdm2- mmu Mdm2- mmu (metabion)	F:CTGAAAAAGCCAAACTGGAA R: AAACAATGCTGCTGGAAGTC	192
m_Nlrp5-ps_2F m_Nlrp5-ps_2R	GGGACACCGCCCTGTTATATT ACTGTTGTTTTCTGCAGGAGT	93
m_Plin4_2F m_Plin4_2R	TCAGTGGAGGAGTGTGGTCA TCATGTCTGTCATCTGGAAGGC	304
m_Rxrb_2F m_Rxrb_2R	TCATGTCTTGGGCCACTCG GCATCTCTTTTCTCACCCCC	87
m_Rxrg_1F m_Rxrg_1R	GCCACAGCCTCTCAACACTAT GACCAGGGGAGCCACCAAAG	314
m_Sez6l_1F m_Sez6l_1R	ATGCATTGGAAGCAGAAGCG AATGTCTGAGGAGGTCCCGA	333
m_Sgk1_1F m_Sgk1_1R	TCTTTTGGGCTCTTTCCGGG TTGAGAGGGACTTGGCGGA	273
m_Siah1a_1F m_Siah1a_1R	AACTGACAAGCCATCTGCGT CCTTGACTGCTGCTCTGCTA	365
m_Sod3_1F m_Sod3_1R	CTGACAGGTGCAGAGAACCTC TGGCTGATGGTTGTACCCTG	275
m_Traf3_1F m_Traf3_1R	GCAACACAGGCTTGCTGGA GCGCTTGTAGTCACGGATCT	155
m_Trim32_1F m_Trim32_1R	ACTGACGTGGAAGGCGGGAA CGGGGCCAACAGAACCGATG	217
m_Trim32_3F m_Trim32_3R	AAAGCAGGACCTCTTGACGG TATGTTCCCGTCTGCCTTGG	183

2.11 RNAscope

RNAscope is an *in situ* hybridization method, which visualizes single RNA molecules. An RNAscope probe for Meg3 was specifically designed (Advanced Cell Diagnostics; San Francisco, California, USA; Mm-Meg3-O3: 20ZZ probe targeting 2501-3613 of NR_003633.3). This probe detects only uc007paq.3/uc029rxy.3/uc007pau.4 of UCSC genes and NCBI RefSeq NR_027651.2 and NR_003633.3, but does not detect transcript variant 3 of NCBI RefSeq NR_027652.1.

RNAscope was performed according to the manufacturer's protocol (RNAscope Multiplex Fluorescent V2 Assay, Advanced Cell Diagnostics) with minor modifications. Briefly, brains were fresh-frozen and stored at − 80 °C until further processing. Brains were then embedded in Tissue Tak and cut in 10 µm coronal section using a cryostat. Slices were mounted on Superfrost Plus slides and stored at − 80 °C for up to three months.

Thawed sections were post-fixed in 4 % PFA in 0.1 M PBS for 3 h at RT. After sequential dehydration in 50 % ethanol, 70 % ethanol and two times in 100 % ethanol, sections were dried for 5 min at RT and blood residues were removed by a hydrogen peroxidase step for 10 min at RT. Sections were permeabilized by Protease III treatment for 10 min and washed with PBS. The RNAsope probe targeting Meg3 (#Mm-Meg3-O3) was pre-heated to 40 °C and sections were completely covered with the probe and incubated at 40 °C for 2 h. After probe hybridization, sections were stored in 5x SSC buffer at RT overnight. The next day, sections were washed twice for 2 min in RNAscope Wash buffer and sequentially incubated with RNAscope Amp-I and Amp-II for 30 min each and Amp-III solution for 15 min, with two washing steps with Wash buffer in-between each treatment. Signal was developed using the TSA Plus fluorophore Cy5 (1:5000). Sections were mounted with Roti-Mount FluorCare DAPI. Images were captured using the Leica DM4 B.

If RNAscope was combined with immunohistochemical stainings, immunohistochemical stainings were performed after RNAscope signal development with TSA fluorophores. Slices were washed three times with dH$_2$O for 2 min at RT and blocked with 3 % BSA in PBST for 1 h at RT in the humidity control tray under slightly shaking conditions. Blocking solution was removed and the primary antibody solution (mouse anti-NeuN 1:100 in 3 % BSA in PBST) was added and incubated overnight at 4 °C. After three washing steps with PBST for 5 min at RT, secondary antibody solution (goat anti-mouse 1:500 in 3 % BSA in PBST) was added and incubated for 1 h at RT. After three final washing steps for 10 min, slices were air-dried and mounted with Roti-Mount FluorCare DAPI.

2.12   Protein quantification

Proteins were dissolved in PSB-TCEP buffer (see 2.7). The protein quantification assay (#740967 Macherey-Nagel GmbH & Co KG) was used to determine protein concentrations. For this purpose, a BSA dilution series (1/0.75/0.5/0.3/0.2/0 µg/µl) was prepared. 20 µl of each dilution and 5 µl of the samples were pipetted into one well of a 96-well plate and added up to a total volume of 60 µl with PSB. After adding 40 µl of the Quantification Reagent, the plate was incubated for 30 min at RT with gentle shaking. Light extinction was photometrically measured at 570 nm using FLUORstar OPTIMA (BMG labtech, Ortenberg, Germany).

2.13   Western blot analysis

15-30 µg of proteins isolated from the mouse brain septum were loaded onto Criterion™ TGX Stain-Free™ Precast Gels (Bio-Rad) for electrophoretic separation at 140 V for 1.5 h. A prestained protein ladder (Fermentas Inc., Glen Bumie, USA) was used as size marker. Proteins were transferred to the nitrocellulose membrane using Trans-Blot® Turbo™ Midi Nitrocellulose Transfer Packs (Bio-Rad). The gel and membrane were stacked in between layers of blotting papers and placed into the Semi-dry Trans-Blot® Turbo™ Transfer System (Bio-Rad). After blotting for 30 min (25 V, 1 A), the membrane was activated by 2.5 min of UV light exposure using the ChemiDoc XRS+ System (Bio-Rad). After blocking the membrane in Blocking solution (see Table 2) at RT for 1 h, it was incubated with the primary antibody at 4 °C overnight (Table 9). After three washing steps in Tris-buffered saline with 0.1 % Tween-20 (TBS-T, pH 7.6) for 10 min, the membrane was incubated with the secondary antibody for 1 h at RT. After three washing steps in TBS-T and one final washing step in TBS, bands were visualized *via* a chemiluminescent reaction with ECL western blot detection reagents (GE Healthcare, UK) or Super Signal West Dura Extended Duration Substrate (Thermo Fisher Scientific), and images were acquired with the ChemiDoc XRS+ System (Bio-Rad).

All images were analyzed with Image Lab software (Bio-Rad, Munich, Germany) and abundance of the target protein was normalized to total protein of the lane. For reuse of the blots, primary and secondary antibodies were removed by incubating the membrane in Restore Western Blot Stripping Buffer (#21059, Thermo Fisher Scientific) for 15 min at RT. After three TBS-T washing steps, the membrane was blocked in blocking solution for 30 min. The protocol for antibody staining was repeated when required with another primary antibody.

Table 9 List of antibodies used in Western blot.

Target	Size [kDa]	Host, clonality	Company	Blocking solution	Primary antibody dilution (o.n. 4 °C)	Secondary antibody dilution (1 h, RT)
AKT	60	rabbit, pAB	Cell Signaling Technologies #9272	5 % milk in TBS-T 1 h RT	1:1000 5 % milk in TBS-T	1:5000 TBS-T
p-AKT Ser473	60	rabbit, mAB D25E6	Cell Signaling Technologies #4060	5 % milk in TBS-T 1 h RT	1:1000 5 % BSA in TBS-T	1:5000 5 % milk in TBS-T
p-ATK Thr308	60	rabbit, mAB D9E	Cell Signaling Technologies #13038	5 % milk in TBS-T 1 h RT	1:1000 5 % milk in TBS-T	1:5000 5 % milk in TBS-T
MDM2-HRP	60/90	mouse, mAB SMP14	Santa Cruz SC-965	5 % milk in TBS-T 1 h RT	1:500 5 % milk in TBS-T	-
P53	53	mouse, mAB 1C12	Cell Signaling Technologies #2524	5 % milk in TBS-T 1 h RT	1:1000 5 % milk in TBS-T	1:2000 5 % milk in TBS-T
p-PI3 Kinase P85 (Tyr458)/ p55 (Tyr199)	60/85	rabbit, pAB	Cell Signaling Technologies #4228	5 % milk in TBS-T 1 h RT	1:1000 5 % BSA in TBS-T	1:5000 5 % milk in TBS-T 2 h RT
P85	85	rabbit, mAB 19H8	Cell Signaling Technologies #4257	5 % milk in TBS-T 1 h RT	1:1000 5 % BSA in TBS-T	1:5000 5 % milk in TBS-T
PTEN	54	rabbit, mAB D4.3	Cell Signaling Technologies #9188	5 % milk in TBS-T 1 h RT	1:1000 5 % BSA in TBS-T	1:5000 TBS-T
SGK1	48 (observed 65)	rabbit, pAB	Abcam ab59337	5 % milk in TBS-T 1 h RT	1:1000 5 % BSA in TBS-T	1:5000 TBS-T

mAB: monoclonal antibody; pAB: polyclonal AB; RT: room temperature; o.n.:over night.

2.14 Statistical analysis

Data were analysed using GraphPad Prism (version 8, GraphPad Software). Behavioural and molecular experiments were statistically analysed performing parametric one way (factor conditioning) or two-way (factors conditioning x time) analysis of variance (ANOVA), followed by Bonferroni post hoc correction if appropriate (other post hoc corrections are indicated in the corresponding figure legend). For non-parametric data, the Kruskal-Wallis ANOVA on ranks and the Dunn's test were applied (other post hoc corrections are indicated in the corresponding figure legend). To compare two groups, separate parametric t-tests or non-parametric Mann-Whitney U tests were performed. Statistical significance was accepted at $p \leq 0.05$. n represents the number of animals. As indicated in the figure legend, data are represented as mean $\pm$ standard error of the mean (SEM). Statistical analysis for normal distribution and equal variance was performed. However, for consistency, all data are represented as mean.

2.15 Experimental design

Experimental design I – RNA-Seq approach

In order to identify RNA molecules that are regulated in context of social fear, male CD1 mice were exposed to the SFC paradigm and brains were collected 90 min after the last behavioural assessment. Samples were taken after acquisition as well as after social fear extinction training and RNA isolated from the septum was used for RNA-Seq.

Experimental design II – Validation of differential RNA expression

To validate RNA-Seq data, SFC was performed and brains were collected at different time points (acquisition: 90 min, 3 h, 24 h; extinction: 30 min, 90 min, 3 h). RNA and proteins were isolated in parallel and used to quantify RNA expression *via* qPCR and, for certain candidates and downstream signalling factors, proteins levels *via* Western blot analysis.

Experimental design III – Characterization of lncRNA Meg3 in context of social fear

As Meg3 turned out to be dynamically regulated during SFC and in dependence of social fear extinction success, antisense LNA GapmeRs (0.1 nmol per animal) were locally microinfused into the septum in order to knockdown Meg3 (i) before social fear acquisition, (ii) before social fear extinction training and (iii) before extinction training combined with a social fear recall test 3 weeks after extinction training to test long-term effects of the knockdown. Regulation of the PI3K/AKT signalling pathway, which is potentially regulated by Meg3, was investigated with Western blot analyses. Following the RNAscope result of a nuclear localization of Meg3 within the septum in context of social fear, alterations on chromatin and histone modification level were assessed by ATAC-Seq and CUT&RUN for H3K27me3. Samples from SFC$^-$/Ext$^+$, SFC$^+$/Ext$^+$(suc) and SFC$^+$/Ext$^+$ (unsuc) were used for a general characterization of SFC and Meg3 knockdown and corresponding control samples for a direct link to Meg3 regulation. All samples were harvested 90 min after social fear extinction training.

Experimental design IV – Monitoring neurotransmitter release and effects of septum damage on social fear extinction

To monitor neurotransmitter release during social fear extinction, microdialysis probes were unilaterally implanted, while control mice underwent sham surgery. As microdialysis resulted in completely impaired social fear extinction, I aimed to test whether slight mechanic damage/lesions of the LS influence social fear extinction. Therefore, implantation of microdialysis probes or sham surgeries were performed as mentioned before, but the animals were tested in SFC without performing microdialysis itself.

RESULTS

3   Results

3.1   Total RNA-Seq

3.1.1   Sequencing approach I

To obtain an overview of regulated RNAs during the SFC protocol, I started with a total RNA-Seq approach. The brain septum was microdissected from mice that were exposed to SFC (Figure 9A). Three animals were conditioned by receiving 2 ± 0 electric foot shocks during social fear acquisition and sacrificed 90 min after social fear acquisition (SFC$^+$/Ext$^-$). Thus, shock control animals (n = 2) also received two shocks, which were not paired with the contact to the conspecific during the acquisition phase. In this way, changes in RNA expression caused by the shock itself can be detected. Mice of the context group (n = 2) were exposed to the context including the procedure of exchanging two empty cages without receiving any shocks. In this way, effects of the handling procedure during the acquisition can be assessed. Unconditioned animals were allowed to freely explore the presented conspecific without receiving electric foot shocks (SFC$^-$/Ext$^-$).

Additionally, three SFC$^-$ and three SFC$^+$ mice (two shocks during acquisition, day1) were exposed to social fear extinction training (SFC$^-$/Ext$^+$, SFC$^+$/Ext$^+$; day2). The investigation time during social fear extinction training of these animals is shown in Figure 9B. SFC$^-$/Ext$^+$ mice showed low investigation levels of the non-social stimuli, whereas investigation time increased when social stimuli were presented, indicating social motivation and that they were not socially fearful. SFC$^+$/Ext$^+$ mice investigated similarly the non-social stimuli, except of mouse #2 that has not investigated stimuli at all. When social stimuli were presented, all SFC$^+$/Ext$^+$ animals were socially fearful, as they did not investigate the first social stimulus. Investigation levels of mouse #5 increased with the number of presented social stimuli resulting in investigation levels comparable to SFC$^-$/Ext$^+$ mice at the end of the social fear extinction training. Animals #2 and #4 stayed fearful and did not investigate presented social stimuli during extinction training. These animals showed active movements in the home cage specifically avoiding the area, where the social stimulus was presented. Therefore, animals were considered to show strong and specific social avoidance, which could not be extinguished during social fear extinction training.

All animals were sacrificed 90 min after the last behavioural assessment and RNA isolated from the septum was used for library preparation followed by total RNA-Seq.
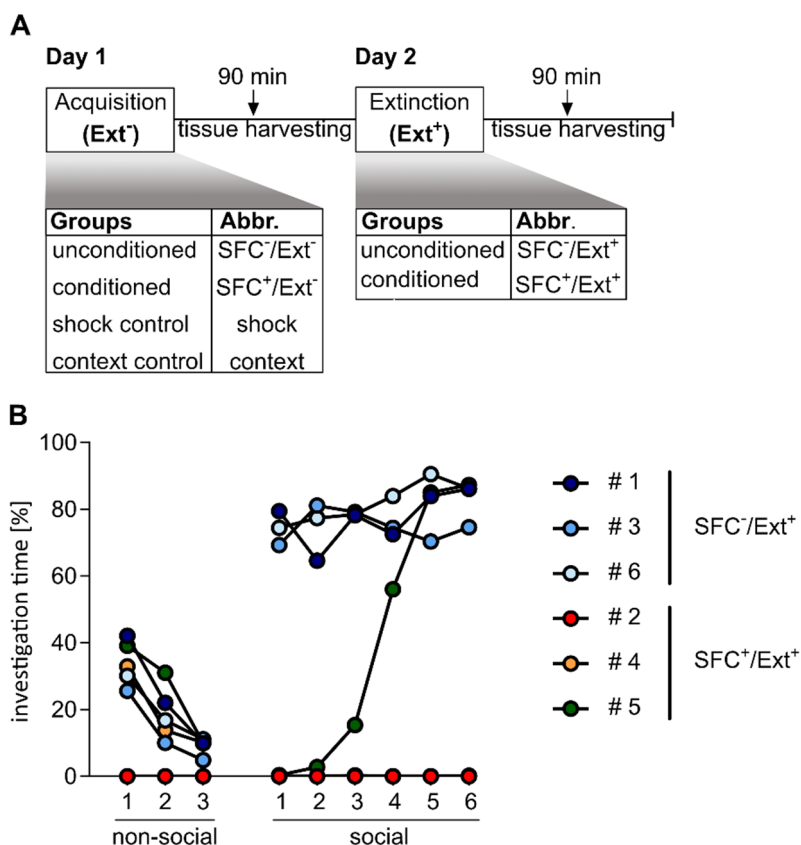
Figure 9 Groups and behavioural data of mice used for total RNA-Seq.

(A) Schematic overview of groups used for total RNA-Seq. (B) Investigation levels during social fear extinction training of SFC⁻/Ext⁺ and SFC⁺/Ext⁺ samples that were used for total RNA-Seq.

Two different mapping strategies were performed (using StringTie and STAR algorithms), both resulting on an average of 82 % alignment (excluding rRNAs) to the mouse genome (version mm10). Total number of mapped reads varied from 41.6 - 74.9 million reads per sample, which is a sufficient sequencing depth for the detection of low-expressed RNA candidates like some lncRNAs. Different strategies of analysis were also used to perform differential expression analysis, Ballgown based on FPKM values and DESeq2 for count-based analysis (for details see 2.6.1.3).

Data for all possible comparisons within the groups gained after social fear acquisition (including context and shock control groups), within the groups gained after extinction as well as the comparison of acquisition and extinction groups are available. However, in the subsequent sections, I will mainly focus on the comparison of SFC⁻ vs. SFC⁺ animals that were subjected social fear extinction training (SFC⁻/Ext⁺ vs. SFC⁺/Ext⁺), as this comparison reveals the most translational aspect. Interestingly, during the examination of the FPKM values I

observed that for some RNA candidates and their transcripts, FPKM values varied drastically within the SFC$^+$/Ext$^+$ group. Here, it was mainly animal #5 that revealed strongly different values. Looking closer on the behavioural experiment, it showed that animal #5 exhibited high investigation levels of the conspecific at the end of the social fear extinction training, and hence, had a successful extinction of social fear (Figure 9B, green), whereas animal #2 and #4 (Figure 9B, red and orange) stayed socially fearful. One of the lncRNAs that showed differential expression was Meg3 (Table 10). Reads from the sequencing were aligned to seven different RNA variants of Meg3. For four variants (uc007par.2, uc007pat.2, uc011ysb.1, uc007pav.2), FPKM values were similar within the behavioural triplets of the SFC$^-$/Ext$^+$ and SFC$^+$/Ext$^+$ groups. For the Meg3 variants uc007paq.3, uc029rxy.2, and uc007pau.3, animal #5 showed strikingly upregulated values compared to animal #2 and #4. Noteworthy, the differences within SFC$^+$/Ext$^+$ triplets only affect the variants that have the alternatively long exon 10 in common (compare also Figure 5). This alternative exon 10 increases the transcript length immensely (11460-12939 nt) compared to the other variants (728-1913 bp).

Table 10 FPKM values of Meg3 variants in samples with unsuccessful (#2, #4) and successful extinction (#5).

| | | | | FPKM values | | | | | |
| | | | | SFC$^-$/Ext$^+$ | | | SFC$^+$/Ext$^+$ | | |
	UCSC ID	# of exons	length	#1	#3	#6	#2	#4	#5
Meg3	uc007paq.3	9	11460	2.81	6.25	3.73	3.68	3.26	**26.88**
	uc029rxy.2	7	12939	16.22	18.70	22.46	19.64	13.14	**26.95**
	uc007pau.3	5	11472	89.91	95.58	96.45	68.19	64.05	**82.00**
	uc007par.2	10	1913	15.27	18.41	18.31	24.44	11.86	16.74
	uc007pat.2	8	1762	2.89	1.51	3.64	5.31	4.14	3.12
	uc011ysb.1	5	728	1.69	3.34	2.90	2.87	2.60	2.74
	uc007pav.2	5	870	18.29	19.25	22.20	24.66	17.29	26.03

So far, the observation of successfully and unsuccessfully social fear-extinguishing mice was accepted as natural variability in behaviour and neglected as important factor. As the differences in susceptibility and the ability to overcome social fear might be based on differential regulation of particular RNA candidates and, for sure, on altered signalling pathways, we decided to take a closer look at the factor "extinction success". Therefore, we performed additional RNA-Seq (Seq II) from animals exhibiting successful extinction (SFC$^+$/Ext$^+$ (suc)) compared to those that failed to show successful extinction (SFC$^+$/Ext$^+$ (unsuc)).

3.1.2 Sequencing approach II combined with approach I

In the second RNA-Seq approach, I wanted to address changes in RNA expression that are linked to the outcome of the social fear extinction training. Therefore, I added two mice that successfully extinguished social fear (animal #19, #20), and two mice that were still fearful at the end of their social fear extinction training (animal #17, #18). These samples were combined with sample #5 in the SFC$^+$/Ext$^+$ (suc) and sample #4 in the SFC$^+$/Ext$^+$ (unsuc) group (Figure 10A). For the differential expression analysis, samples from Seq I and Seq II were combined and re-evaluated. Sample #2 (SFC$^+$/Ext$^+$) was finally excluded as it has not even investigated the non-social stimuli, which could be interpreted as a general lack of motivation.
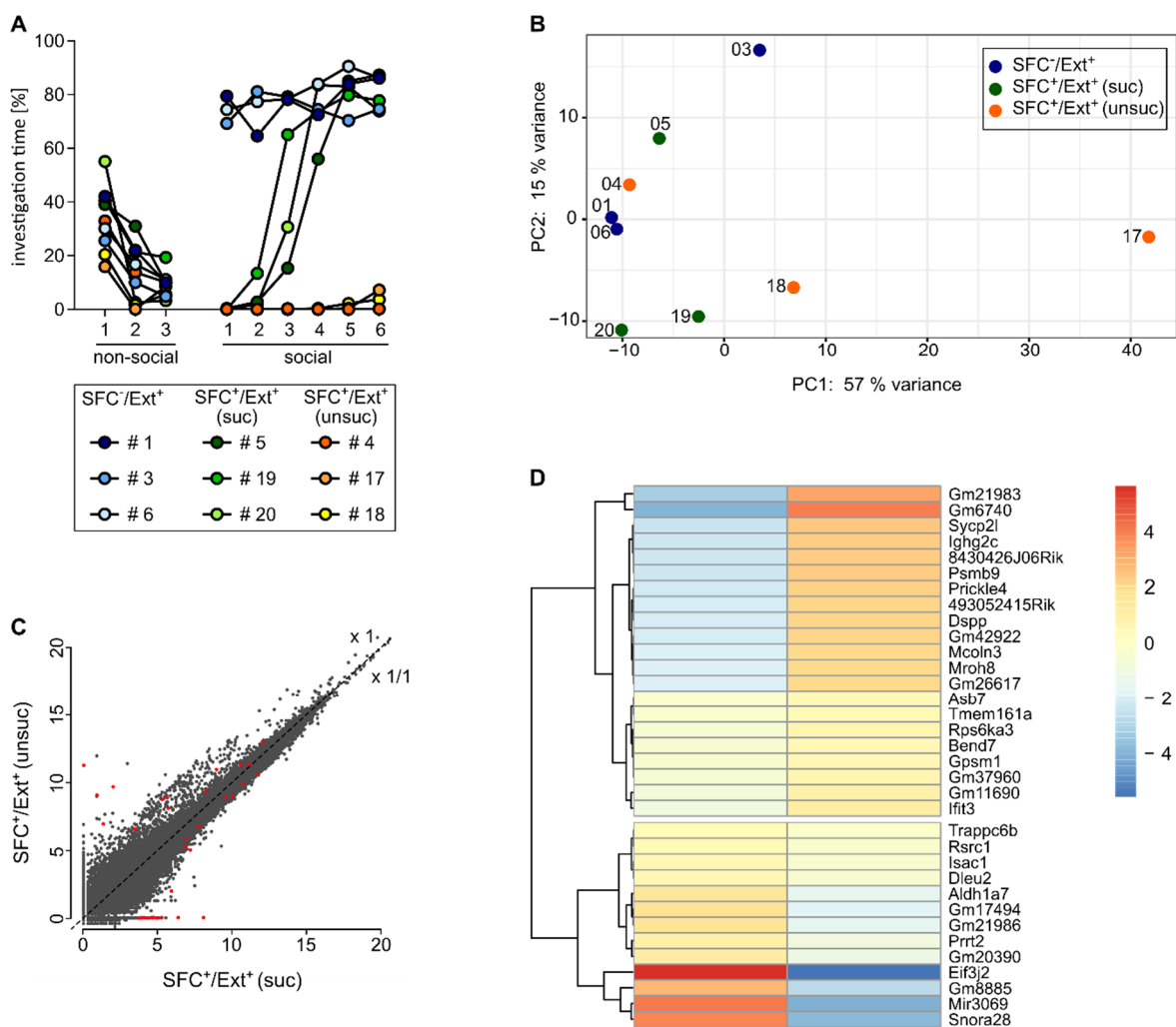

Figure 10 Gene-based alterations in RNA transcription in SFC$^+$/Ext$^+$ (suc) and SFC$^+$/Ext$^+$ (unsuc) mice.

(A) Septum samples were taken 90 min after extinction training from unconditioned and conditioned mice that showed successful or unsuccessful social fear extinction (SFC$^+$/Ext$^+$ (suc), and SFC$^+$/Ext$^+$ (unsuc)). (B) shows the PCA plot. (C) Scatter plot (log$_2$ mean of normalized counts) of top-regulated genes (red dots) listed in (D) the heatmap for the comparison of SFC$^+$/Ext$^+$ (suc) vs. SFC$^+$/Ext$^+$ (unsuc).

Focusing on the comparison of successful and unsuccessful social fear extinction, principal component analysis (PCA) revealed a high variation between, but also within the groups (Figure 10B). Principal component 1 explained 57 % of variance, component 2 resulted in 15 %. In total, 1,775 RNAs were found to be significantly regulated ($p < 0.05$), hereby 1,691 being changed for more than 25 %. Top 34 regulated RNAs and their distribution are shown in Figure 10C, D. Gene ontology analysis (Enrichr, Chen et al., 2013) of these 34 genes revealed that they are mainly associated with biological processes like protein maturation, regulation of SNARE complex assembly and DNA-template transcription in response to stress, metallo-sulfur cluster assembly and response to lipids.

As already observed in Seq I, there were some candidates for which the different variants of one RNA were differentially expressed. Focusing only on the comparison of SFC+/Ext+ (suc) vs. SFC+/Ext+ (unsuc) on a transcript-based levels, PCA revealed that principal component 1 explained 23 % of variance, and component 2 15 % (Figure 11A). 2,615 transcripts ($p < 0.05$ and at least 25 % fold change) were regulated and, out of these, 401 transcripts were altered with a significant adjusted $p_{(adj)}$-value (< 0.05). Regarding the regulation of Meg3 variants, combined analysis of Seq I and Seq II resulted in similar differential regulation of the longer Meg3 variants, as it was already indicated in Seq I. Meg3 variants uc027rxy.2 and uc007pau.3 are significantly different in SFC+/Ext+ (unsuc) vs. SFC+/Ext+ (suc), albeit in an opposing way. The other Meg3 variants were not significantly changed in their levels (Figure 11B).

B

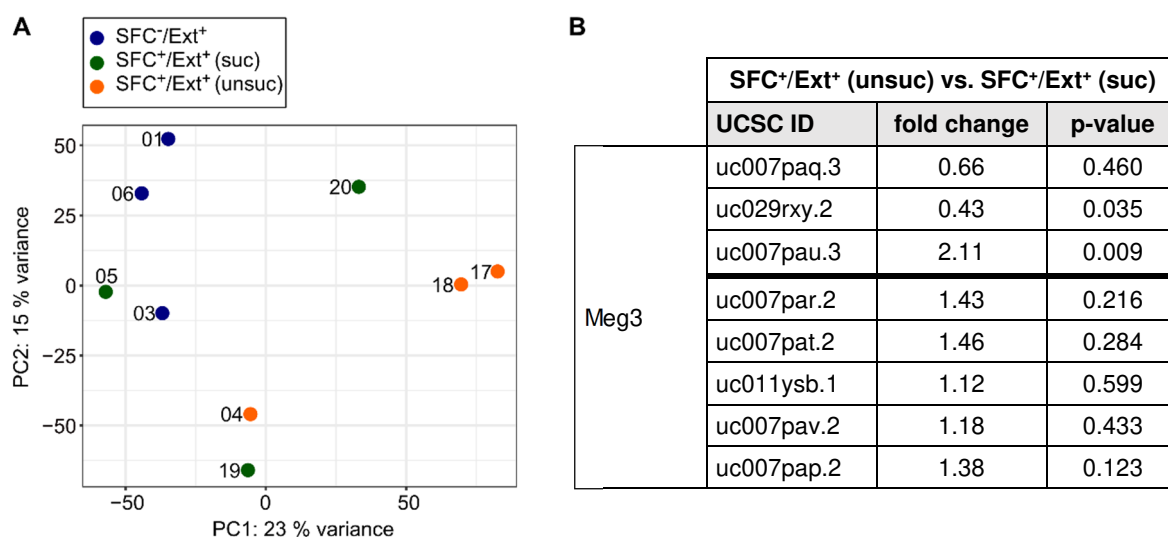| SFC+/Ext+ (unsuc) vs. SFC+/Ext+ (suc)			
	UCSC ID	fold change	p-value
Meg3	uc007paq.3	0.66	0.460
	uc029rxy.2	0.43	0.035
	uc007pau.3	2.11	0.009
	uc007par.2	1.43	0.216
	uc007pat.2	1.46	0.284
	uc011ysb.1	1.12	0.599
	uc007pav.2	1.18	0.433
	uc007pap.2	1.38	0.123

Figure 11 Transcript-based alterations in RNA transcription in SFC+/Ext+ (suc) and SFC+/Ext+ (unsuc) mice.

(A) shows the PCA plot. (B) Fold changes and p-values of Meg3 transcripts in SFC+/Ext+ (suc) vs. SFC+/Ext+ (unsuc) mice based on transcript-based analysis.

Other candidates, which were shown to be regulated by the RNA-Seq approaches, were chosen for subsequent qPCR validation (Table 11). After the validation of Meg3 expression and the expression of listed RNA candidates in Table 11, Meg3 showed a strong regulation depending on extinction success (see 3.2.1, Figure 12), representing an interesting candidate especially regarding the translational aspect to humans. For this reason, the main part of my thesis and subsequent experiments focused on the lncRNA Meg3. qPCR results of the other validated RNA candidates are shown in 3.6.

Table 11 Validated RNA candidates and their RNA-Seq data.

Gene-ID	name	fold change	p-value
SFC⁻/Ext vs. SFC⁺/Ext⁺			
Seq I: gene-based analysis			
Hcrtr2	Hypocretin (orexin) receptor 2	1.49	0.00009 (p_{adj} = 0.043)
Sgk1	Serum and glucocorticoid regulated kinase 1	0.65	0.00001 (p_{adj} = 0.008)
Sirt1	Sirtuin 1	1.14	0.039
Seq II: gene-based analysis			
Crfr2	Corticotropin releasing factor receptor 2	0.63	0.000358
Gm13157	Non-coding RNA	3.59	0.007
Irak1	Interleukin 1 receptor associated kinase 1	0.65	0.00009 (p_{adj} = 0.008)
Nlrp5-ps	NLR family, pyrin domain containing 5, pseudogene	2.24	0.052
Plin4	Perilipin 4	0.54	0.015

3.2   Meg3 – a lncRNA involved in social fear

In this section, I characterized the dynamic and spatial regulation of Meg3 expression during the SFC paradigm and addressed potential factors like learning processes and social interaction that might be important for Meg3 regulation. Additionally, Meg3 loss-of-function studies were performed to determine the role of Meg3 on behavioural phenotypes during SFC and the PI3K/AKT signalling pathway as potential component of Meg3 downstream signalling was examined.

3.2.1   Dynamic regulation of Meg3 expression levels during the SFC paradigm

The RNA-Seq approach revealed that the long Meg3 variants were differentially regulated after social fear extinction, here in an extinction success-dependent manner. To confirm RNA-Seq data, Meg3 expression levels should be validated 90 min after social fear extinction training by qPCR. Therefore, male SFC$^+$ mice were conditioned during social fear acquisition on day 1 receiving 2.2 ± 0.1 electric foot shocks. During the social fear extinction training on day 2, SFC$^-$ and SFC$^+$ mice showed similar investigation levels for three non-social stimuli (empty cages). SFC$^-$ mice showed high investigation levels (first stimulus 66.60 % ± 2.60 %) of the social stimuli throughout the extinction training indicating that they were not socially fearful. All SFC$^+$ mice showed significantly low investigation levels for the first social stimulus (0.46 % ± 2.99 %). Interestingly, most of SFC$^+$ mice showed a gradual extinction of their social fear, which is reflected by increasing investigation times over repeated presentations of social stimuli (Figure 12A). Here, investigation levels were not significantly different compared to SFC$^-$ from the fourth social stimulus on. These animals were assigned to the SFC$^+$/Ext$^+$ (suc) group after behaviour scoring. In contrast, a small subset of SFC$^+$ mice showed less social investigation overall and less than 45 % investigation time for the mean of the fifth and sixth stimuli. Therefore, they were assigned to the SFC$^+$/Ext$^+$ (unsuc) group. Of note, the number of shocks were similar for the SFC$^+$/Ext$^+$ (suc) and SFC$^+$/Ext$^+$ (unsuc) mice (2.2 ± 0.1 vs. 2.1 ± 0.2). RNA was isolated from the septum of animals that were sacrificed 90 min after social fear extinction training. Meg3 levels were determined *via* qPCR. SFC$^+$/Ext$^+$ (unsuc) mice had significantly decreased Meg3 levels (relative fold change 0.72 ± 0.062) compared to the SFC$^-$/Ext$^+$ and SFC$^+$/Ext$^+$ (suc) group (relative fold change 1.04 ± 0.071; Figure 12B) and Meg3 levels positively correlated with the mean of the fifth and sixth stimuli's investigation time (Figure 12C). Taken together, these findings reveal that Meg3 is differentially regulated 90 min after extinction training in animals with successful social fear extinction and those that fail to extinguish social fear, thereby confirming the RNA-Seq data.
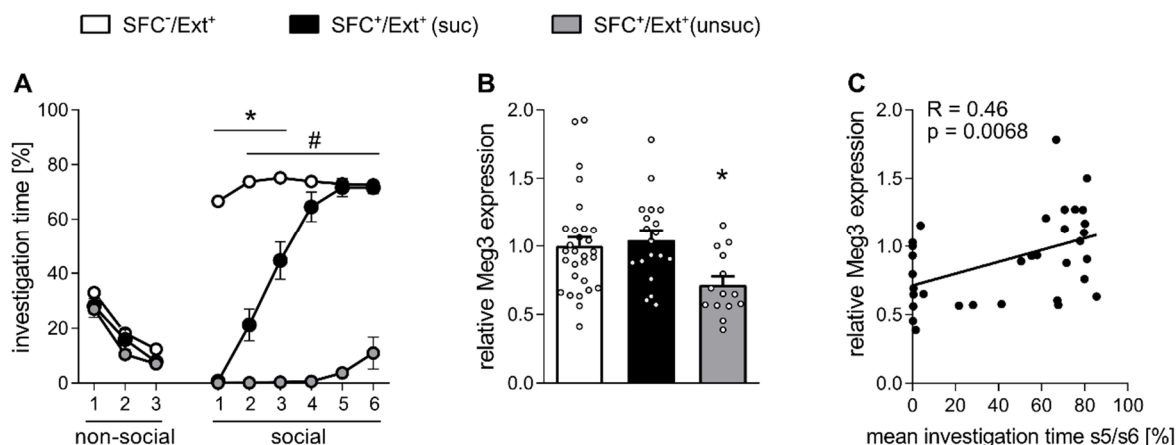
Figure 12 Meg3 expression 90 min after social fear extinction.

(A) SFC$^+$/Ext$^+$ (suc) mice successfully extinguished social fear and showed a comparable investigation time of the social stimuli to SFC$^-$ mice at the end of extinction training. In contrast, SFC$^+$/Ext$^+$ (unsuc) did not extinguish social fear and showed significantly less investigation levels even at the end of the extinction training compared to SFC$^-$/Ext$^+$ and SFC$^+$/Ext$^+$ (suc) (*$p < 0.05$ SFC$^-$/Ext$^+$ vs. SFC$^+$/Ext$^+$ (suc) and SFC$^+$/Ext$^+$ (unsuc); #$p < 0.05$ SFC$^+$/Ext$^+$ (unsuc) vs. SFC$^-$/Ext$^+$ and SFC$^+$/Ext$^+$ (suc)). (B) Meg3 levels remained comparable between SFC$^+$/Ext$^+$ (suc) and SFC$^{-/}$Ext$^+$, but were significantly decreased in SFC$^+$/Ext$^+$ (unsuc) mice ($p < 0.05$ vs. SFC$^+$/Ext$^+$ (suc) and vs. SFC$^{-/}$Ext$^+$). (C) Meg3 expression levels of all SFC$^+$ mice correlated with the mean of the fifth and sixth stimuli's investigation levels ($p = 0.0068$). Data represent (A) mean investigation time $\pm$ SEM, (B) mean fold change + SEM vs. SFC$^-$/Ext$^+$ and (C) relative Meg3 expression levels plotted against mean investigation time of the fifth and sixth stimuli. n(SFC$^-$) = 29, n(SFC$^+$/Ext$^+$ (suc)) = 19, n(SFC$^+$/Ext$^+$ (unsuc)) = 14.

Statistics:

Number of shocks during social fear acquisition

Mann-Whitney U tests: $p = 0.74$ SFC$^+$/Ext$^+$ (suc) vs. SFC$^+$/Ext$^+$ (unsuc)

Social fear extinction (Figure 12A)

Two way ANOVA: group effect: $F(2, 59) = 174.6$; $p < 0.0001$;

group x time: $F(16, 472) = 44.44$; $p < 0.0001$

Bonferroni's post hoc analysis:

$p < 0.05$ SFC$^-$/Ext$^+$ vs. SFC$^+$/Ext$^+$ (suc) and SFC$^+$/Ext$^+$ (unsuc) for social stimuli 1-3;

$p < 0.05$ SFC$^+$/Ext$^+$ (unsuc) vs. SFC$^-$/Ext$^+$ and SFC$^+$/Ext$^+$ (suc)

Meg3 levels (Figure 12B)

One way ANOVA on Ranks: $H = 9.569$; $DF = 2$; $p = 0.0084$

Dunn's test: $p = 0.0312$ SFC$^+$/Ext$^+$ (unsuc) vs. SFC$^-$/Ext$^+$ and $p = 0.0095$ SFC$^+$/Ext$^+$ (unsuc) vs. SFC$^+$/Ext$^+$ (suc)

Pearson Correlation (Figure 12C)
R = 0.4618; p = 0.0068

In order to get insights in the dynamic regulation of Meg3 during the SFC paradigm, RNA levels were additionally investigated 90 min, 3 h and 24 h after social fear acquisition and 3 h after social fear extinction training (Figure 13A-E). Context and shock groups were added for the 90 min and 3 h acquisition time point to evaluate whether the protocol procedure or physical pain (randomly given shocks, without association to a social stimulus) altered Meg3 levels. Neither 90 min nor 3 h after acquisition Meg3 was altered, whereas 24 h after social fear acquisition, SFC$^+$ mice revealed significantly decreased Meg3 levels (Figure 13D). Animals that were exposed to social fear extinction training were assigned to the successful or unsuccessful extinction group according to their behaviour as previously explained in 2.3.2 (data not shown). 3 h after extinction training, mice of the SFC$^+$/Ext$^+$ (unsuc) expressed significantly less Meg3 levels than SFC$^+$/Ext$^+$ (suc) (Figure 13E).

Regarding the overall Meg3 fold changes over time and behavioural testing (Figure 13F), a trend was found for Meg3 being decreased in SFC$^+$ mice over time after social fear acquisition. Meg3 data of the 90 min time point after extinction training, which were already shown in Figure 12B, were included in the timeline. After social fear extinction training, Meg3 levels of SFC$^+$/Ext$^+$ (unsuc) mice were significantly downregulated 90 min after extinction training compared to SFC$^+$/Ext$^+$ (suc). Using separate statistics, I compared the baseline level of Meg3 before the extinction training (24 h after acquisition; 0.71 ± 0.06) with levels after extinction training (Figure 13F), and found that SFC$^+$/Ext$^+$ (suc) mice showed significantly upregulated Meg3 levels 90 min (1.04 ± 0.07) and 3 h (1.09 ± 0.09) after social fear extinction training, and therefore, restored Meg3 levels comparable to SFC$^-$/Ext$^+$ mice. In contrast, Meg3 levels of SFC$^+$/Ext$^+$ (unsuc) mice (0.72 ± 0.06) were not different compared to the levels before the extinction training when measured 90 min after social fear extinction training. SFC$^+$/Ext$^+$ (unsuc) still displayed downregulated Meg3 levels even 3 h after social fear extinction training (0.76 ± 0.14; Figure 13F), indicating a long-lasting effect of social fear conditioning on Meg3 levels in case the extinction success is missing.

In summary, Meg3 was found to be dynamically regulated in conditioned animals during SFC with a strong negative correlation to social fear levels at the end of the extinction training. This

indicates an extinction success-dependent regulation of Meg3 and an inverse regulation regarding acquisition and extinction learning.
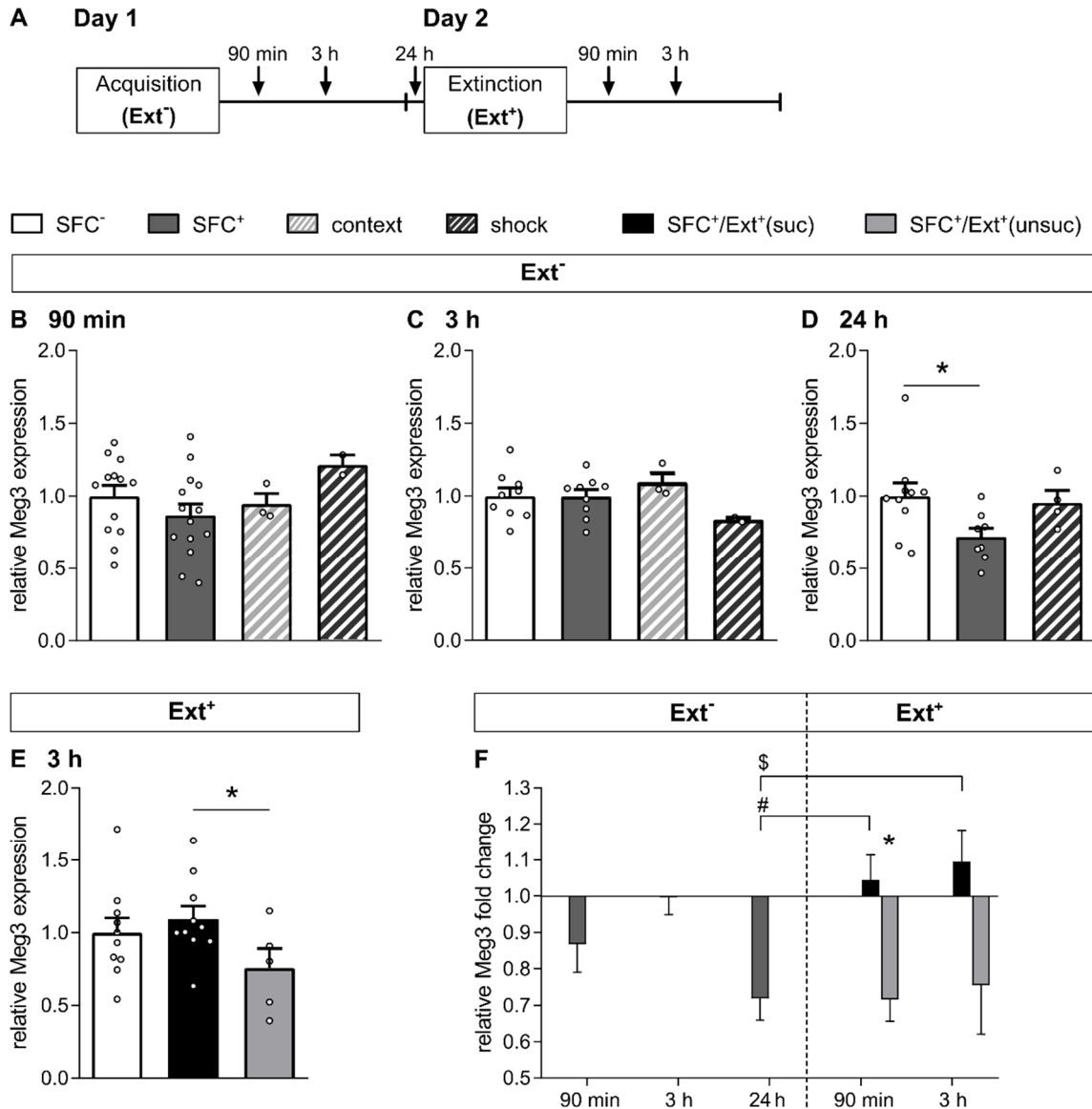

Figure 13 Dynamic Meg3 expression during the SFC paradigm.

(A) Schematic overview of time points, which were investigated for Meg3 levels. Meg3 was not differentially regulated (B) 90 min and (C) 3 h after social fear acquisition. (D) Nevertheless, SFC+ animals showed decreased levels 24 h after social fear acquisition (*p = 0.0274). (E) 3 h after social fear extinction, Meg3 levels were downregulated in the SFC+/Ext+ (unsuc) group (*p = 0.0498). (F) Regarding relative fold changes over time, Meg3 was regulated by trend after social fear acquisition (p = 0.061). 90 min after extinction training, SFC+/Ext+ (unsuc) showed significantly decreased levels of Meg3 compared to SFC+/Ext+ (suc) (*p < 0.05) and comparison to the baseline levels of Meg3 before extinction (24 h after social fear acquisition) revealed that SFC+/Ext+ (suc) successfully restored Meg3 levels 90 min (#p = 0.0102) and 3 h ($p < 0.05) after extinction training. Data represent mean fold change + SEM for (B)-(E). In (F), data represent mean fold change +/- SEM vs. the respective SFC- group. Ext-: n(SFC-) = 9-10; n(SFC+) = 8-9; n(context) = 3; n(shock) = 2-4; Ext+ 90 min/3 h: n(SFC-) = 29/10; n(SFC+/Ext+ (suc)) = 19/10; n(SFC+/Ext+ (unsuc)) = 14/5.

Statistics:

Meg3 levels 90 min after social fear acquisition (Figure 13B)
One way ANOVA: $F_{(3, 28)} = 1.239$; $p = 0.3143$
Meg3 levels 3 h after social fear acquisition (Figure 13C)
One way ANOVA: $F_{(3, 19)} = 1.250$; $p = 0.3197$
Meg3 levels 24 h after social fear acquisition (Figure 13D)
One way ANOVA: $F_{(2, 19)} = 3.395$; $p = 0.0549$ Separate statistics: t-test: $p = 0.0274$ SFC$^-$/Ext$^-$ vs. SFC$^+$/Ext$^-$
Meg3 levels 3 h after social fear extinction training (Figure 13E)
One way ANOVA: $F_{(2, 22)} = 2.134$; $p = 0.1422$ Separate statistics: t-test: $p = 0.0498$ SFC$^+$/Ext$^+$ (suc) vs. SFC$^+$/Ext$^+$ (unsuc)
Relative Meg3 fold change over time (Figure 13F)

After acquisition: one way ANOVA: $F_{(2, 28)} = 3.083$; $p = 0.0616$
 After extinction: two way ANOVA: group effect $F_{(1, 44)} = 13.28$; $p = 0.00007$;
     group x time: $F_{(1, 44)} = 0.003449$; $p = 0.9534$
     Bonferroni's post hoc analysis: $p < 0.05$ 90 min SFC$^+$/Ext$^+$ (suc) vs. SFC$^+$/Ext$^+$ (unsuc)
 24 h after acquisition compared with time points after extinction:
     One way ANOVA: $F_{(4, 51)} = 5.587$; $p = 0.0008$
     Bonferroni's post hoc analysis: $p < 0.05$ 24 h SFC$^+$ vs. 3 h SFC$^+$/Ext$^+$ (suc)
     Separate statistics: t-test: $p = 0.0102$ 24 h SFC$^+$ vs. 90 min SFC$^+$/Ext$^+$ (suc)

3.2.2 Specific regulation of Meg3 in the context of fear extinction learning

During SFC, learning and memory processes are always linked to a social component and associative learning processes. In order to determine possible factors, which might be responsible for the regulation of Meg3 within the brain septum, several control experiments were performed.

First, I tested whether social interaction *per se* is sufficient to induce Meg3 alterations. Hence, mice were single-housed and known objects (empty cages) that were already presented overnight in the home cage, were three times presented in the home cage during behavioural testing.

Afterwards, six different stimuli, either six different empty cages (non-social group) or six different conspecifics (social group), were presented consecutively. The number and duration of presentations followed the original social fear extinction protocol to keep the conditions comparable. Known empty cages were similarly investigated by all mice (Figure 14A). Both groups of mice investigated the first novel stimulus at a similar level (non-social 52.6 % ± 7.4 %, social 56.4 % ± 7.8%). The social group continued to investigate the conspecifics over the series of presentation whereas investigation time of the non-social objects declined significantly over time from the third stimulus on (Figure 14A). Nevertheless, Meg3 levels in the septum were not altered between the non-social and social group (Figure 14B).

In a second approach, I aimed to test whether Meg3 is activity-dependently regulated and whether Meg3 levels stay low in mice, which were not given the opportunity to extinguish social fear as they were confronted with empty cages (SFC$^+$ non-social) instead of social stimuli during social fear extinction training (Figure 14C). Data from SFC$^+$/Ext$^+$ (suc) and (unsuc) mice of chapter 3.2.1 (Figure 12), which underwent normal social fear extinction training, were used for the comparison with animals that investigated empty cages as stimuli instead of conspecifics during extinction training (in the experiments with non-social stimuli, some mice were also exposed to social stimuli (normal social fear extinction training) in order to be able to combine the new data of non-social extinction training with previous data from 3.2.1). The SFC$^+$ non-social group showed similar investigation levels for the first unknown stimulus like for the first presentation of the known empty cage, indicating that they were not fearful of the unknown empty cage *per se*. Over presentations, the investigation time decreased from 35.9 % ± 6.7 % to 16.6 % ± 5.8 %. From the third stimulus on, investigation times of the SFC$^+$ non-social and SFC$^+$/Ext$^+$ (unsuc) group were significantly different from the SFC$^+$/Ext$^+$ (suc) group. Regarding Meg3 levels 90 min after extinction training, SFC$^+$/Ext$^+$ (suc) mice had significantly elevated levels of Meg3 (1.04 ± 0.07) compared to SFC$^+$/Ext$^+$ (unsuc) (0.72 ± 0.06) and SFC$^+$ non-social (0.80 ± 0.04) (Figure 14D). Meg3 levels of the SFC$^-$ social and SFC$^-$ non-social group did not show significant changes (data not shown).

Results from the first two control experiments showed that extinction learning processes are necessary for Meg3 regulation. In the next step, I asked whether the social aspect during this type of learning is important. In order to dissect the social component from the associative learning processes during SFC, I exchanged the social stimulus with a white ball during the SFC protocol. Hence, conditioned animals received an electric foot shock when investigating the white ball. In this way, the timeframe and the type of learning stayed the same and I referred to it as operant fear conditioning (OFC).

Unconditioned mice (OFC⁻) showed high investigation levels for the first presented white ball stimulus (66.1 % ± 7.0 %), whereas subsequently a fast decline in investigation levels over the stimulus presentations was observed (last stimulus: 21.6 % ± 7.9 %; Figure 14E). Interestingly, three behavioural phenotypes were observed within the conditioned OFC group (OFC⁺). For a subset of animals fear conditioning against the white ball did not manifest fear (OFC⁺(not fearful)) as animals showed high investigation of the first present white ball stimulus (69.2 % ± 4.3 %). OFC⁺(fearful, suc) mice were fearful against the first stimulus but reached investigation levels comparable to OFC⁻ over stimulus presentations. A few animals showed a delay in fear extinction and started to approach stimuli only with the fifth and sixth stimuli (OFC⁺(fearful, unsuc)). Shock numbers were variable between non-fearful animals, OFC⁺(fearful, suc) and OFC⁺(fearful, unsuc) animals (3.5 ± 0.3, 1.8 ± 0.2, 2.5 ± 1.5 shocks according to mentioned order). The decline of investigation levels in OFC⁻ mice in combination with general lower investigation levels of OFC⁺ mice compared to SFC⁺ mice during the SFC paradigm complicate and prevent a clear definition of and a separation in successful and unsuccessful extinction in context of OFC. No difference in Meg3 levels was found between the groups 90 min after extinction training (Figure 14F).

Taken together, control experiments revealed that learning processes during extinction training are necessary to induce restoration of Meg3 levels within the septum of conditioned mice. Whether learning has to be linked to a social component could not be clarified and has to be further investigated.
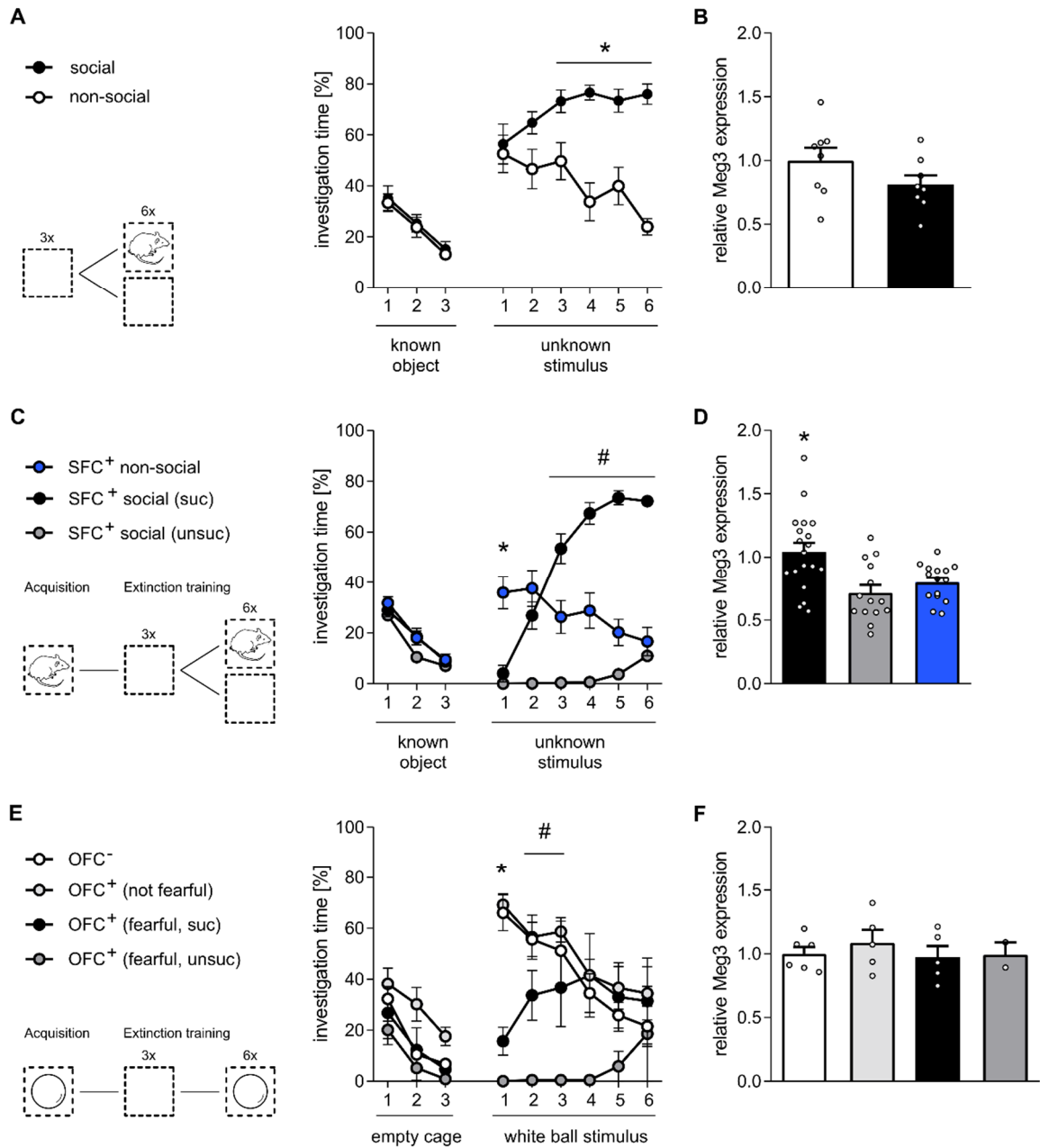
Figure 14 Control experiments for the identification of factors that regulate Meg3 within the septum.

(A) Mice show higher investigation times for social stimuli than for non-social stimuli (*p < 0.05). Repeated social interaction does not alter (B) Meg3 levels 90 min after the last stimulus presentation (n = 8 per group). (C) SFC+ non-social mice showed significantly more investigation of the first unknown stimulus than SFC+ social (suc) and (unsuc) (*p < 0.05). From the third stimulus on, SFC+ social (suc) mice explored presented objects longer than SFC+ social (unsuc) and SFC+ non-social mice (#p < 0.011) (n = 14 -19). (D) SFC+ non-social animals had similar Meg3 levels as SFC+ social (unsuc) animals 90 min after extinction training whereas SFC+ social (suc) had significantly higher levels (*p < 0.05 vs. SFC+ non-social and SFC+ social (suc)). (E) During OFC, conditioned animals showed either no fear (OFC+(not fearful)) or fear during the first white ball presentation, which was followed by successful or unsuccessful extinction (*p < 0.001 OFC+(fearful, suc) and OFC+(fearful, unsuc) vs. OFC- and OFC+(not fearful); # p < 0.01 OFC+(fearful, unsuc) vs. OFC-, OFC+(not fearful) and OFC+(fearful, suc)). n(OFC-) = 6, n(OFC+(not fearful) and OFC+(fearful, suc)) = 5; n(OFC+(fearful, unsuc)) = 2. (F) There was no difference in Meg3 levels between the groups. Data represent mean investigation levels ± SEM for A, C, E, and mean fold change + SEM vs. respective control group for B, D, F.

Statistics:

Social interaction and corresponding Meg3 levels (Figure 14A, B)

Two way ANOVA: group effect $F_{(1, 14)} = 28.27$; $p = 0.0001$;

group x time: $F_{(8, 112)} = 7.908$; $p < 0.0001$

Bonferroni's post hoc analysis: $p < 0.05$ social vs. non-social for unknown stimuli 3-6

t-test: $p = 0.1537$ non-social vs. social

Extinction behaviour and corresponding Meg3 levels (Figure 14C, D)

Two way ANOVA: group effect $F_{(2, 51)} = 40.58$; $p < 0.0001$;

group x time: $F_{(18, 402)} = 31.39$; $p < 0.0001$

Bonferroni's post hoc analysis: $p < 0.0007$ SFC[+] non-social vs. SFC[+]/Ext[+] (suc) and vs. SFC[+]/Ext[+] (unsuc) for the first unknown stimulus; $p < 0.011$ SFC[+]/Ext[+] (suc) vs. SFC[+] non-social and vs. SFC[+]/Ext[+] (unsuc) for unknown stimuli 3-6

One way ANOVA: $F_{(2, 45)} = 8.145$; $p = 0.001$

Bonferroni's post hoc analysis: $p < 0.05$ Meg3 levels SFC[+]/Ext[+] (suc) vs. SFC[+] non-social and vs. SFC[+]/Ext[+] (unsuc)

Operant fear conditioning and corresponding Meg3 levels (Figure 14E, F)

Two way ANOVA: group effect $F_{(3, 126)} = 16.18$; $p < 0.0001$;

group x time: $F_{(24, 126)} = 1.504$; $p < 0.0777$

Bonferroni's post hoc analysis: $p < 0.001$ OFC[+] (fearful, suc) and OFC[+] (fearful, unsuc) vs. OFC[-] and OFC[+] (not fearful); $p < 0.01$ OFC[+] (fearful, unsuc) vs. OFC[-], OFC[+] (not fearful) and OFC[+] (fearful, unsuc)

One way ANOVA: $F_{(3, 14)} = 0.3781$; $p = 0.7702$

3.2.3 Nuclear localization of Meg3 in neurons of the brain septal region

Meg3 is known to be mainly localized in the nucleus but there is also evidence of a cytoplasmic function for some cases (Reddy et al., 2017; Sanli et al., 2018; Tan et al., 2017). To get insights into potential action sites, I determined the localization of Meg3 in the septum in the context of social fear. Therefore, I established a RNAscope probe for unfixed septum slices that fluorescently labels single Meg3 RNA molecules. As shown in Figure 15A and B, Meg3 is

exclusively localized within the nucleus suggesting known Meg3 functions in regulating chromatin states. Co-staining with NeuN, a marker for neurons, revealed that Meg3 is mainly expressed in neurons (Figure 15C), indicating that social fear extinction behaviour is primarily affected by neuronal Meg3. Therefore, manipulations of Meg3 will in the first place result in neuronal changes and further experiments like ATAC-Seq (see 3.3) should address cell-type specific alterations in context of Meg3.
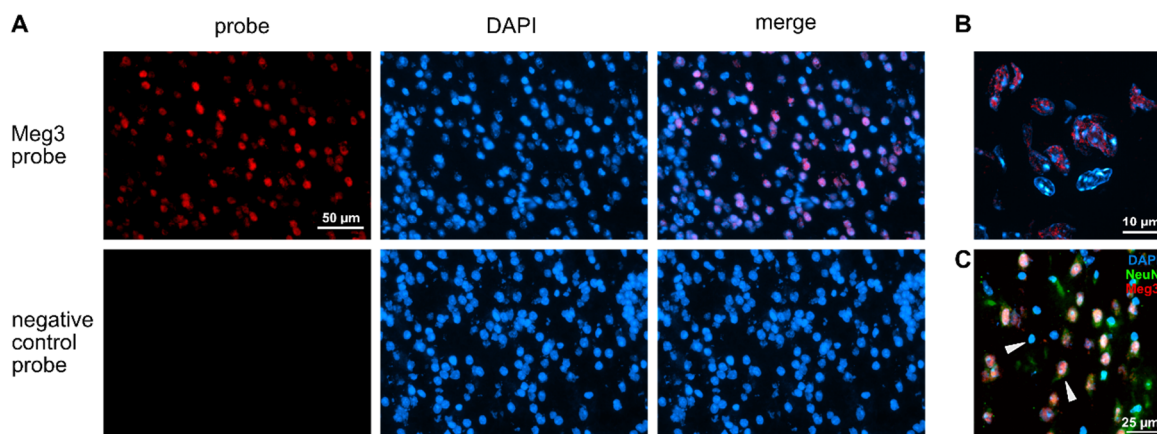

Figure 15 Nuclear localization of Meg3 within neurons of the septum.

(A) The upper panel shows a strong red signal for Meg3 RNA molecules, whereas no signal was detected for the negative control (lower panel). (B) High-resolution image (63x) shows nuclear localization of Meg3. (C) Co-staining of Meg3 with NeuN indicates mainly neuronal expression.

3.2.4 Meg3 loss-of-function studies

3.2.4.1 Establishment of specific LNA antisense GapmeRs for Meg3 variants

To address the effects of Meg3 levels on behaviour, I aimed to perform Meg3 knockdown experiments for different time points during SFC. For the knockdown of specific Meg3 variants, I designed four different LNA antisense GapmeRs and tested them with a concentration of 0.2 nmol/280 nl per animal. GapmeR1 and GapmeR2 showed no knockdown effect, whereas GapmeR3 and GapmeR5 decreased Meg3 level (Figure 16A). As GapmeR5 decreased Meg3 levels most efficiently, I performed knockdown with decreasing GapmeR5 concentrations (Figure 16B) and an incubation time of 72 h. Overall, a decline in the knockdown rate was observable with decreased concentrations. As a concentration of 0.1 nmol per animal showed the same effect as 0.2 nmol, the concentration of 0.1 nmol in 280 nl per animal was chosen for future experiments (Figure 16B). GapmeRs were labelled with fluorescein (FAM-label) to determine the distribution within the septum *via* fluorescence microscopy. I found that bilateral

infusions (from Bregma +0.3 mm anteroposterior, ±0.5 mm mediolateral and −3.4 mm and −3.0 mm dorsoventral axis) resulted in a GapmeR distribution within the whole septum without diffusing into other brain regions (Figure 16C). Knockdown by GapmeR5 was also confirmed with RNAscope. Here, almost no signal for Meg3 molecules could be detected within the septum of knockdown brains (lower panel Figure 16D).
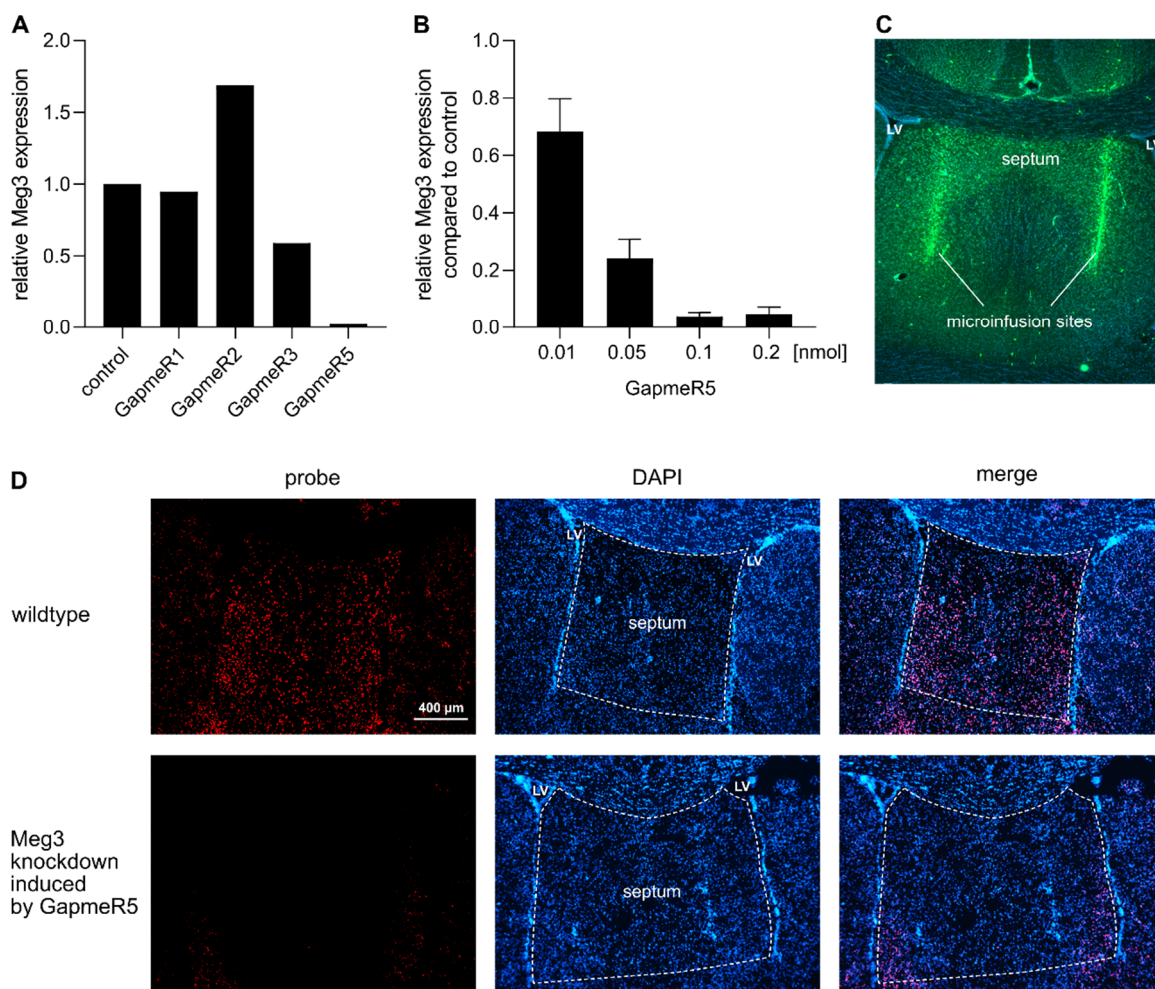

Figure 16 Establishment of antisense LNA GapmeRs for *in vivo* knockdown experiments.

(A) Differents antisense LNA GapmeRs for Meg3 knockdown were tested with GapmeR5 being the most efficient one. (B) Dose-response curves revealed 0.1 nmol in 280 nl per animal as the most efficient concentration for *in vivo* experiments within the septum. (C) FAM-labeling of GapmeRs (green) and (D) RNAscope for Meg3 (red) confirmed specific distribution of GapmeRs and Meg3 knockdown specifically within the mouse brain septum. LV: lateral ventricle, blue = DAPI, probe = specific RNAscope probe for Meg3.

3.2.4.2 Meg3 knockdown effects on social fear extinction

Based on the fact that Meg3 is downregulated in SFC$^+$ mice before the social fear extinction training and that it stays at low levels in SFC$^+$/Ext$^+$ (unsuc) (see 3.2.1), I asked the question whether downregulation of Meg3 before and during the social fear extinction training affects the extinction process towards a less successful extinction of social fear.

To address this, I microinfused antisense LNA GapmeRs, established in 3.2.4.1, and scrambled controls into the septum the day after social fear acquisition and tested social fear extinction behaviour 72 h after surgery (Figure 17A). For the SFC$^+$ control group, only animals with successful social fear extinction were included in the analysis to ensure that animals with normal/higher Meg3 levels were compared to Meg3 knockdown animals. Meg3 knockdown did not affect investigation behaviour of non-social stimuli at the beginning of the extinction training. SFC$^-$ control and SFC$^-$ knockdown animals showed similar interest in social stimuli, indicated by high investigation levels all over the presentation period (Figure 17B). SFC$^+$ control and SFC$^+$ knockdown mice received a similar number of shocks (1.86 ± 0.14 vs. 2.1 ± 0.18) during social fear acquisition and were fearful when the first social stimulus was presented during social fear extinction training. Over the presentations, both groups extinguished SFC-induced social fear, although the SFC$^+$ knockdown animals showed lower investigation at the end of the extinction training compared to SFC$^-$ knockdown (57.30 % ± 10.14 % vs. 83.33 % ± 1.38 %). SFC$^+$ knockdown mice investigated less than SFC$^+$ control mice (79.32 % ± 2.33 %; Figure 17B), however, statistical analysis could not reveal significant differences. Nevertheless, these data indicate that Meg3 knockdown shifts investigation times of conditioned animals towards a lower level and therefore, the experiment should be repeated to increase sample size. Efficient knockdown of Meg3 was confirmed by measuring Meg3 RNA levels with qPCR (Figure 17C) or by validating the microinfusion sites and GapmeR distribution in perfused brain slices by fluorescence microscopy (images not shown).
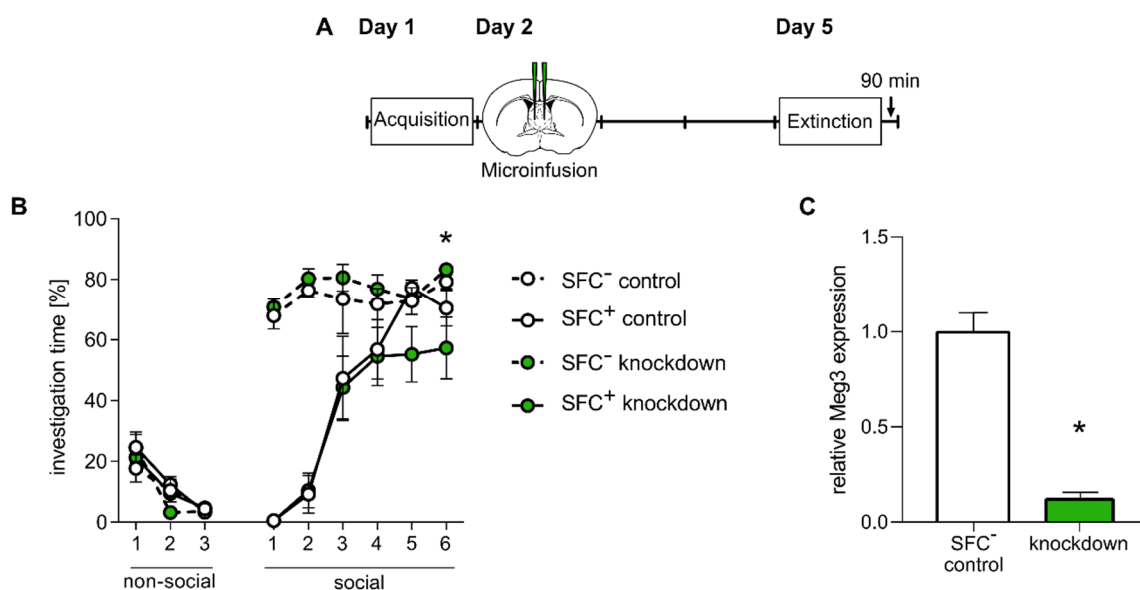
Figure 17 Meg3 knockdown before social fear extinction training.

(A) Schematic timeline for behavioural testing and microinfusion of antisense LNA GapmeRs targeting Meg3. (B) Meg3 knockdown had no effects on social preference as SFC⁻ control and SFC⁻ knockdown mice show similar and high investigation levels of the social stimuli. SFC⁺ control and SFC⁺ knockdown mice were socially fearful at the beginning of the extinction training and extinguished SFC-induced social fear over the extinction training. SFC⁺ knockdown mice were more fearful than SFC⁻ knockdown mice at the end of the extinction training ($*p < 0.05$) and showed a tendency to lower investigation levels at the end of the extinction training compared to SFC⁺ controls. (C) Knockdown animals revealed significantly less Meg3 levels than compared to SFC⁻ control 90 min after social fear extinction training ($*p < 0.0001$). Data represent (B) mean investigation time ± SEM and (C) mean fold change + SEM vs. SFC⁻ control. n(SFC⁻ control, SFC⁻ knockdown, SFC⁺ control) = 7; n(SFC⁺ knockdown) = 10.

Statistics:

Number of shocks during social fear acquisition for control and knockdown mice
t-test: p = 0.34
Meg3 knockdown before social fear extinction training (Figure 17B)
Two way ANOVA: group effect $F_{(3, 27)} = 16.35$; $p = 0.0001$; group x time: $F_{(24, 216)} = 9.171$; $p < 0.0001$ Bonferroni's post hoc analysis: $p < 0.05$ SFC⁻ knockdown vs. SFC⁺ knockdown for social stimulus 6
Meg3 levels 90 min after extinction training in knockdown animals (Figure 17C)
t-test: $p < 0.0001$ SFC⁻ control vs. knockdown animals

3.2.4.3   Meg3 knockdown effects on social fear acquisition

As Meg3 was regulated after social fear acquisition and by learning/memory processes during extinction training, I wanted to test whether social fear acquisition is also affected by Meg3 knockdown. Hence, antisense LNA GapmeRs were applied two days before social fear acquisition *via* microinfusions (Figure 18A) and social fear extinction training was performed 72 h after knockdown, comparable to the time line of the previous experiments in 3.2.4.2. For both groups, SFC$^+$ control and knockdown, two shocks on average were sufficient to induce social avoidance during social fear acquisition (SFC$^+$ control: 2.5 ± 0.22; SFC$^+$ knockdown: 2.29 ± 0.29; Figure 18B). Fear memory consolidation was likewise not affected as all SFC$^+$ control and SFC$^+$ knockdown animals showed fear and no investigation of the first social stimulus (Figure 18C). During the extinction training, investigation time increased for both SFC$^+$ groups, but similar to the specific knockdown prior to extinction training (Figure 17B), SFC$^+$ knockdown seemed to stay at lower investigation levels than SFC$^+$ control. SFC$^+$ knockdown were significantly different in investigation times for the fourth stimulus compared to its SFC$^-$ knockdown and to SFC$^-$ control for the fourth and fifth stimulus (Figure 18C). Efficient knockdown of Meg3 was confirmed by measuring Meg3 RNA levels with qPCR (Figure 18D) or by validating the microinfusion sites and GapmeR distribution in perfused brain slices (not shown).

In summary, Meg3 knockdown had no effect on social fear acquisition. SFC$^+$ knockdown animals seem to investigate social stimuli to a less extent than SFC$^+$ control mice, which is similar to observations made when knockdown was specifically induced affecting only the extinction behaviour (see 3.2.4.2). However, sample size should be further increased to achieve more powerful statistics.
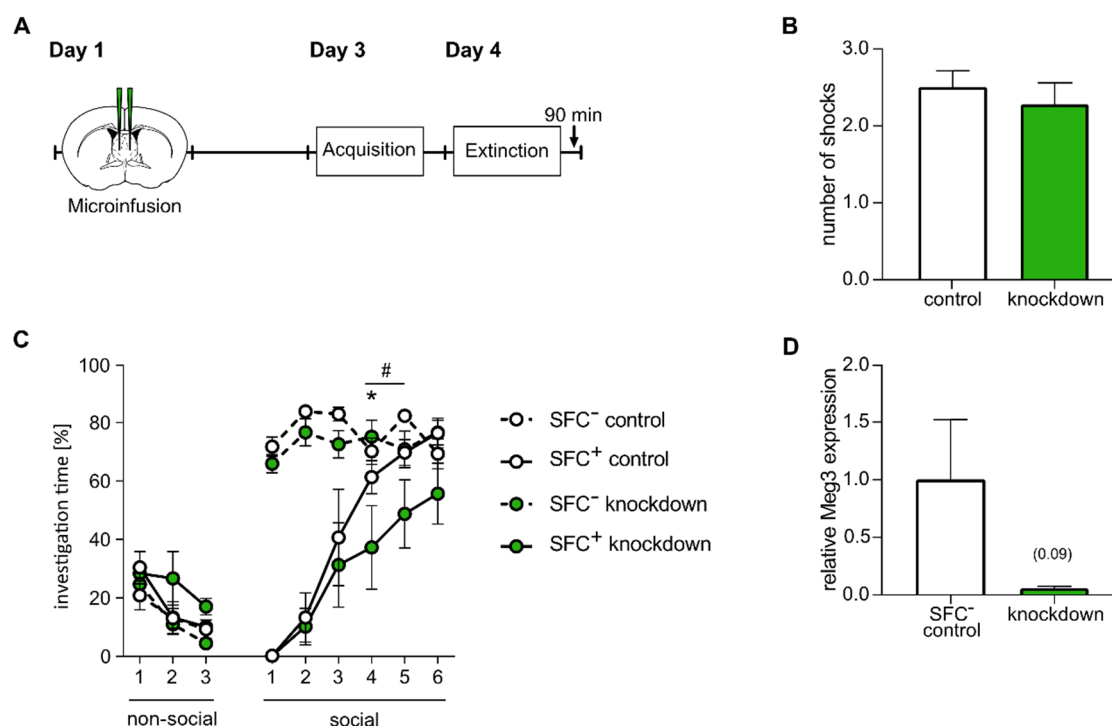
Figure 18 Meg3 knockdown before social fear acquisition.

(A) Schematic timeline for behavioural testing and microinfusion. (B) Meg3 knockdown had no effect on the number of electric foot shocks needed to induce social avoidance during social fear acquisition. (C) SFC⁻ control and SFC⁻ knockdown mice showed similar and high investigation levels of the social stimuli. SFC⁺ control and SFC⁺ knockdown mice were socially fearful at the beginning and extinguished SFC-induced social fear over the extinction training. SFC⁺ knockdown mice were more fearful than SFC⁻ knockdown until the fourth stimulus (*p < 0.01) and the SFC⁻ control until fifth stimulus (#p < 0.01). SFC⁺ knockdown mice generally seem to show lower investigation levels compared to SFC⁺ control mice. (D) Knockdown animals revealed less Meg3 levels than compared to SFC⁻ control mice 90 min after social fear extinction training (p < 0.09; because of SEM in SFC⁻ control (for Meg3 levels n = 2)). Data represent (C) mean investigation time ± SEM and (B, D) mean number of shocks/fold change + SEM vs. respective control group. n(SFC⁻ control) = 7; n(SFC⁺ control) = 6; n(SFC⁻ knockdown) = 5; n(SFC⁺ knockdown) = 7.

Statistics:

Number of shocks during social fear acquisition (Figure 18B)
t-test: p = 0.577
Meg3 knockdown before social fear acquisition (Figure 18C)
Two way ANOVA: group effect $F_{(3, 20)}$ = 12.97; p = 0.0001; group x time: $F_{(24, 160)}$ = 8.185; p < 0.0001 Bonferroni's post hoc analysis: p < 0.01 SFC⁻ knockdown vs. SFC⁺ knockdown social stimuli 1-4; p < 0.01 SFC⁻ control vs. SFC⁺ knockdown for social stimuli 1-5
Meg3 levels 90 min after extinction training in knockdown animals (Figure 18D)
t-test: p < 0.09 SFC⁻ control vs. knockdown animals (high SEM in SFC⁻ control, n = 2)

3.2.4.4 Meg3 knockdown effects on long-term extinction memory

In a last approach, I determined whether Meg3 knockdown affects long-term memory formation, as Meg3 was shown to regulate LTP (Tan et al., 2017). Therefore, Meg3 knockdown was induced 72 h before extinction training and effectiveness of long-term memory formation and storage was tested during social fear recall 21 days later (Figure 19A). SFC$^+$ control and SFC$^+$ knockdown mice received a similar number of shocks (2.22 ± 0.15 vs. 2.21 ± 0.11). During social fear extinction training, SFC$^+$ control mice displayed significantly less investigation of the conspecific until the third stimuli, for SFC$^+$ knockdown, significant differences in investigation time were present until the fourth stimuli (Figure 19B). During social fear recall, three weeks after the extinction training (Figure 19B), SFC$^+$ knockdown animals showed lower investigation levels than SFC$^-$ controls (43.44 % ± 6.94 % vs. 69.07 % ± 2.80 %) but not compared to SFC$^-$ knockdown (60.71 % ± 3.50 %) and SFC$^+$ control mice (52.00 % ± 5.66 %). There was no difference in investigation time when the second stimulus was presented among the groups. Meg3 levels were significantly downregulated to 12.09 % ± 5.33 % even 23 days after knockdown induction and FAM-labelled GapmeRs were still mainly localized within the septum (Figure 19D, C).
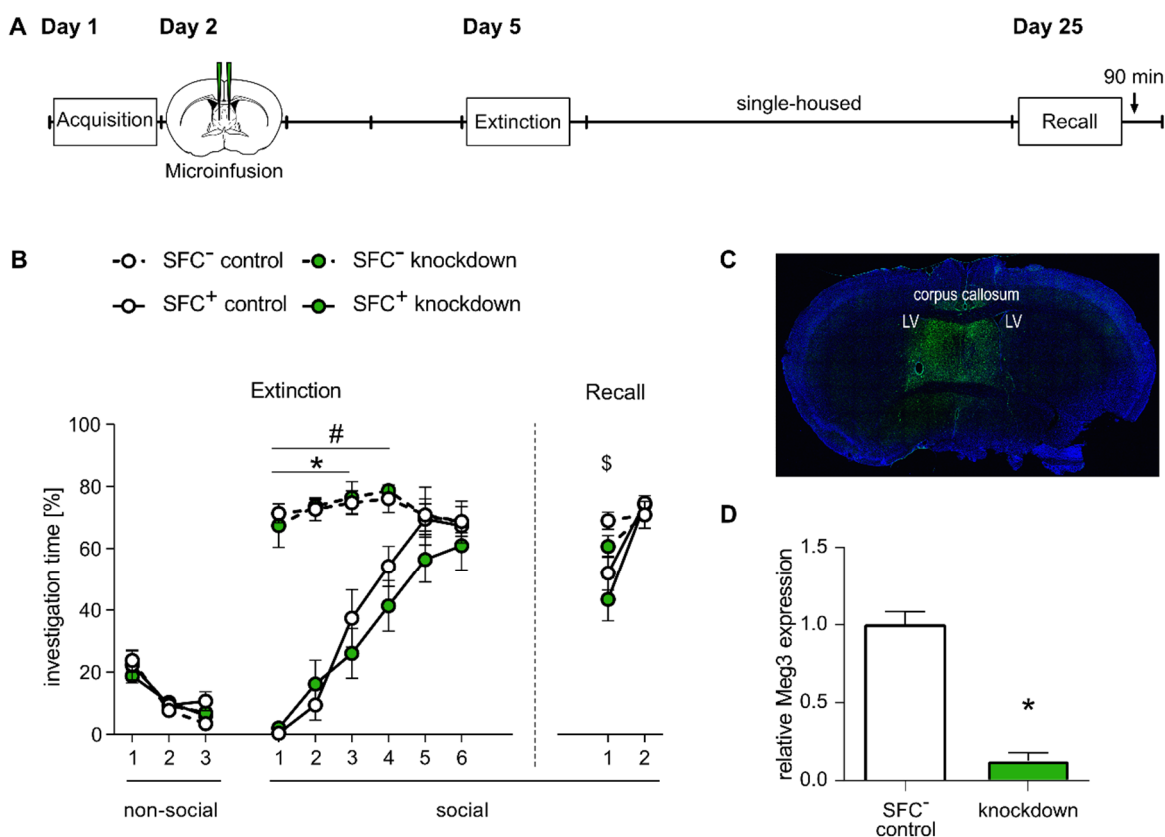

Figure 19 Meg3 knockdown effects on long-term social fear extinction memory.

(A) Schematic timeline for behavioural testing and microinfusion. (B) SFC$^-$ control and SFC$^-$ knockdown mice show similar and high investigation levels of the social stimuli. SFC$^+$ control and knockdown mice were socially

fearful at the beginning of the extinction training and extinguished SFC-induced social fear over the extinction training. SFC$^+$ knockdown mice spent significantly less investigation time until the fourth stimulus than SFC$^-$ knockdown mice (#p = 0.01). SFC$^+$ control mice were significantly different to SFC$^-$ control mice until the third stimulus (*p = 0.01). SFC$^+$ knockdown animals were more fearful than SFC$^-$ control animals ($p = 0.01 SFC$^-$ control vs. SFC$^+$ knockdown). (C) Knockdown animals revealed less Meg3 levels compared to SFC$^-$ controls 90 min after social fear recall (p < 0.0001). (D) FAM-labelled GapmeRs were still distributed within the septum 23 days after microinfusion. Data represent mean investigation time ± SEM and mean fold change + SEM vs. SFC$^-$ control. n(SFC$^-$ control) = 6; n(SFC$^+$ control) = 9; n(SFC$^-$ knockdown = 6; n(SFC$^+$ knockdown) = 14.

The presented results show that antisense LNA GapmeRs are highly efficient and still present 23 days after microinfusion, thus, providing a useful tool for long-term experiments. Animals showed already similar investigation times during the second social stimulus presentation during social fear recall suggesting minor Meg3 knockdown effects on long-term extinction memory tested after 3 weeks.

Statistics:

Number of shocks during social fear acquisition for control and knockdown mice
t-test: p = 0.97
Meg3 knockdown before social fear extinction (Figure 19B)

Extinction:
 Two way ANOVA: group effect F(3, 31) = 15.63; p = 0.0001;
                 group x time: F(24, 248) = 9.419; p < 0.0001
 Bonferroni's post hoc analysis: p < 0.001 SFC$^-$ control vs. SFC$^+$ control for social stimuli 1-3; p < 0.0001 SFC$^-$ knockdown vs. SFC$^+$ knockdown for social stimuli 1-4
 Recall:
 Two way ANOVA: time effect F(1, 31) = 22.18; p < 0.0001;
                 group x time: F(3, 31) = 3.772; p < 0.0204
 Bonferroni's post hoc analysis: p = 0.01 SFC$^-$ control vs. SFC$^+$ knockdown for social stimulus 1

Meg3 levels 90 min after social fear recall (Figure 19D)
t-test: p < 0.0001 SFC$^-$ control vs. knockdown animals

3.2.5 Regulation of the PTEN/PI3K/AKT signalling pathway in context of social extinction

Due to the profound differential expression of Meg3 after social fear extinction, I investigated the PTEN/PI3K/AKT signalling pathway that was shown to be regulated by Meg3 in plasticity studies in context of learning (Tan et al., 2017).

First, I assessed the activity of PI3K and AKT in the septum 90 min after social fear extinction training. Protein as well as RNA samples were isolated in parallel, and therefore, behavioural data are already included in 3.2.1. Phosphorylation levels of the PI3K regulatory subunit P85 and AKT at Ser473 and Thr308 were not changed in SFC$^-$, SFC$^+$ (suc) and SFC$^+$ (unsuc) animals (Figure 20A, B, D, E). Total P85 and AKT protein levels were unchanged and also the lipid phosphatase PTEN, a negative regulator of the PI3K/AKT signalling pathway, was not differentially expressed (Figure 20C, F, G).

In a second step, I investigated the protein and phosphorylation levels 3 h after social fear extinction training. Western blot analyses revealed a differentially activated PI3K/AKT signalling pathway in conditioned mice with unsuccessful extinction. Phosphorylation levels of P85 (relative fold change of 1.7 ± 0.34) and AKT at Ser308 (relative fold change 1.79 ± 0.22) were significantly increased in SFC$^+$ (unsuc) animals (Figure 20H, I, K), whereas no differences were detected for phosphorylation levels of AKT Thr308 (Figure 20L). Total P85 and PTEN protein levels were unchanged in all the groups (Figure 20L, J, N), while total AKT was significantly downregulated in SFC$^+$ (suc) compared to SFC$^-$ 3 h after social fear extinction (relative fold change 0.89 ± 0.03, Figure 20M).

The presented data show for the first time that the PI3K/AKT signalling pathway is involved in learning and memory processes in context of social fear extinction. Here, the differential activation is specifically linked to the extinction success that was already shown to be important for Meg3 regulation (Figure 12).

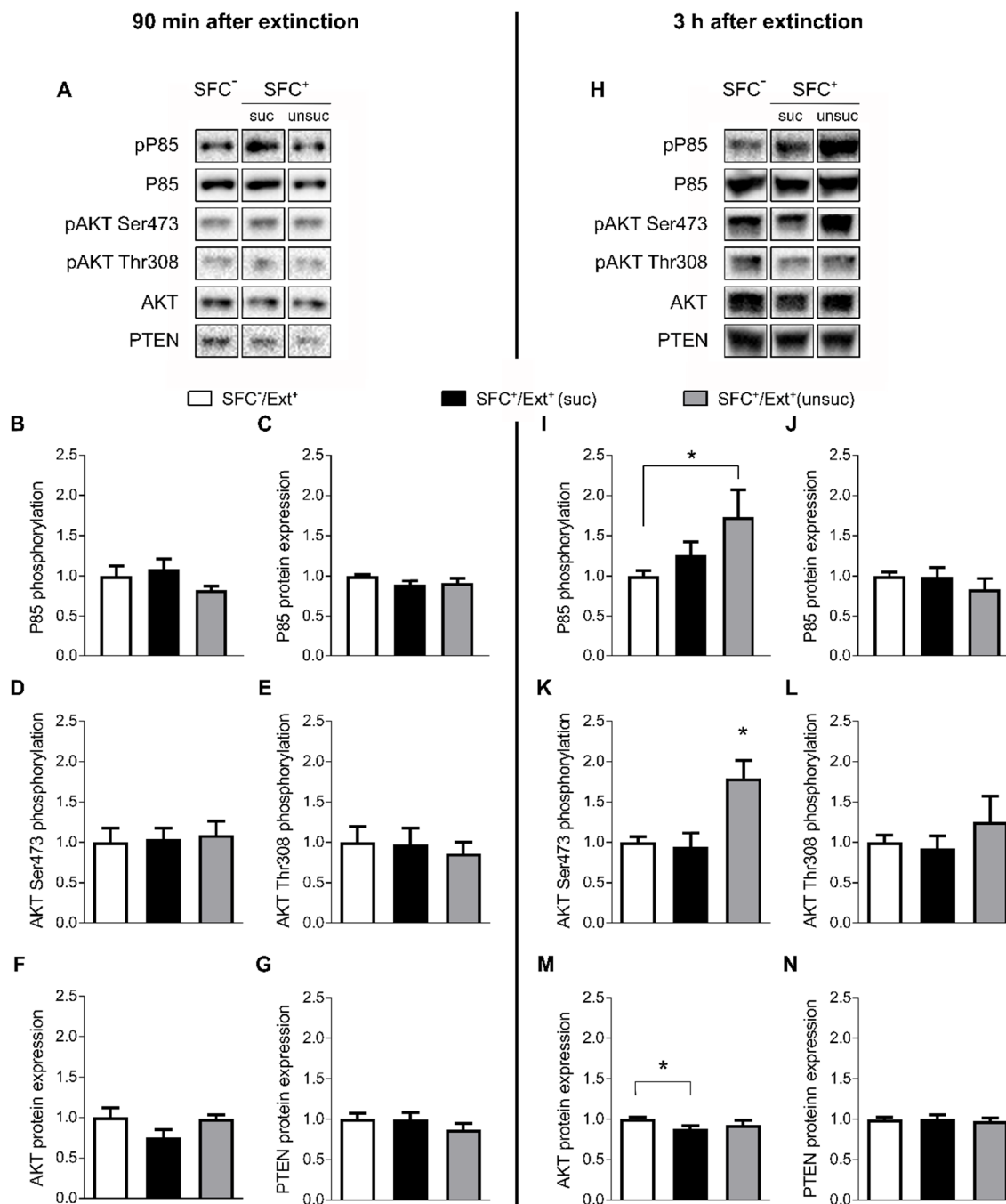**90 min after extinction**

3 h after extinction

Figure 20 Regulation of the PTEN/PI3K/AKT signalling pathway after social fear extinction training.

(A) and (H) show representative blots for pP85, pAKT Ser473 and pAKT Thr308 as well as for total P85, total AKT and PTEN expression 90 min and 3 h after social fear extinction training. (B-G) No changes were found for septal proteins and phosphorylation levels 90 min after social fear extinction training. (I, K) 3 h after extinction, P85 (*p = 0.05) and AKT Ser473 (*p = 0.01) were significantly more phosphorylated in SFC+ (unsuc) animals, (J, L, N) whereas AKT Thr308 phosphorylation and total P85 and PTEN were unchanged. (M) Total AKT was significantly lower expressed in SFC+ (suc) compared to SFC- (*p = 0.05). Abundance of the target protein was normalized to the total amount of protein in each lane. Data are presented as mean fold changes + SEM compared to respective SFC-. 90 min: n = 7-13 animals per group; 3 h: n = 5-10 animals per group.

Statistics:

90 min after social fear extinction: protein expression/phosphorylation levels (Figure 20B-G)

B) One way ANOVA: $F_{(2, 28)}$ = 1.046; p = 0.3646

C) One way ANOVA: $F_{(2, 28)}$ = 2.010; p = 0.1529

D) One way ANOVA: $F_{(2, 30)}$ = 0.07354; p = 0.9293

E) One way ANOVA: $F_{(2, 30)}$ = 0.1168; p = 0.8901

F) One way ANOVA: $F_{(2, 29)}$ = 1.725; p = 0.1960

G) One way ANOVA: $F_{(2, 33)}$ = 0.7878; p = 0.4632

3 h after social fear extinction: protein expression/phosphorylation levels (Figure 20I-N)

I) One way ANOVA: $F_{(2, 20)}$ = 4.251; p = 0.0289

Bonferroni's post hoc analysis: p = 0.0257 SFC$^-$ vs. SFC$^+$ (unsuc)

J) One way ANOVA: $F_{(2, 20)}$ = 0.7659; p = 0.4781

K) One way ANOVA: $F_{(2, 20)}$ = 8.654; p = 0.002

Bonferroni's post hoc analysis: p = 0.01 SFC$^-$ vs. SFC$^+$ (unsuc); p = 0.01 SFC$^+$ (suc) vs. SFC$^+$ (unsuc)

L) One way ANOVA: $F_{(2, 20)}$ = 0.8480; p = 0.4431

M) One way ANOVA: $F_{(2, 20)}$ = 3.585; p = 0.0467

Bonferroni's post hoc analysis: p = 0.05 SFC$^-$ vs. SFC$^+$ (suc)

N) One way ANOVA: $F_{(2, 20)}$ = 0.09983; p = 0.9054

Moreover, I started to assess the changes in PI3K/AKT signalling pathway in Meg3 knockdown mice and according control groups. One day after social fear acquisition, animals were microinfused with either antisense LNA GapmeRs (knockdown) or control antisense oligonucleotides (control). After an incubation time of 72 h, animals were exposed to conspecifics during social fear extinction training and brains were collected 90 min after extinction training. Western blot analyses revealed an upregulation of pP85 in SFC$^+$/Ext$^+$ control animals compared to their corresponding SFC$^-$/Ext$^+$ control group (Figure 21A, B). This upregulation was not observable in the SFC$^+$/Ext$^+$ knockdown group. However, Meg3 knockdown animals, SFC$^-$ as well as SFC$^+$, seem to have elevated basal pP85 levels compared

to SFC⁻ control animals. No significant changes were found for total P85, AKT Ser473, AKT Thr308, total AKT and PTEN (Figure 21C-G).

Due to partially small sample size, results have to be interpreted with caution and samples size has to be increased. Nevertheless, the differences in P85 activation indicate that Meg3 influences the PI3K/AKT signalling pathway in the context of social fear extinction.
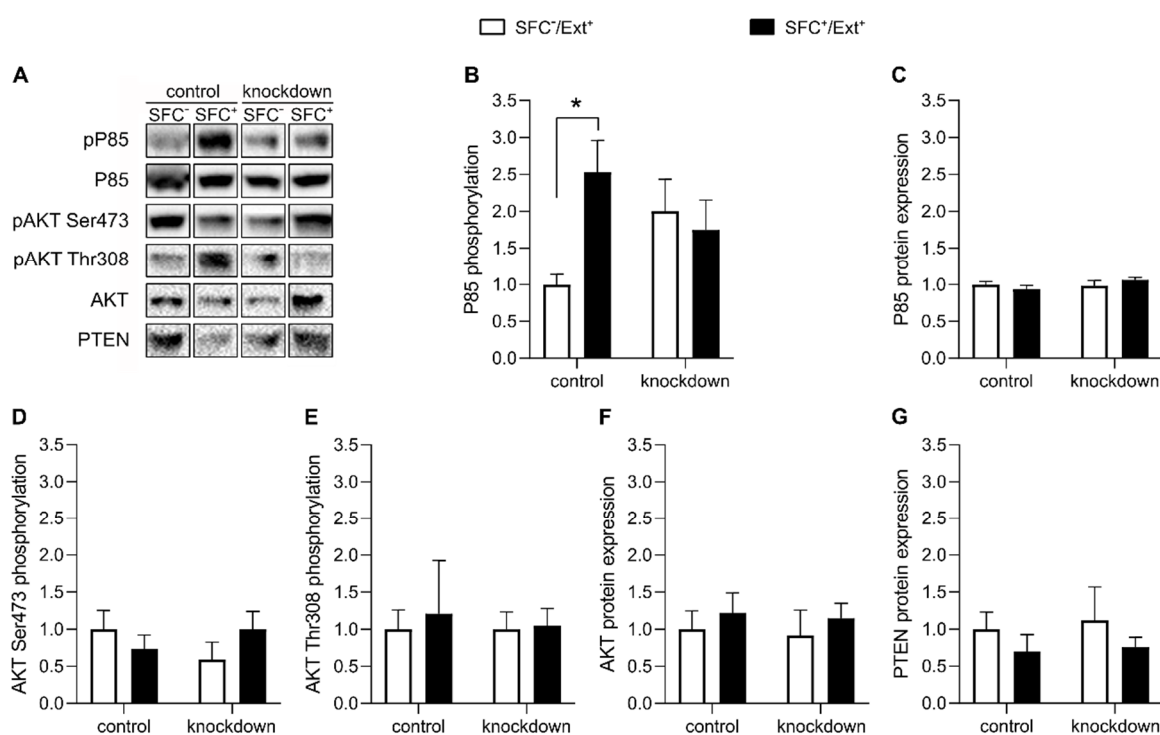

Figure 21 PTEN/PI3K/AKT signalling pathway after Meg3 knockdown.

(A) shows representative blots for pP85, pAKT Ser473 and pAKT Thr308 as well as for total P85, total AKT and PTEN expression in control and Meg3 knockdown mice 90 min after social fear extinction training. (B) Phosphorylation levels of P85 (pP85) are significantly upregulated in SFC⁺/Ext⁺ control mice (separate statistics: *p = 0.0323 vs. SFC⁻/Ext⁺ control). (C-G) No differences were found for phosphorylation levels of AKT Ser473 and AKT Thr308, nor for total P85, total AKT and PTEN. Abundance of the target protein was normalized to the total amount of protein in each lane. Data represent mean fold changes + SEM compared to respective SFC⁻/Ext⁺ control group. n(SFC⁻/Ext⁺ control) = 3-6; n(SFC⁺/Ext⁺ control) = 4-6; n(SFC⁻/Ext⁺ knockdown) = 4-6; n(SFC⁺/Ext⁺ knockdown) = 6-9.

Statistics:

PTEN/PI3K/AKT signalling pathway after Meg3 knockdown and social fear extinction training (Figure 21B-G)

B) Two way ANOVA: treatment effect $F(1, 15) = 0.06371$; $p = 0.8041$;

   treatment x SFC: $F(1, 15) = 4.095$; $p = 0.0612$

separate statistics: t-test: $p = 0.0323$ SFC$^+$/Ext$^+$ control vs. SFC$^-$/Ext$^+$ control

C) Two way ANOVA: treatment effect $F(1, 14) = 0.8693$; $p = 0.3670$;

   treatment x SFC: $F(1, 14) = 1.688$; $p = 0.2149$

D) Two way ANOVA: treatment effect $F(1, 21) = 0.8086$; $p = 0.7789$;

   treatment x SFC: $F(1, 21) = 1.816$; $p = 0.1921$

E) Two way ANOVA: treatment effect $F(1, 22) = 0.04362$; $p = 0.8362$;

   treatment x SFC: $F(1, 22) = 0.03972$; $p = 0.84839$

F) Two way ANOVA: treatment effect $F(1, 22) = 0.09273$; $p = 0.7636$;

   treatment x SFC: $F(1, 22) = 0.00044$; $p = 0.9835$

G) Two way ANOVA: treatment effect $F(1, 20) = 0.1185$; $p = 0.7343$;

   treatment x SFC: $F(1, 20) = 0.01395$; $p = 0.9072$

3.3 Identification of differentially accessible chromatin regions after social fear extinction training

Meg3 showed exclusive nuclear localization and neuronal expression within the septum in context of social fear (see 3.2.3). Therefore, I investigated whether Meg3 plays a role in the regulation of chromatin states as it was described in other contexts (Mondal et al., 2015; Sanli et al., 2018), and in general, how chromatin states are changed after social fear extinction training. In order to determine chromatin regions with altered accessibility, I performed ATAC-Seq in collaboration with Dr Igor Ulitsky and Dr Rotem Tov-Perry, Weizmann Institute of Science, Israel. Samples were collected 90 min after social fear extinction training (for behavioural data see Appendix Figure 29) and cell nuclei from the septum were FAC-sorted for neuronal nuclei. ATAC-Seq revealed 9,541 differentially expressed peaks with $p_{(non-adjusted)} < 0.05$. A peak is defined as a region of 140 bp with −70 and +70 bp around the peak summit. Thresholds were set to ≥ 5 reads per million reads (= MAX) and at least one normalized count within the samples had to be found. Most of the peaks were found intronic and in intergenic regions, but only approximately 10 % were located in promoter transcription start sites (Figure

22A). When MAX was set to a more stringent threshold (MAX = 20), 71 peaks were found to be different in SFC⁺/Ext⁺ (suc) vs. SFC⁺/Ext⁺ (unsuc) and 45 in SFC⁺ control vs. SFC⁺ knockdown. As SFC⁺/Ext⁺ (suc) vs. SFC⁺/Ext⁺ (unsuc) and SFC⁺ control vs. SFC⁺ knockdown display differential regulation of Meg3, I compared whether gene loci are similarly accessible in both comparisons. Here, I found two genes, *doublecortin-like kinase 3 (Dclk3)* and *Cwc22 associated protein (Cwc22),* which showed similar accessibility in SFC⁺/Ext⁺ (suc) and SFC⁺ control than compared to the according groups SFC⁺/Ext⁺ (unsuc) and SFC⁺ knockdown with lower Meg3 levels (Figure 22B). Thus, *Dclk3* and *Cwc22* represent gene loci whose accessibility might be regulated by Meg3 and therefore, should be addressed in future studies.

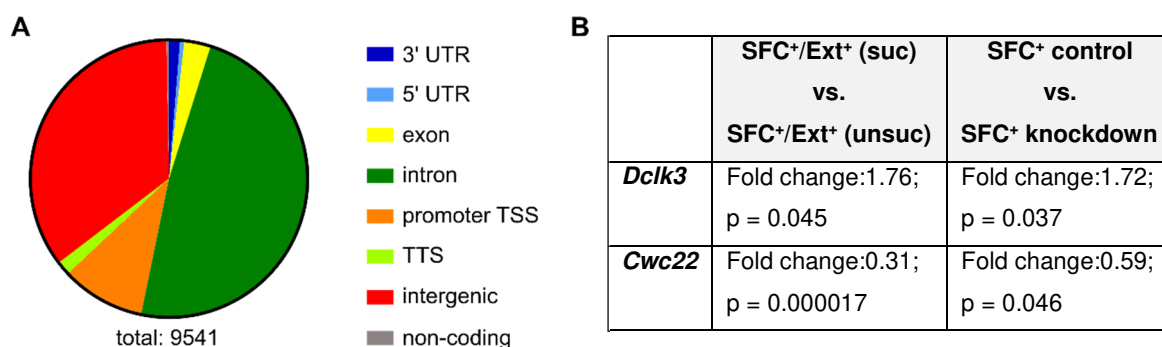|	SFC⁺/Ext⁺ (suc) vs. SFC⁺/Ext⁺ (unsuc)	SFC⁺ control vs. SFC⁺ knockdown
Dclk3	Fold change:1.76; p = 0.045	Fold change:1.72; p = 0.037
Cwc22	Fold change:0.31; p = 0.000017	Fold change:0.59; p = 0.046

Figure 22 Open chromatin analysis of septum samples after social fear extinction training.

(A) Bar plots of the percentage of ATAC peaks found in different regions of the genome in SFC⁻/Ext⁺, SFC⁺/Ext⁺ (suc) and SFC⁺/Ext⁺ (unsuc) as well as SFC⁺ control and SFC⁺ knockdown (Meg3) groups. Peaks are summarized into 3' untranslated region (3' UTR), 5' untranslated region (5' UTR), exons, introns, promoter transcription start sites (TSS), transcription termination sites (TTS), intergenic regions and non-coding regions. In total, 9,541 peaks were found. (B) Differential peaks at the *Dclk3* and *Cwc22* loci were found in SFC⁺/Ext⁺ (suc) vs. SFC⁺/Ext⁺ (unsuc) and SFC⁺ control vs. SFC⁺ knockdown.

3.4 CUT&RUN for H3K27me3 modification after social fear extinction

CUT&RUN is used to identify DNA regions that are bound by specific factors or by histones. Several studies have shown that Meg3 interacts with the PRC2 thereby supporting tri-methylation of lysine 27 of histone 3 (H3K27me3), an event that is usually linked to repression and inactive chromatin regions. For this reason, I performed CUT&RUN for H3K27me3 with samples from SFC⁻ and SFC⁺ mice as well as SFC⁺ control and SFC⁺ knockdown mice sacrificed 90 min after social fear extinction training (behavioural data see Appendix Figure 30). CUT&RUN peaks were correlated with the peaks found in ATAC-Seq (3.3). Thresholds for the fold changes were set to ≥ 25 % with p < 0.01. The correlations of SFC⁺/Ext⁺ (suc) vs.

SFC[+]/Ext[+] (unsuc) and SFC[+] control vs. SFC[+] knockdown are shown as representative examples (Figure 23). As seen in Figure 23A, the principle expectation that increased levels of H3K27me3 modification, which usually has repressive effects, lead to chromatin silencing, was fulfilled in the comparison SFC[+]/Ext[+] (suc) vs. SFC[+]/Ext[+] (unsuc): here, 50 peaks for increased H3K27me3 levels were linked to lower ATAC-Seq signals, indicating less accessible chromatin at these regions. In contrast, the comparison of SFC[+] control vs. SFC[+] knockdown revealed in total less regulated H3K27me3 peaks (16 increased, 46 decreased). Moreover, decreased H3K27me3 led here to reduced chromatin accessibility (Figure 23B).

Overall, many regions with concordant H3K27me3 and ATAC-Seq signals originate from the variable *Cwc22* gene. Detailed bioinformatical analysis and evaluation of the localization of the signal peaks within the *Cwc22* gene and others are necessary to limit the number of potential genes that might be regulated by Meg3. These genes potentially regulated by Meg3 will be addressed in future experiments to identify the downstream signalling of Meg3 after social fear extinction.
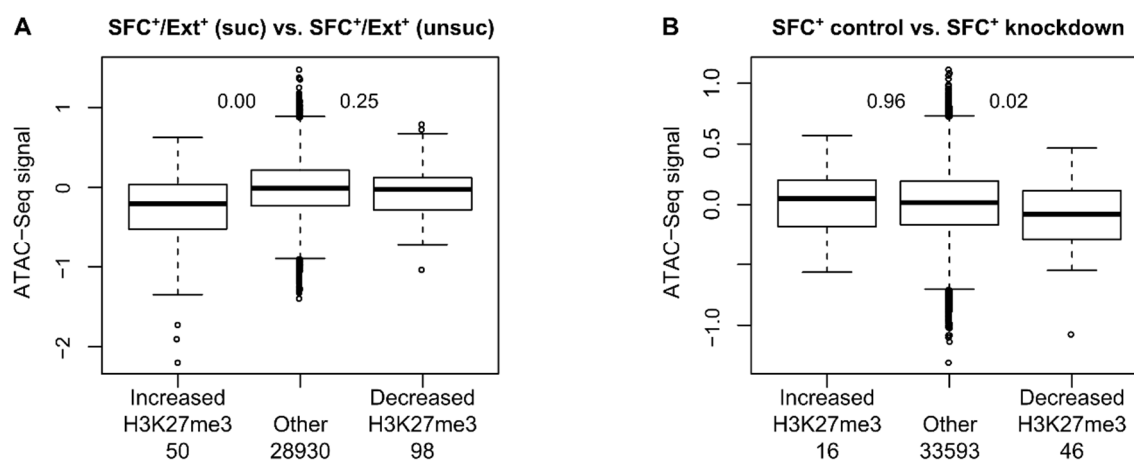

Figure 23 Correlation of ATAC-Seq peaks with CUT&RUN H3K27me3 signals.

(A) Correlation of ATAC-Seq peaks with H3K27me3 signals of SFC[+]/Ext[+] (suc) vs. SFC[+]/Ext[+] (unsuc) and (B) SFC[+] control vs. SFC[+] knockdown. The y-axis shows $\log_2$-fold change and number between the boxes represent p-values of Wilcoxon rank-sum test (vs. Other). Numbers below the names on the x-axis indicate how many peaks meet the criteria (threshold fold change $\geq$ 25 %, $p < 0.01$).

3.5 Meg3 expression in the HPC in the context of social fear extinction

Some studies revealed that Meg3 is regulated in the context of memory formation or loss within the HPC (Tan et al., 2017; Yi & Chen, 2019). To address the question whether the long Meg3

variants are also regulated within the HPC and especially in the context of social fear extinction memory, I determined the RNA level of the specific Meg3 variants within the HPC 90 min and 3 h after social fear extinction training (Figure 24). Here, I differentiated between dorsal and ventral HPC (dHPC, vHPC), which are known to have different roles in cognitive and affective functions. 90 min after social fear extinction training, no differences in Meg3 levels in neither the dHPC nor the vHPC were detected. Nevertheless, a trend for downregulated Meg3 in the dHPC was found in the SFC$^+$/Ext$^+$ (suc) group 3 h after social fear extinction, whereas no alterations were found for the vHPC (Figure 24).

Taken together, results indicate that the long Meg3 variants addressed in this thesis are poorly or temporally differently regulated within the HPC after social fear extinction training than Meg3 variants investigated after learning processes during non-social memory formation (Tan et al., 2017).
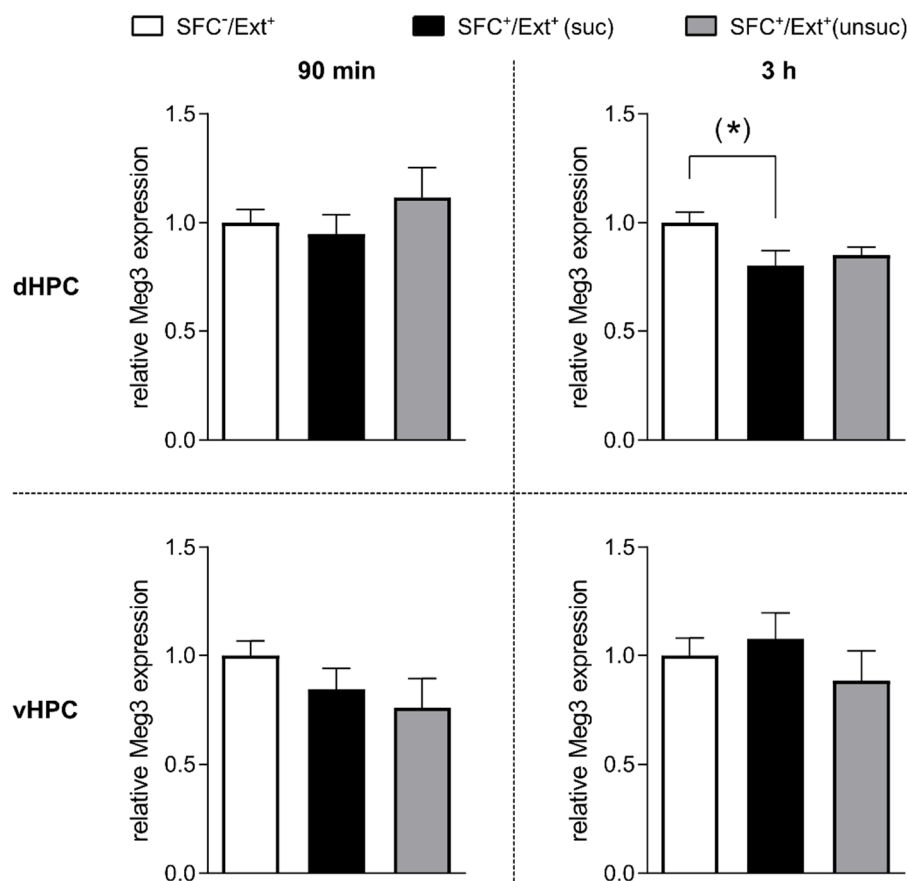

Figure 24 Meg3 expression within the HPC after social fear extinction.

No changes in Meg3 levels were found 90 min after social fear extinction training within the dHPC and vHPC. After 3 h, dorsohippocampal Meg3 was by trend downregulated in SFC$^+$/Ext$^+$ (suc) (separate statistics: (*)p = 0.0573 SFC$^+$/Ext$^+$ vs. SFC$^-$/Ext$^+$). 90 min: n(SFC$^-$/Ext$^+$) = 11, n(SFC$^+$/Ext$^+$ (suc)) = 10, n(SFC$^+$/Ext$^+$ (unsuc)) = 10; 3 h: n(SFC$^-$/Ext$^+$) = 5, n(SFC$^+$/Ext$^+$ (suc)) = 7, n(SFC$^+$/Ext$^+$ (unsuc)) = 2.

Statistics:

Meg3 expression levels within the HPC (Figure 24)

dHPC

90 min: One way ANOVA: $F(2, 22) = 0.6311$; $p = 0.5414$

3 h: One way ANOVA: $F(2, 11) = 2.550$; $p = 0.1231$;

   separate statistics: t-test: (*)$p = 0.0573$ SFC$^-$/Ext$^+$ vs. SFC$^+$/Ext$^+$

vHPC

90 min: One way ANOVA: $F(2, 22) = 1.577$; $p = 0.2291$

3 h: One way ANOVA: $F(2, 15) = 0.5460$; $p = 0.5903$

3.6   Validation of additional RNA candidates

RNA-Seq analysis revealed several RNA candidates that were differentially regulated in gene-based and transcript-based analyses. Samples for the validation include samples, which were also used for Meg3 validation. Behavioural data are not shown.

Sgk1

Sgk1 mRNA was significantly upregulated in the septum of SFC$^+$/Ext$^+$ (unsuc) mice (1.51 ± 0.30; Figure 25A) 90 min after social fear extinction. The levels seem to get balanced 3 h after extinction training (Figure 25B). No differences in RNA levels were found 30 min after social fear extinction (that might be due to low animal numbers in the SFC$^+$/Ext$^+$ (unsuc) group (n = 2)) (Figure 25C). On a protein level, SGK1 was significantly decreased in SFC$^+$/Ext$^+$ (unsuc) mice at the 90 min time point compared to SFC$^+$/Ext$^+$ (suc) and SFC$^-$/Ext$^+$ animals (Figure 25D, E). After 3 h, SGK1 levels were restored or even seemed to be slightly increased, nevertheless, effects were not significant (Figure 25F).

Monitoring Sgk1 mRNA and protein levels identified again the success of the social fear extinction training as an important factor for inducing Sgk1 transcription and translation and revealed a dynamic Sgk1 expression regulation after social fear extinction.
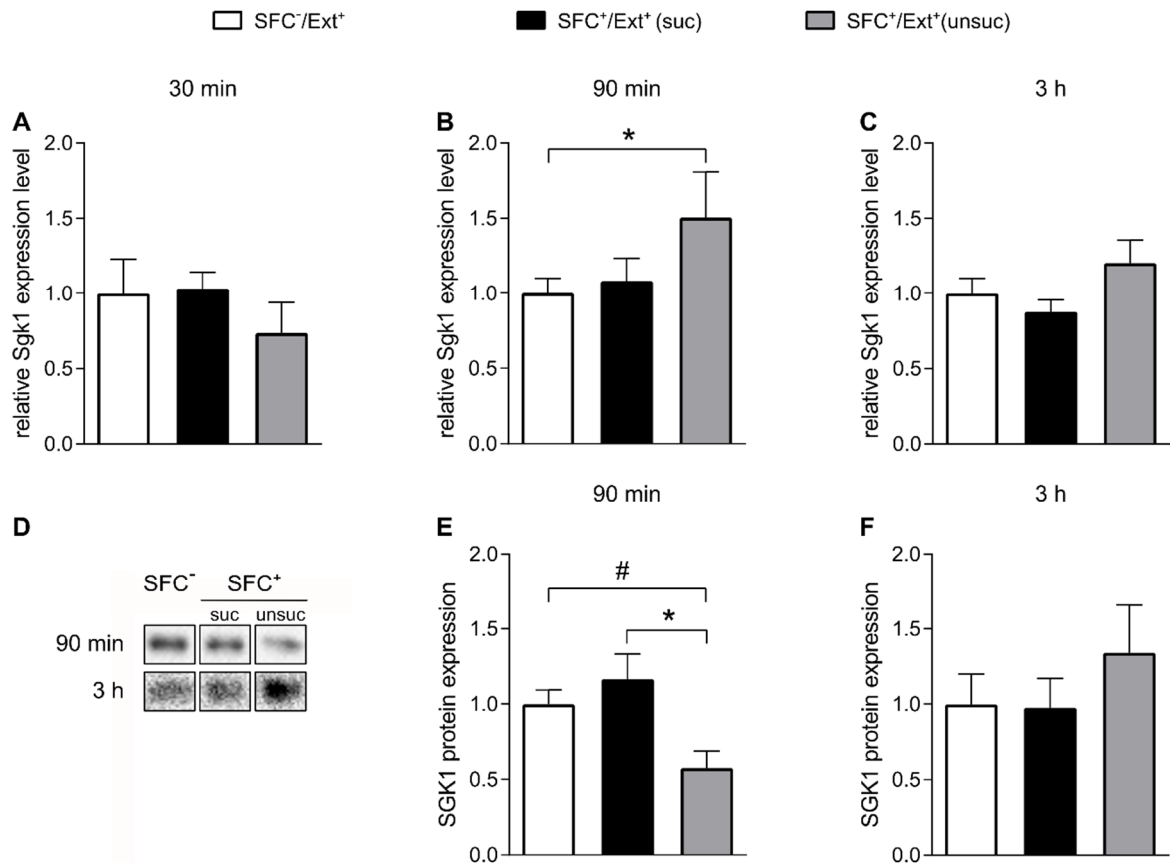
Figure 25 Sgk1 mRNA and protein levels after social fear extinction.

(A-C) Sgk1 mRNA levels were assessed 30 min, 90 min and 3 h after social fear extinction training. After 90 min, SFC$^+$/Ext$^+$ (unsuc) showed increased Sgk1 levels (separate statistics: *p = 0.0507 vs. SFC$^-$/Ext$^+$). (D) Representative blots for SGK1 levels at 90 min and 3 h after social fear extinction training. (E) Protein levels were significantly decreased in SFC$^+$/Ext$^+$ (unsuc) after 90 min (*p = 0.05 vs. SFC$^+$/Ext$^+$ (suc); separates statistics: #p = 0.0098 vs. SFC$^-$/Ext$^+$). (F) No difference was found after 3 h. Abundance of the target protein was normalized to the total amount of protein in each lane. Data are presented as mean fold changes + SEM compared to respective SFC$^-$. For mRNA levels: 30 min: n(SFC$^-$/Ext$^+$) = 7, n(SFC$^+$/Ext$^+$ (suc)) = 5, n(SFC$^+$/Ext$^+$ (unsuc)) = 2; 90 min: n(SFC$^-$/Ext$^+$) = 20, n(SFC$^+$/Ext$^+$ (suc)) = 12, n(SFC$^+$/Ext$^+$ (unsuc)) = 6; 3 h: n(SFC$^-$/Ext$^+$) = 10, n(SFC$^+$/Ext$^+$ (suc)) = 10, n(SFC$^+$/Ext$^+$ (unsuc)) = 4. For protein levels: 90 min: n(SFC$^-$/Ext$^+$) = 12, n(SFC$^+$/Ext$^+$ (suc)) = 11, n(SFC$^+$/Ext$^+$ (unsuc)) = 8; 3 h: n(SFC$^-$/Ext$^+$) = 10, n(SFC$^+$/Ext$^+$ (suc)) = 8, n(SFC$^+$/Ext$^+$ (unsuc)) = 5.

Statistics:

Sgk1 mRNA levels in the septum after social fear extinction training (Figure 25A-C)

30 min: One way ANOVA: $F_{(2, 11)}$ = 0.2945; p = 0.7506

90 min: One way ANOVA: $F_{(2, 35)}$ = 2.152; p = 0.1314

   separate statistics: t-test: p = 0.0507 SFC⁻/Ext⁺ vs. SFC⁺/Ext⁺ (unsuc)

3 h: One way ANOVA on Ranks: H = 5.056; DF = 2; p = 0.0798

SGK1 protein levels in the septum after social fear extinction training (Figure 25E, F)

90 min: One way ANOVA: $F_{(2, 28)}$ = 4.779; p = 0.0164

   Bonferroni's post hoc analysis: p = 0.05 SFC⁺/Ext⁺ (unsuc) vs. SFC⁺/Ext⁺ (suc)

   separate statistics: t-test: p = 0.0098 SFC⁺/Ext⁺ (unsuc) vs. SFC⁻/Ext⁺

3 h: One way ANOVA: $F_{(2, 20)}$ = 0.6211; p = 0.5474

Other coding and non-coding RNAs

In addition to the above described RNAs, I validated Crfr2, sCrfr2 and Irak1 mRNA levels 90 min after social fear extinction training in an extinction success-dependent manner (Figure 26A-C). Here, no significant differences in expression levels were found. For Plin4, Gm13157 and the non-coding RNA Nlrp5-ps, differential regulation in SFC⁻ vs. SFC⁺ could not be confirmed (Figure 26D-F). One problem was that even SFC⁻ animals showed high variance in the expression levels. Hcrtr2 mRNA was not regulated at 90 min, but increased 3 h after social fear extinction training (1.44 ± 0.26; Figure 26G). For Sirt1, a similar regulation was observed for 90 min and 3 h after extinction training, but statistics reached no significance (Figure 26H).
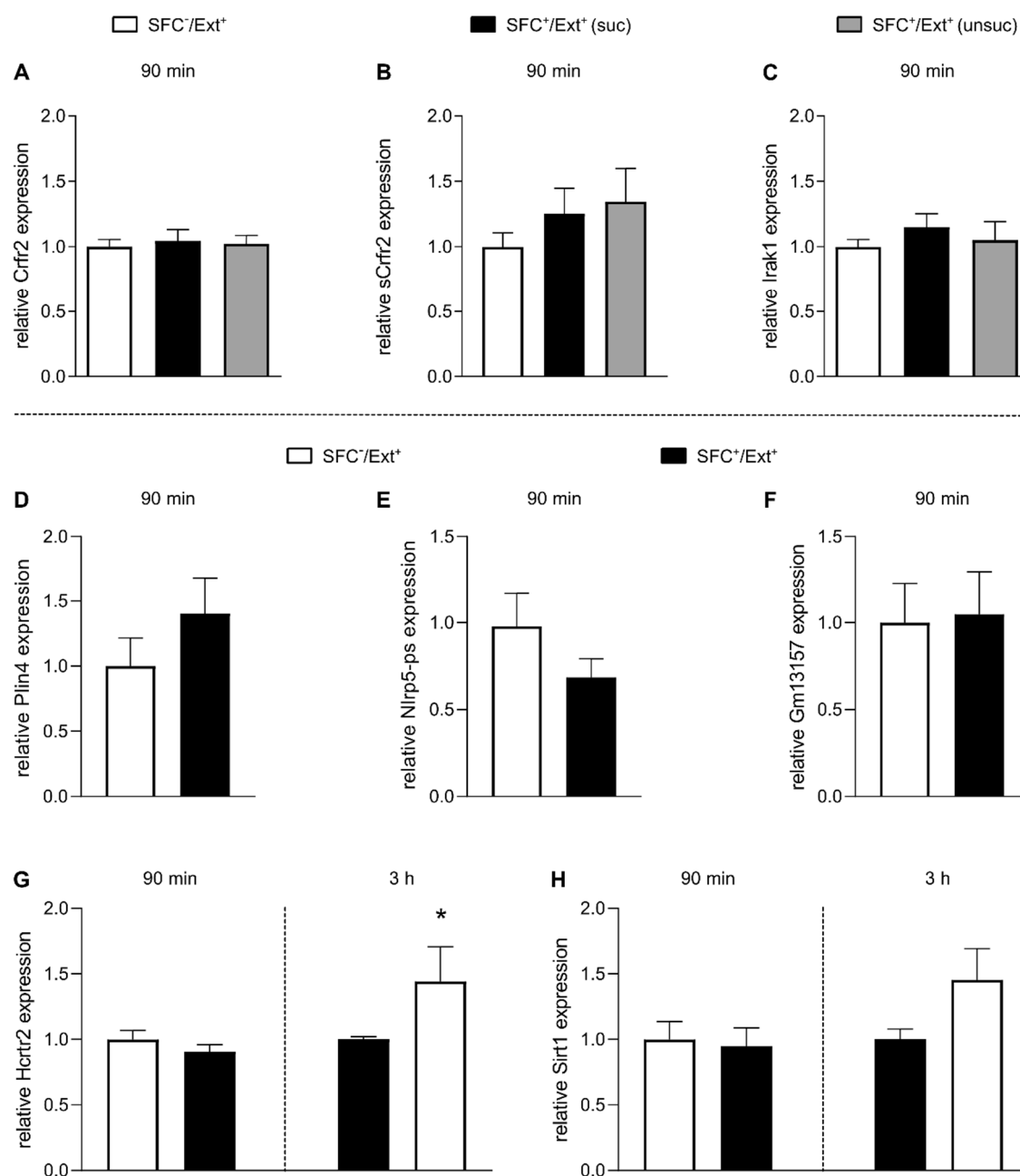
Figure 26 RNA-Seq based validation of additional RNA candidates.

(A-F) Crfr2, sCrfr2, Irak1, Plin4, Nlrp5-ps and Gm13157 RNA showed no significant regulation in SFC⁺/Ext⁺ compared to SFC⁻/Ext⁺ 90 min after social fear extinction training. (G, H) Hcrtr2 and Sirt1 mRNA expression levels were additionally investigated for 3 h after social fear extinction training. Here, Hcrtr2 was significantly upregulated in SFC⁺/Ext⁺ (*p = 0.0096). Data represent mean fold change + SEM compared to respective SFC⁻/Ext⁺. Crfr2/sCrfr2/Irak1: n(SFC⁻/Ext⁺) = 14-20, n(SFC⁺/Ext⁺ (suc)) = 11-13, n(SFC⁺/Ext⁺ (unsuc)) = 5-8; 90 min: n(SFC⁻/Ext⁺) = 16-18, n(SFC⁺/Ext⁺) = 12-17; 3 h: n(SFC⁻/Ext⁺) = 7-8, n(SFC⁺/Ext⁺) = 12.

Statistics:

RNA levels in the septum after social fear extinction training (Figure 26)
A) One way ANOVA on Ranks: H = 0.2061; DF = 2; p = 0.9021
B) One way ANOVA on Ranks: H = 1.598; DF = 2; p = 0.4497
C) One way ANOVA on Ranks: H = 1.577; DF = 2; p = 0.4545
D) Mann-Whitney U tests: p = 0.3473
E) Mann-Whitney U tests: p = 0.05246
F) Mann-Whitney U tests: p > 0.999
G) 90 min: t-test: p = 0.2855; 3 h: Mann-Whitney U tests: p = 0.0096
H) 90 min: Mann-Whitney U tests: p = 0.5391; 3 h: Mann-Whitney U tests: p = 0.2268

3.7   Impairment of social fear extinction by lesions of the LS

Initially, I aimed to identify neurotransmitter systems that play a role during social fear extinction, and to strengthen the role of the LS for social fear extinction. Therefore, neurotransmitter release within the LS should be measured by microdialysis. In a pilot experiment (data not shown), microdialysis probes were unilaterally implanted into the LS and microdialysis was performed during the social fear extinction training. Surprisingly, conditioned animals did not show any social fear extinction behaviour. Subsequently, I wanted to test whether the procedure of microdialysis by diluting neurotransmitter availability within the LS was responsible for the observed abolishment of social fear extinction. For this purpose, I implanted unilaterally microdialysis probes into the LS but without performing microdialysis during the extinction training. Moreover, I added control animals that were sham-operated, meaning they received the same time of anaesthesia, holes were drilled for inserting screws and the wound was closed using dental cement but no microdialysis probe was implanted.

Conditioned sham-operated (SFC$^+$ sham) animals and conditioned animals with implanted microdialysis probe (SFC$^+$ probe) received a similar number of shocks (2.2 ± 0.3 vs. 2.8 ± 0.6). SFC$^-$ sham mice showed no fear when the first social stimulus was presented (Figure 27). SFC$^+$ sham mice were fearful at the beginning as mice showed low investigation of the social stimulus. From the third stimulus on, SFC$^+$ sham displayed similar investigation levels than SFC$^-$ sham. Implantation of the microdialysis probe had no impact on social motivation as SFC$^-$ probe mice spent similar investigation times on the social stimuli as the SFC$^-$ sham group. Mice of the SFC$^+$

probe group showed strong social fear all over the first seven social stimuli. Even after increasing the number of presented social stimuli to 12, SFC^+ probe mice could not extinguish social fear and showed significantly less investigation time than SFC^- probe until the stimulus 8 and for SFC^- sham until the end of extinction training (Figure 27).

The strongly impaired social fear extinction of conditioned mice with unilaterally implanted microdialysis probe emphasize the importance of an intact LS for social fear extinction. Even an unilateral lesion of the LS caused by the implantation of a microdialysis probe, which is a well established and regularly used tool in behavioural neuroscience, was sufficient to inhibit the extinction of social fear although prolonged training sessions were applied.
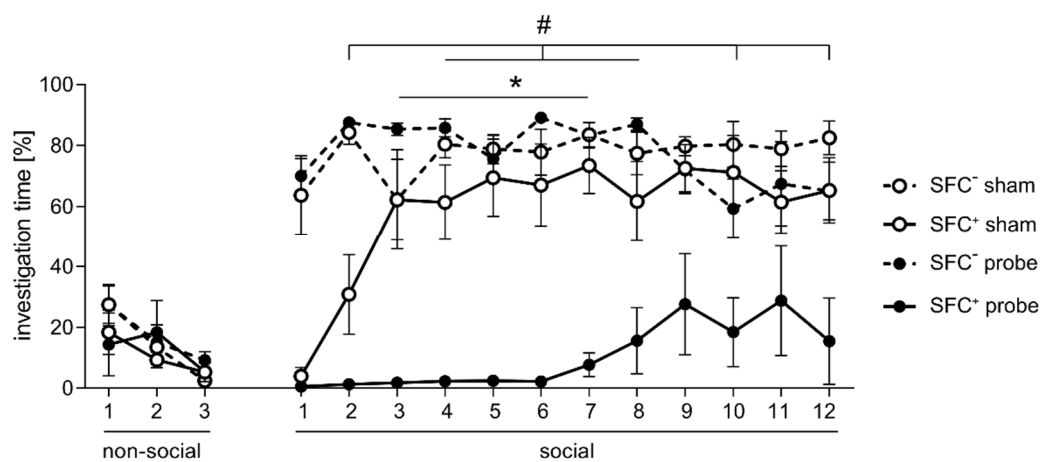

Figure 27 Damage of the LS impairs social fear extinction.

Unilateral implantation of a microdialysis probe into the LS impairs social fear extinction in SFC^+ probe mice (*$p < 0.05$ vs. SFC^+ sham; #$p < 0.05$ vs. SFC^- control), whereas social investigation is not altered by damage from probe implantation in SFC^- probe mice. Data represent mean investigation time ± SEM. n(SFC^- sham/probe) = 4/6; n(SFC^+ sham/probe) = 6/5.

Statistics:

Extinction behaviour (Figure 27)
Two way ANOVA: group effect $F(3, 18) = 20.96$; $p < 0.0001$;   group x time: $F(42, 252) = 5.674$; $p < 0.0001$ Bonferroni's post hoc analysis: $p < 0.05$ SFC^+ probe vs. SFC^+ sham for social stimuli 3-7; $p < 0.05$ SFC^+ probe vs. SFC^- sham for social stimuli 2, 4-8, 10, 12; $p < 0.05$ SFC^+ probe vs. SFC^- probe for social stimuli 2, 4-8

DISCUSSION

4   Discussion

In the course of this thesis, I was able to depict for the first time the involvement of a lncRNA in social fear extinction regulation. More precisely, I characterized the dynamic regulation of the lncRNA Meg3 and factors that are important for its regulation during SFC. I could reveal a region-specific regulation within the septum and that antisense LNA GapmeR-induced knockdown of Meg3 tends to decrease social fear extinction behaviour. Moreover, I demonstrated a differential activation of the PI3K/AKT signalling pathway in animals with successful and unsuccessful extinction and in control vs. Meg3 knockdown animals. All the experiments included in this thesis focused on the septum, which has repeatedly been proven to play an important role in the extinction of social fear (Menon et al., 2018; Zoicas et al., 2014). Furthermore, I successfully generated a comprehensive profile of characteristics of SFC based on transcriptomic data, chromatin accessibility and H3K27me3 histone modifications.

4.1   Dynamic regulation of the lncRNA Meg3 within the septum in the context of social fear

Development of SAD is often triggered by foregoing negative events and experiences that are linked to a social situation (Brook & Schmidt, 2008). For mice, such an event is mimicked during the acquisition phase of the SFC paradigm, in which the social contact to an unknown conspecific is punished by pairing the contact with an electric foot shock (Toth et al., 2012). During associative and extinction learning including memory formation and consolidation processes, plasticity events take place, which weaken existing and strengthen new or already established synapses (El-Boustani et al., 2018; Hagena & Manahan-Vaughan, 2012; Ho et al., 2011). Intriguingly, lncRNAs embody many different functions within the brain and overall, they are accepted to be regulated by neuronal activity and to control neuronal plasticity (Maag et al., 2015). In line with this, I found variants of the lncRNA Meg3 containing the alternative long exon 10A (Figure 5) to be dynamically regulated within the septum, a brain region highly and differentially activated during SFC (Menon et al., 2018; Zoicas et al., 2014). Interestingly, septal Meg3 was regulated in an inverse manner for social fear acquisition and social fear extinction learning. 24 h after associative learning during social fear acquisition, SFC$^+$ animals displayed significantly downregulated levels, whereas animals that underwent social fear extinction training and successfully extinguished social fear restored Meg3 to a level comparable to SFC$^-$ mice (Figure 13).

Abovementioned opposing regulation might be based on different types of learning during fear acquisition and fear extinction. Different theories characterize fear acquisition typically as associative learning about a positive relationship between a neutral stimulus and an aversive stimulus, whereas fear extinction is rather described as a new learning process about their negative relationships that dissociates the conditioned and aversive stimulus. The acquisition memory itself stays intact after fear extinction, as spontaneous recovery is still observed (Rescorla & Heth, 1975; Tronson et al., 2013). Another model associates fear extinction with a value change and reinterpretation of the conditioned stimulus when the confrontation is less aversive than expected, which consequently induces a feeling of safety (Gershman et al., 2010; Redish et al., 2007). In this context, several molecules such as protein kinases PKC, CDK5, PKA and FYN within the HPC, or GTPase proteins Ras and Rab interactor 1 within the amygdala have been shown to play opposite roles in fear acquisition and extinction in contextual fear conditioning (Ahi et al., 2004; Bliss et al., 2010; Fischer et al., 2002; Isosaka et al., 2008). This inverse relationship could also explain the expression pattern of Meg3 in the context of social fear. This idea is further supported by the fact that mice lacking a successful extinction learning process, and therefore, also the regain of social contact (SFC$^+$/Ext$^+$ (unsuc)), still expressed Meg3 at lower levels than SFC$^-$/Ext$^+$ and SFC$^+$/Ext$^+$ (suc) mice (Figure 12) resulting in a positive correlation of Meg3 levels with investigation levels at the end of extinction training. To rule out that social contact is responsible for Meg3 regulation, I quantified Meg3 levels after repeated social interaction. Here, I could not observe any effects on Meg3 expression levels indicating that learning processes are responsible for its regulation (Figure 14). This is also supported by reduced Meg3 levels in mice that were not allowed to extinguish social fear during social fear extinction training as they were only exposed to novel empty cages instead of different conspecifics. These findings demonstrate that the maintenance of social fear goes along with the maintenance of reduced Meg3 levels. To shed further light on whether learning processes have to involve a social component for Meg3 regulation within the septum, I performed operant fear conditioning with an inanimate object, i.e. a white ball, as neutral stimulus. Unfortunately, low fear acquisition rates and reduced investigation levels of the neutral stimuli during extinction training were observed. Non-social stimuli depict a less arousing stimulus compared to social ones, as the latter also activates sensory senses with e.g. odour, vocalization, and active movements (Jacobs & Smith, 1960; Ryan et al., 2009). Therefore, the object might have been less interesting and distinguishable, resulting in low fear acquisition und reduced motivation to investigate the object. Adding an attractive odour to the white ball or increasing its size might help to raise attractiveness and prominence as stimulus and lead to

more defined behavioural readouts for future experiments assessing the importance of social learning.

The striking difference in Meg3 expression levels in SFC^+/Ext^+ (suc) and SFC^+/Ext^+ (unsuc) mice 90 min after social fear extinction training drives the attention also on the topic "susceptibility and resilience". Susceptibility and resilience are extensively discussed for various interventions and in case of non-responders for SAD treatments, which are represented by the SFC^+/Ext^+ (unsuc) mice. Why do some animals easily extinguish social fear and others are resistant to extinction training, and how might Meg3-signalling be involved? From a translational point of view, social fear extinction training is equivalent to exposure therapies in humans. For humans, numerous therapeutic approaches are available, but still revealing a high rate of non-responders (de Menezes et al., 2007). Current treatment options usually use a combination of cognitive behavioural therapies and medication (Leichsenring & Leweke, 2017). However, traditional behavioural therapies that include relaxation training, identification and modification of negative thoughts, soft skill training and exposure to feared situations, seem to be less effective for SAD than for other types of anxiety, which is also reflected by an increased number of needed sessions (Robinson et al., 2019). Application of effect-cumulative substances like D-cycloserine, a broad-spectrum antibiotic and partial N-methyl-D-aspartate receptor agonist, prior to extinction/exposure therapy in animal models for conditioning and SAD patients indeed improved extinction augmentation, however positive effects diminished after the first sessions (Hofmann et al., 2006; Sartori et al., 2016). Other current pharmacological interventions mainly use antidepressants, benzodiazepines and anticonvulsants, being cautiously applied due to partially tremendous side-effects (Blanco et al., 2013). The first-line pharmacological treatments are selective serotonin reuptake and serotonin norepinephrine reuptake inhibitors that have a favourable-side effect profile and high efficacy. Benzodiazepines show partial effects, nevertheless, they should be avoided due to sedative effects, impairment of cognition and abuse potential (Blanco et al., 2013; Farach et al., 2013). However, even in promising clinical trials, there is still a high rate of non-responders to medications and only 35 - 65 % of pharmacologically treated patients show positive, symptom-alleviative effects (Davidson, 2003). Different sources of non-response are possible. In some cases, the intake-period of particular drugs is too abruptly stopped, which was exemplified by a study showing that 27.7 % of non-responders to 8 weeks-paroxetine treatment (selective serotonin reuptake inhibitor) showed treatment effects after 12 weeks (Stein et al., 2002). Asides from that, several studies investigated optimal treatment duration suggesting a time frame between 3 to 6 months after the patient responded to treatment in order decrease the relapse rate that occurs after a

short treatment period (Blanco et al., 2013). Other important factors are that some patients do not follow their medication plan and therefore, optimal doses and duration of treatment are not guaranteed. Moreover, there is only sparse literature available investigating the influence of co-morbid psychiatric disorders like depression on non-response. Hence, interfering properties stay elusive. Other reasons for non-response, but also higher susceptibility for certain diseases may include individual metabolic characteristics and differential molecular signalling caused by genetics or environmental factors (Royer et al., 2019).

Using the analogy of social fear extinction training and exposure therapy for humans, mice of the SFC$^+$/Ext$^+$ (unsuc) group that do not show proper social fear extinction, can be classified as non-responders to extinction training or as animals with higher susceptibility to social fear, and hence, overcoming this fear is more difficult for them. As I found Meg3 to be differentially regulated in SFC$^+$ animals, which showed different extinction patterns, one can speculate that Meg3 and its downstream signalling are involved in this different outcome, or that Meg3 may be considered as a marker of extinction success resulting from modified signalling cascades upstream of Meg3 transcription. With respect to upstream signalling of Meg3 expression, hypermethylation of the promoter region and reduced binding of cAMP response element-binding protein at the promoter are the most investigated mechanisms that cause reduced expression of Meg3 (He et al., 2017; Zhao et al., 2006). However, mechanisms for Meg3 regulation during the SFC paradigm were not investigated in the scope of this thesis. Hence, I can only hypothesize that above-mentioned mechanisms are involved in regulating Meg3 expression in SFC$^+$/Ext$^+$ (unsuc) mice and aim to address this question in future research.

Regarding downstream effects, Meg3 was described to induce LTP *in vitro* and *in vivo*, to be regulated after associative learning (Tan et al., 2017) and to improve memory formation in a model of AD within the HPC (Yi & Chen, 2019). These facts and the proven interconnectivity of the HPC and the septum for the evaluation of information and regulation of memory formation and response reactions (Sheehan et al., 2004) led me to hypothesize that social approaches trigger extinction learning that activates the *Meg3* locus within the septum, leading to increased Meg3 expression in successfully extinguishing animals. Meg3 could take over similar regulatory functions as shown in cued fear conditioning during associative learning (Tan et al., 2017), and hence, support LTP and synaptogenesis that finally help to overcome social fear. For studying the functions of Meg3 in SFC, two approaches, overexpression and knockdown, are suitable. I started with loss-of-function experiments to address whether Meg3 knockdown impairs social fear extinction or extinction memory formation. First, I evaluated antisense LNA GapmeRs in their efficiency and distribution and, using the optimal GapmeR

conditions, induced the Meg3 knockdown within the septum after social fear acquisition to influence only the extinction training (Figure 17). Here, SFC[-] knockdown animals showed no altered social motivation as they investigated the social stimuli to a similar level as SFC[-] control animals. SFC[+] knockdown mice were socially fearful at the beginning of the extinction training and extinguished social fear similarly to SFC[+] control. However, SFC[+] knockdown mice tend to investigate the conspecifics less than the SFC[+] control group at the end of the extinction training. A similar gradient of investigation levels was observed when Meg3 knockdown was induced prior to social fear acquisition training (Figure 18). The knockdown did not interfere with social fear acquisition as the same number of shocks was applied to induce social avoidance during acquisition training. In summary, the highly efficient knockdown of the long Meg3 variants resulted only in slightly modified behavioural phenotypes, which were not as pronounced as the naturally occurring extinction behaviour in SFC[+]/Ext[+] (unsuc) mice. Importantly, however, Meg3 mainly takes over regulatory functions that might fine-tune reactions and prime cells for synaptogenesis and therefore, expecting on/off-effects on behaviour would be optimistic. Besides, it is not known whether other compensatory mechanisms already occur, as the incubation time for the antisense LNA GapmeRs was 72 h in order to let the animals recover from anaesthesia and surgery. To determine septal Meg3 knockdown effects on extinction memory formation and its subsequent long-term consolidation, I additionally tested social fear recall three weeks after extinction training with a subset of animals. The time frame of three weeks was chosen based on literature for non-social recall showing time frames of one day for short-term, and up to weeks for long-term recall testing (Mikics et al., 2017; Tumolo et al., 2018). I observed that SFC[+] Meg3 knockdown mice spent significantly less time investigating the first stimulus during recall training than SFC[-] controls, however the investigation time for the second stimulus was similar (Figure 19). The animals were single-housed during the three weeks after extinction training to prevent additional social contact interfering with social fear memory in case extinction memory could not be consolidated due to Meg3 knockdown. Presentations of conspecifics represent strong stimuli as the reaction to such stimuli is important for daily life and survival. Hence, many mouse strains show high grades of sociability and social preference (Hsieh et al., 2017; Moy et al., 2004). Possibly, the period of isolation after the extinction training may have been too long. Thus, even if extinction memory might not have been properly consolidated, there might be a strong inner conflict of social fear with the innate curiosity of novelty and especially territorial defence behaviour when a novel conspecific was presented within the home cage. For some animals, I observed aggressive behaviour towards the presented stimuli, visualized by bite-attacks through

the gaps of the empty wire-mesh cage. One study showed that social isolation for two weeks induced pronounced offensive aggressive behaviour in mice (Zelikowsky et al., 2018), and hence, this possible inner conflict between still manifested social fear and social aggression should be taken into account and a shorter period for social recall training should be considered.

For follow-up experiments, Meg3 overexpression studies are planned to reveal whether Meg3 facilitates LTP in SFC, and therefore, could also improve social fear extinction. However, overexpression of the Meg3 variants of interest is challenging because of the variants' transcript length of more than 11 kb.

4.2   PI3K/AKT signalling in context of social fear extinction and Meg3 KD

Interestingly, two rodent studies positively linked Meg3 expression with activated PI3K/AKT signalling during LTP (Tan et al., 2017; Yi & Chen, 2019). The PI3K/AKT signalling is very well investigated as a promoter of cell survival. Moreover, it is involved in learning and memory processes regulating synaptic plasticity (Horwood et al., 2006). Here, PI3K/AKT signalling regulates AMPAR trafficking and insertion into the membrane (Man et al., 2003; Tan et al., 2017) and is necessary for LTP in different brain areas, which was shown by PI3K inhibition studies in mice and rats (Lin et al., 2001; Opazo et al., 2003; Sanna et al., 2002). Other studies showed that inhibition of PI3K/AKT signalling interferes with fear acquisition, consolidation, extinction and retrieval in animal models for non-social fear learning (Barros et al., 2001; X. Chen et al., 2005; Lin et al., 2001). SFC, like any other associative learning processes, requires enhanced synaptogenesis and synaptic plasticity during learning events and as Meg3 was dynamically regulated, especially within the context of extinction, the PI3K/AKT signalling pathway was likely involved. Western blot analyses exhibited a significantly activated PI3K represented by increased phosphorylated P85, and higher levels of phosphorylated AKT at Ser473 in SFC[+]/Ext[+] (unsuc) samples 3 h after extinction training (day 2, Figure 20). As extinction learning processes are activated during successful extinction, activated PI3K/AKT signalling would have been expected especially in the SFC[+]/Ext[+] (suc) group, however, no changes were found for 90 min and 3 h after social fear extinction training. It is reported that phospho-AKT signalling can be sustained between 1-2 h after stimulation (Bruss et al., 2005; Kubota et al., 2012; Yudushkin, 2019) and therefore, it is possible that the activation peak of PI3K/AKT was missed in SFC[+]/Ext[+] (suc) mice under the assumption that first social approaches already started to induce LTP. By average, SFC[+]/Ext[+] (suc) mice started to approach conspecifics during the second social stimulus presentation and showed comparable

investigation levels to SFC$^-$ mice from the fourth social stimulus on. Considering the time from the first approach in the case of SFC$^+$ or from the fourth stimulus until 90 min after extinction training, phosphorylation levels were investigated approximately 2 h after stimulation, which is probably too late for detecting changes in the SFC$^+$/Ext$^+$ (suc) group. Supporting this, I found total AKT to be downregulated in SFC$^+$/Ext$^+$ (suc) animals 3 h after extinction training, which is in line with findings of a recent study showing that dephosphorylation of AKT goes along with its own degradation (Wei et al., 2019).

In contrast, in the SFC$^+$/Ext$^+$ (unsuc) group, PI3K/AKT signalling just started to become activated 3 h after social fear extinction training. Activation of the PI3K/AKT signalling pathway starts usually with the phosphorylation of the catalytic subunit P85 of PI3K. PI3K then produces PIP3 that recruits inactive AKT from the cytoplasm to the membrane. Phosphorylation of AKT Thr308 by PDK1 activates AKT, whereas additional, but optional, phosphorylation of AKT Ser473 potentiates kinase activity. However, there is convincing evidence, that phosphorylated AKT Ser473 primes AKT conformation for a better interaction with PDK1, therefore facilitating AKT Thr308 phosphorylation (Sarbassov et al., 2005; Scheid et al., 2002; Yang et al., 2002). My results exactly reflect the aforementioned mechanisms. 3 h after social fear extinction training, PI3K was significantly activated and AKT Ser473 phosphorylation was already induced. At this stage, phospho-AKT Ser473 seems to facilitate the phosphorylation of Thr308, indicated by a slight increase of phospho-AKT Thr308 in the SFC$^+$/Ext$^+$ (unsuc) group, without reaching significance yet. Moreover, there is evidence that already partial AKT activation at the Ser473 residue is sufficient to mediate plasticity and memory consolidation (Horwood et al., 2006). The question as to why there is such a delayed activation of the PI3K/AKT observed in SFC$^+$/Ext$^+$ (unsuc) mice, still needs to be discussed and further investigated. One possible explanation could be that animals of the SFC$^+$/Ext$^+$ (unsuc) group do not show any contact to presented social stimuli or start to approach only at the end of the extinction training. After no (or only a few) contact moments, we cannot expect that these mice immediately start to form extinction memory. These contacts can certainly act as a first trigger but as the extinction training is stopped before the animals achieved a long-lasting contact, it is more likely that animals struggle between social fear expression and the uncertainty whether this contact without being linked to an aversive event happened by chance. This might lead to the activation of other LTP-linked signalling pathways such as the TrkB signalling pathway (Minichiello, 2009), and to delayed LTP regulated *via* the PI3K/AKT signalling. As Meg3 was shown to be upregulated with LTP stimulation in *in vitro* and *in vivo* studies (Tan et al., 2017) and to control PI3K/AKT signalling, Meg3 downregulation in

SFC$^+$/Ext$^+$ (unsuc) group 90 min and 3 h after extinction probably contributes to delayed activation of PI3K and AKT.

To elucidate the impact of Meg3 on the PI3K/AKT signalling pathway after social fear extinction training, I determined its activation in control and Meg3 knockdown samples 90 min after social fear extinction (Figure 21). SFC$^+$ control mice showed a strong activation of P85 compared to SFC$^-$ control mice. In contrast, Meg3 knockdown prevented this effect. Interestingly, phosphorylated P85 seemed to be increased under basal conditions in Meg3 knockdown mice, which would be in line with previous findings by Tan et al. showing that Meg3 knockdown, induced 48 h prior to primary neurons stimulation, leads to an activated PI3K/AKT signalling pathway under basal conditions, whereas further activation was prevented during LTP (Tan et al., 2017). Other effects on AKT phosphorylation or PTEN could not be detected, however, the lack of effects has to be taken with caution since some groups were statistically underpowered. Samples were split for RNA/protein analysis and analysis of GapmeR distribution, thus, additional experiments have to be performed to increase sample numbers. Besides, extinction training of the Meg3 knockdown experiments was performed 4 days after social fear acquisition because the antisense LNA GapmeRs were microinfused one day after acquisition and incubation time was 72 h. Hence, the time schedule of Meg3 knockdown experiments differs from the common SFC protocol, which might explain the differences of the SFC$^-$ control and SFC$^+$ control groups of the Meg3 knockdown experiments to the SFC$^-$/Ext$^+$ and SFC$^+$/Ext$^+$ groups of the common SFC experiments.

From a different, namely the metabolic perspective, AKT is also proven to be regulated in the context of insulin signalling (Gabbouj et al., 2019; Kumar et al., 2010). Glucose uptake is essential during learning and memory processes and mainly taken up by neurons *via* the glucose transporter 3 (Clodfelder-Miller et al., 2005; Mergenthaler et al., 2013). One study even showed that intraseptal glucose administration attenuated memory impairment in a morphine-based model for impaired memory (McNay & Pearson-Leary, 2020). Others revealed a special role of phospho-AKT Ser473 during glucose uptake in the periphery and in the brain (Gabbouj et al., 2019; Kumar et al., 2010). Therefore, metabolic processes might also explain and contribute to alterations in AKT signalling. Interestingly, various studies linked peripheral Meg3 signalling to insulin synthesis, secretion and resistance (Sathishkumar et al., 2018; You et al., 2015; Zhu et al., 2016). However, investigation of peripheral Meg3 levels and whether they are linked to altered Meg3 expression within the brain in context of social fear, as well as general changes in metabolism were beyond the scope of this thesis.

In summary, I could show that the PI3K/AKT signalling pathway within the septum is specifically regulated in a time and extinction success-dependent manner, which shows parallels to septal Meg3 regulation. Meg3 knockdown experiments clearly showed a differential regulation of active PI3K, however, an increased samples size and a more detailed time-resolution including earlier time points than 90 min and later time points than 3 h will clarify open questions and above-mentioned hypotheses. Nevertheless, the data point towards a regulatory role of Meg3 for the PI3K/AKT signalling pathway in context of social fear extinction within the context.

4.3 Effects of social fear extinction on chromatin accessibility and H3K27me3 histone modifications

Many studies show that Meg3 functions mainly within the nucleus (Reddy et al., 2017; Zhang et al., 2014). With RNAscope, an *in situ* hybridization technique, I was able to confirm this showing an exclusively nuclear localization of Meg3 after social fear extinction within the septum (Figure 15). Hence, Meg3 likely interacts with factors that modulate transcription and chromatin states resulting in differentially regulated gene expression. So far, Meg3 has been shown to interact with PRC2, which introduce methyl groups at H3K27 (Kaneko et al., 2014; Mondal et al., 2015; Wang et al., 2018). Thus, ATAC-Seq and CUT&RUN for H3K27me3 were performed to identify potential downstream action site of Meg3. ATAC-Seq resulted in specific chromatin profiles of neurons from the septum as neuronal nuclei were FAC-sorted. For CUT&RUN, nuclei from all cell-types had to be used due to the high number of cells needed for the protocol. However, as Meg3 is almost exclusively expressed in neurons (Figure 15; Zhang et al., 2014), differences found in SFC[+] control and SFC[+] Meg3 knockdown groups should represent mainly neuronal expression alterations linked to Meg3. Nevertheless, effects might be diluted due to signals originating from other cell types. Moreover, it has to be taken into account that even if H3K27me3 is usually linked to inactive chromatin region, the combination with other histone modifications, forming a part of the epigenetic code, might result in active chromatin states (Royer et al., 2019). Therefore, more detailed bioinformatical analyses and the combination with ATAC-Seq data are necessary to identify regulated chromatin regions that are relevant in the context of social fear extinction and linked to Meg3. Additionally, identifying genes that are found in the comparison SFC[+]/Ext[+] (suc) vs. SFC[+]/Ext[+] (unsuc) and in SFC[+] control vs. SFC[+] Meg3 knockdown potentially limits the number of regulatory function sites of Meg3 as in both comparisons Meg3 expression levels are differentially expressed in compared groups. These

data will help to get a better understanding of Meg3 downstream signalling, which might be relevant in controlling social fear extinction and its consolidation.

4.4 Time-shifted expression of Sgk1 in mice with successful and unsuccessful extinction

Another RNA candidate that has been chosen for closer examination was the serum and glucocorticoid inducible kinase 1, Sgk1. *Sgk1* is an immediate early gene and its transcription is regulated by various stimuli like serum and glucocorticoids (Lang et al., 2006), which are released for example in the context of fear conditioning (dos Santos Corrêa et al., 2019). SGK1 becomes activated upon PI3K signalling, in which PI3K triggers the phosphorylation of SGK1 at Ser422 by mTORC2, and subsequently at Thr256 by PDK1 (Di Cristofano, 2017). Due to the short half-life of approximately 20 min for mRNA and 30 min for protein (Brickley et al., 2002; Di Cristofano, 2017; Firestone et al., 2003), it is challenging to identify critical time points.

Investigation of Sgk1 expression levels revealed differentially regulated mRNA and protein peaks of the SFC^+/Ext^+ (unsuc) group (Figure 25). Sgk1 mRNA levels seemed to be lower 30 min after social fear extinction training in SFC^+/Ext^+ (unsuc) mice (n = 2), whereas levels were significantly upregulated compared to SFC^-/Ext^+ after 90 min. On a protein level, time-shifted changes were observable as at 90 min, SGK1 was still significantly downregulated in SFC^+/Ext^+ (unsuc), while after 3 h, the levels were restored or even seemed to be higher compared to SFC^+/Ext^+ (suc) and SFC^-/Ext^+. Overall, these findings show parallels to the results for the PI3K/AKT signalling pathway after social fear extinction training. SFC^+/Ext^+ (unsuc) mice display a delayed activation of SGK1 signalling, which is known to be regulated during learning and memory processes. Spatial learning experiments were linked to a significant increase of Sgk1 mRNA levels upon learning in fast learning rats compared to slowly learning rats and spatial memory can be impaired by inactivation of SGK1 through phosphatase 2A (Chao et al., 2007; Tsai et al., 2002). Furthermore, contextual fear conditioning and re-exposure to context increase SGK1 expression and SGK1 phosphorylation facilitates LTP in the HPC (Ma et al., 2006; von Hertzen, 2005). Consequently, I hypothesize that SFC^+/Ext^+ (suc) mice have increased levels of Sgk1 mRNA and protein at the end of or briefly after social fear extinction training, whereas SFC^+/Ext^+ (unsuc) show a delayed expression. The delayed expression might occur as learning processes and LTP are triggered to a less extent, and consequently, to a later time point during or after social fear extinction training than SFC^+/Ext^+ (suc). However, a detailed time resolution of mRNA expression, an increased sample size, as well as the validation of phosphorylation

states will help to get a better understanding of SGK1-mediated mechanisms, which might differentially regulate social fear extinction.

4.5   Validation of the RNA candidates and confirmation of the RNA-Seq approach

High-throughput sequencing technologies generate a mass of data that provide an overview of molecules, chromatin areas or sequences that are changed in context of a particular situation or disorder. These sequencing approaches are popular especially for issues, for which little is known on a molecular, RNA or DNA-based, level. For social fear, there is only sparse knowledge about underlying molecular mechanisms available. Therefore, I aimed for a broad overview on SFC-induced alterations within the septum, a brain region of high importance for social fear regulation, with a particular focus on RNA molecules. Focusing on RNA transcription levels offers opportunities to perform research in different directions: investigating protein levels due to subsequent RNA translation of RNAs identified by RNA-Seq and their consequent downstream signalling, as well as action sites of regulatory non-coding RNAs. Based on the Seq-data (Table 11), I have chosen several RNA candidates to be validated by qPCR. These candidates are either known to be linked to anxiety, fear, plasticity, metabolism and neuronal disorders, or are completely unknown in the relevant contexts (Flores et al., 2017; Han et al., 2018; Nogueiras et al., 2013; Yang et al., 2013). Crfr2 was regulated according to the Seq-data and as CRFR2 signalling, especially within the septum, modifies memory and anxiety (Anthony et al., 2014; Radulovic et al., 1999), I validated the mRNA levels 90 min after social fear extinction training. Interestingly, I found no difference between SFC$^+$ and SFC$^-$ mice. Recent studies showed that different splice variants of Crfr2 exist and that one variant results in a soluble form of the CRFR2 (sCRFR2) that competes for ligand binding (A. M. Chen et al., 2005). Moreover, sCRFR2 positively correlates with levels of anxiety-like behaviour (Winter et al., in preparation). Hence, I determined its expression levels 90 min after social fear extinction training and I found that in general sCrfr2 mRNA levels seemed to be higher in SFC$^+$ animals, but independent of extinction success. This result can be interpreted to be in line with findings from Winter et al., however, samples size has to be increased in order to achieve a valid statement (Figure 26). The regulation of other chosen candidates like Irak1, the IL-1 receptor-associated kinase 1, and Gm13157, a zinc finger protein, could not be verified by qPCR, whereas the fold changes of Plin4 and Nlrp5-ps were changed in the expected direction, but due to high variance within the SFC$^-$ group no significance was reached. Sirt1, a NAD-dependent deacetylase, and Hcrtr2, the orexin receptor 2, were predicted to be upregulated 90 min after social fear extinction but instead, I found a significant up-regulation of Hcrtr2 after 3 h; for

Sirt1, a similar regulation was found. An in-depth analysis of these targets and the mechanisms by which they might regulate social fear extinction was beyond the scope of this thesis, but importantly, the validation of above-mentioned RNA candidates was used as confirmation of the RNA-Seq approach.

Summing up, the RNA-Seq performed during my thesis presents the first approach to broadly characterize social fear acquisition and social fear extinction on a RNA-based level. However, it has to be considered that total septum punches, containing several different cell types like neurons and various glia cells, were used for RNA isolation, and therefore, found effects might be diluted. Due to the high number of groups (in total seven groups), only triplets, which is the minimum of recommended samples, could be used for the unconditioned and conditioned groups. A higher number of samples per group would potentially reveal more significant results, especially as individual variance plays an important factor. Natural variation and variance in behaviour, and therefore in RNA and protein expression levels in the brain, have an impact on sequencing results. Even though the SFC represents a very robust model for inducing social fear and extinction learning, there is still an individual bias, which is in the case of here generated data also represented in the PCA plots (Figure 10B, Figure 11A). The gene expression patterns within one group slightly spread and do not cluster as strong as usually seen e.g. in *in vitro* experiments. This is a common issue and a recent study exemplified this as they found 48 % of tested metabolic genes were differentially expressed in different tissues, including the brain, of fish individuals within one population that were raised under controlled laboratory conditions (Whitehead & Crawford, 2005). Here, the differences are unlikely caused by environmental factors as they were adapted and fed in the same way. The observed differences in expression might origin from the genetic background or heritable epigenetic modifications. Moreover, there are several analysis pipelines available for RNA-Seq analysis and depending on the focus of the research question, some are more suitable than others. In this study, we focused on the analysis that used the aligner StringTie, which is preferably used in order to detect also new, not annotated transcripts. The choice of the RNA-Seq pipeline has tremendous impact on the outcome as a recent study showed that > 12 % of protein coding genes differ in their abundance estimates by more than four-fold even when the same samples and RNA-Seq reads were used in different analysis pipelines (Arora et al., 2020). Nevertheless, RNA-Seq is a powerful tool to study disorders, however, the workflow and analysis pipelines, as well as the RNA candidates for further investigation have to be critically chosen and validated with other methods.

4.6 The important role of the septum especially for social fear extinction

For the Seq-approaches and *in vivo* experiments, I focused on the septum, a highly connected area, receiving mainly input from the HPC and sending projections to the amygdala, hypothalamus and others (Deng et al., 2019; Sheehan et al., 2004). It plays a substantial role as a relay station in context of memory formation, fear, and general emotional reactions. During SFC, the septum has been proven several times to regulate social fear expression (Menon et al., 2018; Zoicas et al., 2014) and the data obtained in the present thesis supports its importance.

I observed that unilateral damage of the LS is sufficient to abolish social fear extinction even if the number of presented conspecifics was increased (Figure 27). Importantly, the damage that was caused by the implantation of a microdialysis probe is usually negligible. Microdialysis is a well established and often used tool to investigate neurotransmitter release within the brain or to apply certain substances (Zapata et al., 2009). This further demonstrates the sensitivity and the importance of the LS for social fear extinction. Other septal lesion studies observed impaired social olfactory recognition and exaggerated freezing behaviour during fear conditioning, which are also important aspects for social fear extinction (Sparks & LeDoux, 1995; Terranova et al., 1994). In future studies, cell type-specific damage induced by antibody-coupled immunotoxins or excitotoxic substances will help to unravel the involvement of cholinergic and GABAergic neurons separately in context of social fear conditioning (Pang et al., 2011; Vuckovich et al., 2004; Wallace & Rosen, 2001; Wetmore et al., 1994).

The role of the septum in SFC is additionally supported as the regulation of the long Meg3 variants was specifically observed within the septum, and not within the HPC. In contrast, other studies found other Meg3 variants to be regulated during fear conditioning paradigms or in AD and other neuropsychological disorders within the HPC (Tan et al., 2017; Yi & Chen, 2019). During the investigation of hippocampal Meg3 levels, separate statistics revealed only a trend for Meg3 variants of interest to be downregulated 3 h after social fear extinction training within the dHPC of successful extinguishing animals (Figure 24). The HPC is a cortical structure, which belongs to the limbic system and is on the longitudinal axis divided into the dorsal, intermediate and ventral HPC. The dHPC is suggested to be responsible for cognitive functions, whereas the ventral part deals with affective issues like emotional behaviour. However, newest studies show that there is a strong link between expression patterns and structural connectivity leading to an even more detailed partition than into CA1, CA3, dentate gyrus and subiculum (Bienkowski et al., 2018). Meg3 is usually strongly regulated in context of learning and memory processes within the HPC, therefore, it is even more surprising that no significant alterations were found after social fear extinction, which involves cognitive as well as affective processes (Tan et al., 2017;

Yi & Chen, 2019). However, those studies investigated the short Meg3 variants, which might be differentially regulated than the long Meg3 variants I focused on during the thesis. Moreover, a more region-specific investigation within HPC subregions might be necessary.

4.7   Conclusion and future perspectives

The present study provides insights into the regulation of RNA molecules after social fear acquisition and social fear extinction in male mice. With a special focus on the lncRNA Meg3, I showed that alternatively spliced Meg3 variants were dynamically regulated specifically within the septum (Figure 28). Here, Meg3 levels were regulated in an extinction-success dependent manner with a negative correlation to fear levels. Moreover, I could show that learning processes are responsible for its regulation. I established a highly efficient and locally applicable knockdown system with antisense LNA GapmeRs and knockdown experiments supported a facilitating role of Meg3 during extinction training. In addition to altered Meg3 levels after social fear extinction, the PI3K/AKT signalling pathway was regulated in dependence of the extinction success. Additionally, I could link these alterations to Meg3, as preliminary results from knockdown experiments showed differences in PI3K activation in control and Meg3 knockdown mice after extinction training.

Taken together, the presented results extend first insights into the molecular complexity of social fear and its extinction, which involves olfactory senses, learning processes as well as memory formation and consolidation, with regard to RNA molecules. They highlight especially the role of one lncRNA in fine-tuning behaviours, in the present case by modifying signalling pathways and chromatin accessibility as revealed by ATAC-Seq and CUT&RUN experiments (see 3.3 and 3.4). The here generated data provide, one the one hand, an overall characterization of the SFC on a RNA and chromatin level for future research, also including social fear acquisition. On the other hand, the characterization of Meg3 and PI3K/AKT signalling pathway (Figure 28) represents pioneer work for deeper research, especially focusing on the translational aspect given with the parallels of extinction training and exposure therapies in humans. Detailed knowledge about Meg3 regulation and its downstream signalling can provide new starting points for the development of therapeutics that support humans during exposure therapies and hence, helps to successfully extinguish social fear.
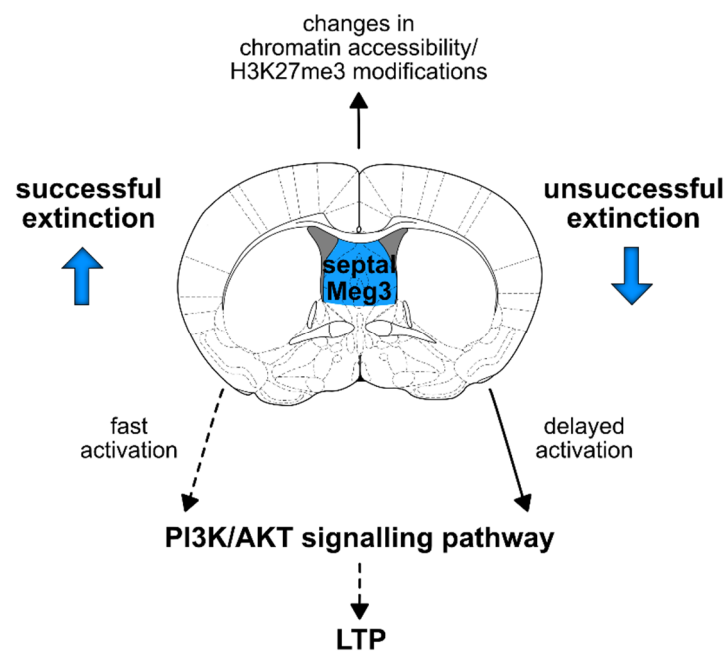
Figure 28 Signalling scheme of known (bold arrows) and hypothetical (dashed arrows) interactions of Meg3 and the PI3K/AKT signalling pathway in the context of social fear extinction.

In future experiments, I want to correlate ATAC-Seq, CUT&RUN and RNA-Seq data to identify additional candidates, and particularly, candidates that are regulated by Meg3. Here, *Cwc22*, coding for a spliceosome-associated protein, and doublecortin-like kinase 3, *Dclk3*, are interesting candidates as their locus accessibility is similarly regulated in SFC$^+$/Ext$^+$ (unsuc) and Meg3 knockdown groups, which represent mice with lower Meg3 levels, compared to their counterparts in SFC$^+$/Ext$^+$ (suc) and control groups, with high Meg3 expression (Figure 22). In case a correlation of these targets with Meg3 expression can be proven, gain- and loss-function studies will help to identify their function and targets.

Additionally, assessing the expression levels of the short Meg3 variant, even if the StringTie/ prepDE.PY/DeSeq2 analysis pipeline did not reveal distinct significances, will give a global overview of the regulation of the Meg3 locus in SFC. The most investigated and abundant Meg3 variant is NR_027652.1 with ~ 1.9 kb (Zhu et al., 2019). Thus, a more detailed temporal resolution of its expression levels and region-specific examination after social fear acquisition and extinction is also from high biological relevance. In parallel, the role of the alternatively long exon 10 will be co-addressed, as a shift in alternative splicing events, like shown for the membrane bound CRFR2 and sCRFR2 in anxiety-like behaviour (Winter et al, in preparation), might be relevant in context of SFC (Figure 5). Depending on the outcome, tools such as plasmid application *via* osmotic minipumps (Yi & Chen, 2019) for specific expression of the

shorter Meg3 variant (~ 1.9 kb) or newest methods like the neuron-optimized CRISPR/dCas9 activation system (Savell et al., 2019), which can induce expression of the *Meg3* locus *in vivo*, will be considered in order to study potential positive effects of Meg3 upregulation in context of social fear extinction.

Moreover, as the here generated data give first indications for a differentially regulated PI3K/AKT signalling pathway after social fear extinction and in Meg3 knockdown mice, collection of more samples will further elucidate its role in social fear and the role of Meg3 in its regulation. In line with this, it would be also interesting to examine more closely the role of mTORC2, as two downstream targets, AKT and SGK1, were regulated after social fear extinction. This will help to complete the characterization of the PI3K signalling pathway in SFC and provide further starting points for treatment options.

In addition, the potential upregulation of sCrfr2 in SFC$^+$ mice should be clarified as in case of confirmation, the CRFR2 system represents a well investigated system providing many tools and background information for focused studies of its role in SFC. The CRFR2 expression is restricted to mainly limbic regions associated with social behaviours (Elharrar et al., 2013; Shemesh et al., 2016; Wagner, 2019). Hence, an involvement in social fear would be plausible. Moreover, Winter and colleagues showed a correlation of sCRFR2 and anxiety-like behaviour after a mild stressor. As the SFC paradigm shows parallels combining stressful events such as a new context and electric foot shocks during social fear acquisition with testing for social fear levels during the extinction training, one could speculate that sCRFR2 might take over similar functions in both contexts.

Last, cell type-specific chemical lesion as already mentioned in 4.6 should be performed to restrict the number of relevant cell types enabling a more focused research on social fear and the septum in order to find specific treatment options for SAD.
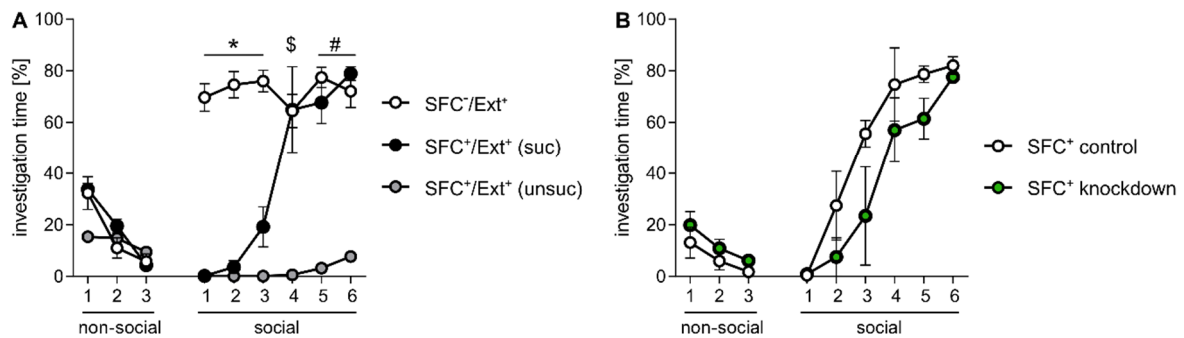
APPENDIX

Appendix

Figure 29 Social fear extinction behaviour of samples used for ATA-Seq.

(A) SFC$^-$/Ext$^+$ mice show significantly higher investigation times for the first three stimuli compared to SFC$^+$/Ext$^+$ (suc) and SFC$^+$/Ext$^+$ (unsuc) (*p < 0.05). SFC$^+$/Ext$^+$ (unsuc) investigated the fourth social stimuli significantly less compared to SFC$^-$/Ext$^+$ ($p = 0.05) and showed decreased investigation levels for stimulus 5 and 6 compared to both groups (#p < 0.05 vs. SFC$^+$/Ext$^+$ (suc) and vs. SFC$^-$/Ext$^+$). Two way ANOVA: group effect $F_{(2, 6)}$ = 67.88, p < 0.0001; group x time $F_{(16, 48)}$ = 24.05, p < 0.0001. Bonferroni's post hoc test: see *p, $p, #p. (B) SFC$^+$ control and SFC$^+$ knockdown mice similarly increased investigation levels of the social stimuli during the social fear extinction training. Two way ANOVA: group effect $F_{(1, 4)}$ = 2.219, p = 0.2105; group x time $F_{(8,032)}$ = 1.735, p < 0.1282. n = 3 per group.
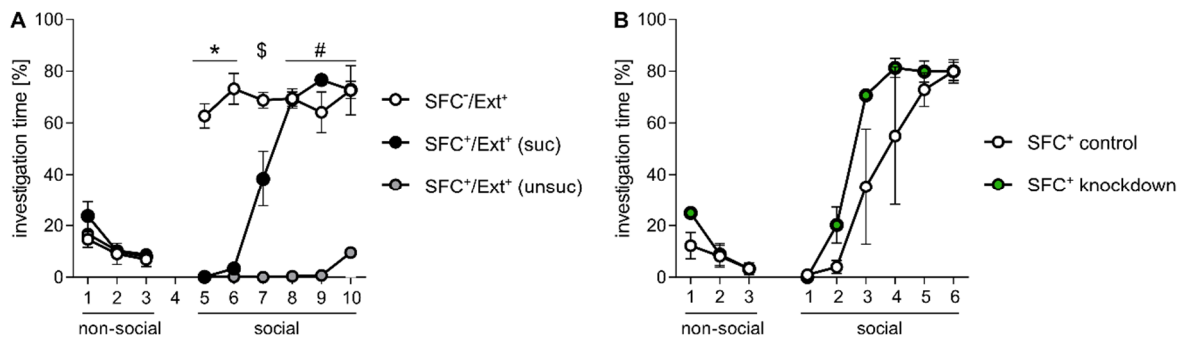

Figure 30 Social fear extinction behaviour of samples used for CUT&RUN.

(A) SFC$^-$/Ext$^+$ mice show significantly higher investigation times for the first two stimuli compared to SFC$^+$/Ext$^+$ (suc) and SFC$^+$/Ext$^+$ (unsuc) (*p < 0.05). SFC$^+$/Ext$^+$ (unsuc) investigated the third social stimuli significantly less compared to SFC$^-$/Ext$^+$ ($p = 0.05) and showed decreased investigation levels for stimulus 4 to 6 compared to both groups (#p < 0.05 vs. SFC$^+$/Ext$^+$ (suc) and vs. SFC$^-$/Ext$^+$). Two way ANOVA: group effect $F_{(2, 6)}$ = 70.58, p < 0.0001; group x time $F_{(16, 48)}$ = 27.05, p < 0.0001. Bonferroni's post hoc test: see *p, $p, #p. (B) SFC$^+$ control and SFC$^+$ knockdown mice similarly increased investigation levels of the social stimuli during the social fear extinction training. Two way ANOVA: group effect $F_{(1, 4)}$ = 2.102, p = 0.2207; group x time $F_{(8, 32)}$ = 1.449, p < 0.2150. n = 3 per group.

REFERENCES

References

Ahi, J., Radulovic, J., & Spiess, J. (2004). The role of hippocampal signaling cascades in consolidation of fear memory. *Behavioural Brain Research*, *149*(1), 17–31.

Ali, M. S. S. H., Cheng, X., Moran, M., Haemmig, S., Naldrett, M. J., Alvarez, S., Feinberg, M. W., & Sun, X. (2019). LncRNA Meg3 protects endothelial function by regulating the DNA damage response. *Nucleic Acids Research*, *47*(3), 1505–1522.

Amato, R., D'Antona, L., Porciatti, G., Agosti, V., Menniti, M., Rinaldo, C., Bellacchio, E., Soddu, S., Fuiano, G., Perrotti, N., Costa, N., Lang, F., Mattarocci, S., & Paggi, M. G. (2009). Sgk1 activates MDM2-dependent p53 degradation and affects cell proliferation, survival, and differentiation. *Journal of Molecular Medicine*, *87*(12), 1221–1239.

Anthony, T. E., Dee, N., Bernard, A., Lerchner, W., Heintz, N., & Anderson, D. J. (2014). Control of stress-induced persistent anxiety by an extra-amygdala septohypothalamic circuit. *Cell*, *156*(3), 522–536.

Aoto, J., Martinelli, D. C., Malenka, R. C., Tabuchi, K., & Südhof, T. C. (2013). Presynaptic neurexin-3 alternative splicing trans-synaptically controls postsynatpic AMPA-receptor trafficking. *Cell*, *154*(1), 1–24.

Arora, S., Pattwell, S. S., Holland, E. C., & Bolouri, H. (2020). Variability in estimated gene expression among commonly used RNA-seq pipelines. *Scientific Reports*, *10*(1), 1–9.

Astuti, D., Latif, F., Wagner, K., Gentle, D., Cooper, W. N., Catchpoole, D., Grundy, R., Ferguson-Smith, A. C., & Maher, E. R. (2005). Epigenetic alteration at the DLK1-GTL2 imprinted domain in human neoplasia: Analysis of neuroblastoma, phaeochromocytoma and Wilms' tumour. *British Journal of Cancer*, *92*(8), 1574–1580.

Baralle, F. E., & Giudice, J. (2017). Alternative splicing as a regulator of development and tissue identity. *Nature Reviews Molecular Cell Biology*, *18*(7), 437–451.

Bardoni, B., Schenck, A., & Mandel, J. L. (2001). The Fragile X mental retardation protein. *Brain Research Bulletin*, *56*(3–4), 375–382.

Barros, D. M., Mello E Souza, T., De Souza, M. M., Choi, H., DeDavid E Silva, T., Lenz, G., Medina, J. H., & Izquierdo, I. (2001). LY294002, an inhibitor of phosphoinositide 3-kinase given into rat hippocampus impairs acquisition, consolidation and retrieval of memory for one-trial step-down inhibitory avoidance. *Behavioural Pharmacology*, *12*(8), 629–634.

Barry, G., Briggs, J. A., Vanichkina, D. P., Poth, E. M., Beveridge, N. J., Ratnu, V. S., Nayler, S. P., Nones, K., Hu, J., Bredy, T. W., Nakagawa, S., Rigo, F., Taft, R. J., Cairns, M. J., Blackshaw, S., Wolvetang, E. J., & Mattick, J. S. (2014). The long non-coding RNA Gomafu is acutely regulated in response to neuronal activation and involved in schizophrenia-associated alternative splicing. *Molecular Psychiatry*, *19*(4), 486–494.

Bhat, S. A., Ahmad, S. M., Mumtaz, P. T., Malik, A. A., Dar, M. A., Urwat, U., Shah, R. A., & Ganai, N. A. (2016). Long non-coding RNAs: Mechanism of action and functional utility. *Non-Coding RNA Research*, *1*(1), 43–50.

Bienkowski, M. S., Bowman, I., Song, M. Y., Gou, L., Ard, T., Cotter, K., Zhu, M., Benavidez, N. L., Yamashita, S., Abu-Jaber, J., Azam, S., Lo, D., Foster, N. N., Hintiryan, H., & Dong, H. W. (2018). Integration of gene expression and brain-wide connectivity reveals the multiscale organization of mouse hippocampal networks. *Nature Neuroscience*, *21*(11), 1628–1643.

Biondi, R. M., Kieloch, A., Currie, R. A., Deak, M., & Alessi, D. R. (2001). The PIF-binding pocket in PDK1 is essential for activation of S6K and SGK, but not PKB. *EMBO Journal*, *20*(16), 4380–4390.

Blanco, C., Bragdon, L. B., Schneier, F. R., & Liebowitz, M. R. (2013). The evidence-based pharmacotherapy of social anxiety disorder. *International Journal of Neuropsychopharmacology*, *16*(1), 235–249.

Bliss, J. M., Gray, E. E., Dhaka, A., O'Dell, T. J., & Colicelli, J. (2010). Fear learning and extinction are linked to neuronal plasticity through Rin1 signaling. *Journal of Neuroscience Research*, *88*(4), 917–926.

Braasch, D. A., & Corey, D. R. (2001). Locked nucleic acid (LNA): Fine-tuning the recognition of DNA and RNA. *Chemistry and Biology*, *8*(1), 1–7.

Brady, J. V., & Nauta, W. J. H. (1955). Subcortical mechanisms in emotional behaviours: the duration of affective changes following septal and habenular lesions in the albino rat. *The Journal of Comparative and Physiological Psychology*, *48*(5), 412–420.

Brickley, D. R., Mikosz, C. A., Hagan, C. R., & Conzen, S. D. (2002). Ubiquitin modification of serum and glucocorticoid-induced protein kinase-1 (SGK-1). *Journal of Biological Chemistry*, *277*(45), 43064–43070.

Briggs, J. A., Wolvetang, E. J., Mattick, J. S., Rinn, J. L., & Barry, G. (2015). Mechanisms of long non-coding RNAs in mammalian nervous system development, plasticity, disease, and evolution. *Neuron*, *88*(5), 861–877.

Briz, V., Restivo, L., Pasciuto, E., Juczewski, K., Mercaldo, V., Lo, A. C., Baatsen, P., Gounko, N. V., Borreca, A., Girardi, T., Luca, R., Nys, J., Poorthuis, R. B., Mansvelder, H. D., Fisone, G., Ammassari-Teule, M., Arckens, L., Krieger, P., Meredith, R., & Bagni, C. (2017). The non-coding RNA BC1 regulates experience-dependent structural plasticity and learning. *Nature Communications*, *8*(1), 1–15.

Brook, C. A., & Schmidt, L. A. (2008). Social anxiety disorder: A review of environmental risk factors. *Neuropsychiatric Disease and Treatment*, *4*(1), 123–143.

Bruss, M. D., Arias, E. B., Lienhard, G. E., & Cartee, G. D. (2005). Increased phosphorylation of Akt substrate of 160 kDa (AS160) in rat skeletal muscle in response to insulin or contractile activity. *Diabetes*, *54*(1), 41–50.

Buenrostro, J. D., Giresi, P. G., Zaba, L. C., Chang, H. Y., & Greenleaf, W. J. (2013). Transposition of native chromatin for fast and sensitive epigenomic profiling of open chromatin , DNA-binding proteins and nucleosome position. *Nature Methods*, *10*(12), 1213–1219.

Bunda, A., Lacarubba, B., Bertolino, M., Akiki, M., Bath, K., Lopez-Soto, J., Lipscombe, D., & Andrade, A. (2019). Cacna1b alternative splicing impacts excitatory neurotransmission and is linked to behavioral responses to aversive stimuli. *Molecular Brain*, *12*(1), 1–14.

Bustin, S., Vandesompele, J., & Pfaffl, M. (2009). PCR technology review: Standardization of qPCR and RT-Qpcr. *Genetic Engineering and Biotechnology News*, *29*(14), 3–6.

Cao, J. (2014). The functional role of long non-coding RNAs and epigenetics. *Biological Procedures Online*, *16*(11), 1–13.

Carninci, P., Kasukawa, T., Katayama, S., Gough, J., Frith, M. C., Maeda, N., Oyama, R., & Ravasi, T. (2005). Transcriptional landscape of the mammalian genome. *Science*, *309*(5740), 1559–1563.

Castel, P., Ellis, H., Bago, R., Toska, E., Razavi, P., Carmona, F. J., Kannan, S., Verma, C. S., Dickler, M., Chandarlapaty, S., Brogi, E., Alessi, D. R., Baselga, J., & Scaltriti, M. (2016). PDK1-SGK1 signaling sustains AKT-independent mTORC1 activation and confers resistance to PI3Kα inhibition. *Cancer Cell*, *30*(2), 229–242.

Cava, C., Bertoli, G., & Castiglioni, I. (2019). Portrait of tissue-specific coexpression networks of noncoding RNAs (miRNA and lncRNA) and mRNAs in normal tissues. *Computational and Mathematical Methods in Medicine*, *2019*, 1–14.

Chabot, B., & Shkreta, L. (2016). Defective control of pre-messenger RNA splicing in human disease. *Journal of Cell Biology*, *212*(1), 13–27.

Chanda, K., Das, S., Chakraborty, J., Bucha, S., Maitra, A., Chatterjee, R., Mukhopadhyay, D., & Bhattacharyya, N. P. (2018). Altered levels of long ncRNAs Meg3 and Neat1 in cell and animal models of Huntington's disease. *RNA Biology*, *15*(10), 1348–1363.

Chao, C. C., Ma, Y. L., & Lee, E. H. Y. (2007). Protein kinase CK2 impairs spatial memory formation through differential cross talk with PI-3 kinase signaling: Activation of Akt and inactivation of SGK1. *Journal of Neuroscience*, *27*(23), 6243–6248.

Chargaff, E. (1950). Chemical specificity of nucleic acids and mechanism of their enzymatic degradation. *Experientia*, *6*(6), 201–209.

Chen, A. M., Perrin, M. H., Digruccio, M. R., Vaughan, J. M., Brar, B. K., Arias, C. M., Lewis, K. A., Rivier, J. E., Sawchenko, P. E., & Vale, W. W. (2005). A soluble mouse brain splice variant of type 2 - corticotropin-releasing factor (CRF) receptor binds ligands and modulates their activity. *Proceedings of the National Academy of Sciences of the United States of America*, *102*(7), 2620–2625.

Chen, E. Y., Tan, C. M., Kou, Y., Duan, Q., Wang, Z., Meirelles, G. V., Clark, N. R., & Ma'ayan, A. (2013). Enrichr: Interactive and collaborative HTML5 gene list enrichment analysis tool. *BMC Bioinformatics*, *14*(28), 1–14.

Chen, X., Garelick, M. G., Wang, H., Li, V., Athos, J., & Storm, D. R. (2005). PI3 kinase signaling is required for retrieval and extinction of contextual memory. *Nature Neuroscience*, *8*(7), 925–931.

Cheng, X., Li, L., Shi, G., Chen, L., Fang, C., & Li, M. (2020). MEG3 promotes differentiation of porcine satellite cells by sponging miR-423-5p to relieve inhibiting. *Cells*, *9*(449), 1–20.

Clark, M. B., Johnston, R. L., Inostroza-Ponta, M., Fox, A. H., Fortini, E., Moscato, P., Dinger, M. E., & Mattick. (2015). Genome-wide analysis of long noncoding RNA turnover. *Methods in Molecular Biology*, *1262*, 305–320.

Clodfelder-Miller, B., De Sarno, P., Zmijewska, A. A., Song, L., & Jope, R. S. (2005). Physiological and pathological changes in glucose regulate brain AKT and glykogen synthase kinase-3. *Journal of Biological Chemistry*, *280*(48), 39723–39731.

Collins, B. J., Deak, M., Arthur, J. S. C., Armit, L. J., & Alessi, D. R. (2003). In vivo role of the PIF-binding docking site of PDK1 defined by knock-in mutation. *EMBO Journal*, *22*(16), 4202–4211.

Core, L. J., Waterfall, J. J., & Lis, J. T. (2008). Nascent RNA sequencing reveals widespread pausing and divergent initiation at human promoters. *Science*, *322*(5909), 1845–1849.

Crick, F. H. (1958). On protein synthesis. *Symposium of the Society for Experimental Biology*, *121*, 138–163.

Crick, F. H. (1970). Central Dogma of Molecular Biology. *Nature*, *227*(8), 561–563.

Cullinan, W. E., Herman, J. P., Battaglia, D. F., Akil, H., & Watson, S. J. (1995). Pattern and time course of immediate early gene expression in rat brain following acute stress. *Neuroscience*, *64*(2), 477–505.

da Rocha, S. T., Edwards, C. A., Ito, M., Ogata, T., & Ferguson-Smith, A. C. (2008). Genomic imprinting at the mammalian Dlk1-Dio3 domain. *Trends in Genetics*, *24*(6), 306–316.

Davidson, J. R. T. (2003). Pharmacotherapy of social phobia. *Acta Psychiatrica Scandinavica*, *108*(417), 65–71.

De France, J. F., Yoshihara, H., McCrea, R. A., & Kitai, S. T. (1975). Pharmacology of the inhibition in the lateral septal region. *Experimental Neurology*, *48*(3), 502–523.

de Menezes, G. B., Fontenelle, L. F., Mululo, S., & Versiani, M. (2007). Treatment-resistant anxiety disorders: social phobia, generalized anxiety disorder and panic disorder. *Revista Brasileira de Psiquiatria*, *29*(2), 55–60.

Deng, K., Yang, L., Xie, J., Tang, H., Wu, G. S., & Luo, H. R. (2019). Whole-brain mapping of projection from mouse lateral septal nucleus. *The Company of Biologists*, *8*(7), 1–9.

Derrien, T., Johnson, R., Bussotti, G., Tanzer, A., Djebali, S., Tilgner, H., Guernec, G., Martin, D., Merkel, A., Knowles, D. G., Lagarde, J., Veeravalli, L., Ruan, X., Ruan, Y., Lassmann, T., Carninci, P., Brown, J. B., Lipovich, L., Gonzalez, J. M., … Guigó, R. (2012). The GENCODE v7 catalog of human long noncoding RNAs: Analysis of their gene structure, evolution, and expression. *Genome Research*, *22*(9), 1775–1789.

Di Cristofano, A. (2017). SGK1: The dark side of PI3K signaling. *Current Topics in Developmental Biology*, *123*, 49–71.

Ding, X., Liu, S., Tian, M., Zhang, W., Zhu, T., Li, D., Wu, J., Deng, H. T., Jia, Y., Xie, W., Xie, H., & Guan, J. S. (2017). Activity-induced histone modifications govern Neurexin-1 mRNA splicing and memory preservation. *Nature Neuroscience*, *20*(5), 690–699.

dos Santos Corrêa, M., Vaz, B. dos S., Grisanti, G. D. V., de Paiva, J. P. Q., Tiba, P. A., & Fornari, R. V. (2019). Relationship between footshock intensity, post-training corticosterone release and contextual fear memory specificity over time. *Psychoneuroendocrinology*, *110*, 1–8.

El-Boustani, S., Ip, J. P. K., Breton-Provencher, V., Knott, G. W., Okuno, H., Bito, H., & Sur, M. (2018). Locally coordinated synaptic plasticity of visual cortex neurons in vivo. *Science*, *360*(6395), 1349–1354.

Elharrar, E., Warhaftig, G., Issler, O., Sztainberg, Y., Dikshtein, Y., Zahut, R., Redlus, L., Chen, A., & Yadid, G. (2013). Overexpression of corticotropin-releasing factor receptor type 2 in the bed nucleus of stria terminalis improves posttraumatic stress disorder-like symptoms in a model of incubation of fear. *Biological Psychiatry*, *74*(11), 827–836.

Fallah, H., Azari, I., Neishabouri, S. M., Oskooei, V. K., Taheri, M., & Ghafouri-Fard, S. (2019). Sex-specific up-regulation of lncRNAs in peripheral blood of patients with schizophrenia. *Nature Scientific Reports*, *9*(1), 1–8.

Farach, F. J., Pruitt, L. D., Jun, J. J., Jerud, A. B., Zoellner, L. A., & Roy-Byrne, P. P. (2013). Pharmacological treatment of anxiety disorders: Current treatment and future directions. *Journal of Anxiety Disorders*, *23*(8), 833–843.

Fehm, L., Beesdo, K., Jacobi, F., & Fiedler, A. (2008). Social anxiety disorder above and below the diagnostic threshold: Prevalence, comorbidity and impairment in the general population. *Social Psychiatry and Psychiatric Epidemiology*, *43*(4), 257–265.

Fehm, L., Pelissolo, A., Furmark, T., & Wittchen, H. U. (2005). Size and burden of social phobia in Europe. *European Neuropsychopharmacology*, *15*(4), 453–462.

Firestone, G., Giampaolo, J., & O'Keeffe, B. (2003). Stimulus-dependent regulation of serum and glucocorticoid inducible protein kinase (SGK) transcription, subcellular localization and enzymatic activity. *Cellular Physiology and Biochemistry*, *13*(1), 1–12.

Fischer, A., Sananbenesi, F., Schrick, C., Spiess, J., & Radulovic, J. (2002). Cyclin-dependent kinase 5 is required for associative learning. *Journal of Neuroscience*, *22*(9), 3700–3707.

Flores, Á., Herry, C., Maldonada, R., & Berrendero, F. (2017). Facilitation of contextual fear extinction by orexin-1 receptor antagonism is associated with the activation of specific amygdala cell subpopulations. *International Journal of Neuropsychopharmacology*, *20*(8), 654–659.

Franke, T. F. (2008). PI3K/Akt: Getting it right matters. *Oncogene*, *27*(50), 6473–6488.

Franklin, R. E., & Gosling, R. G. (1953a). The structure of sodium thymonucleate fibres. I. The influence of water content. *Acta Crystallographica*, *6*, 673–677.

Franklin, Rosalind E., & Gosling, R. G. (1953b). Evidence for 2-chain helix in crystalline structure of sodium deoxyribonucleate. *Nature*, *172*, 156–157.

Frith, M. C., Bailey, T. L., Kasukawa, T., Mignone, F., Kummerfeld, S. K., Madera, M., Sunkara, S., Furuno, M., Bult, C. J., Quackenbush, J., Kai, C., Kawai, J., Carninci, P., Hayashizaki, Y., Pesole, G., & Mattick, J. S. (2006). Discrimination of non-protein-coding transcripts from protein-coding mRNA. *RNA Biology*, *3*(1), 40–48.

Fuller, C. W., Middendorf, L. R., Benner, S. A., Church, G. M., Harris, T., Huang, X., Jovanovich, S. B., Nelson, J. R., Schloss, J. A., Schwartz, D. C., & Vezenov, D. V. (2009). The challenges of sequencing by synthesis. *Nature Biotechnology*, *27*(11), 1013–1023.

Furlanis, E., Traunmüller, L., Fucile, G., & Scheiffele, P. (2019). Landscape of ribosome-engaged transcript isoforms reveals extensive neuronal-cell-class-specific alternative splicing programs. *Nature Neuroscience*, *22*(10), 1709–1717.

Gabbouj, S., Natunen, T., Koivisto, H., Jokivarsi, K., Takalo, M., Marttinen, M., Wittrahm, R., Kemppainen, S., Naderi, R., Posado-Fernández, A., Ryhänen, S., Mäkinen, P., Paldanius, K. M. A., Doria, G., Poutiainen, P., Flores, O., Haapasalo, A., Tanila, H., & Hiltunen, M. (2019). Intranasal insulin activates Akt2 signaling pathway in the hippocampus of wild-type but not in APP/PS1 Alzheimer model mice. *Neurobiology of Aging*, *75*, 98–108.

Galarza, M., Merlo, A. B., Ingratta, A., Albanese, E. F., & Albanese, A. M. (2004). Cavum septum pellucidum and its increased prevalence in schizophrenia: A neuroembryological classification. *Journal of Neuropsychiatry and Clinical Neurosciences*, *16*(1), 41–46.

García-Martínez, J. M., & Alessi, D. R. (2008). mTOR complex 2 (mTORC2) controls hydrophobic motif phosphorylation and activation of serum- and glucocorticoid-induced protein kinase 1 (SGK1). *Biochemical Journal*, *416*(3), 375–385.

Gejman, R., Batista, D. L., Zhong, Y., Zhou, Y., Zhang, X., Swearingen, B., Stratakis, C. A., Hedley-Whyte, E. T., & Klibanski, A. (2008). Selective loss of MEG3 expression and intergenic differentially methylated region hypermethylation in the MEG3/DLK1 locus in human clinically nonfunctioning pituitary adenomas. *Journal of Clinical Endocrinology and Metabolism*, *93*(10), 4119–4125.

Georgiades, P., Watkins, M., Surani, M. A., & Ferguson-Smith, A. C. (2000). Parental origin-specific developmental defects in mice with uniparental disomy for chromosome 12. *Development*, *127*(21), 4719–4728.

Gershman, S. J., Blei, D. M., & Niv, Y. (2010). Context, learning, and extinction. *American Psychological Association*, *117*(1), 197–209.

Greek, R., & Rice, M. J. (2012). Animal models and conserved processes. *Theoretical Biology and Medical Modelling*, *9*(1), 1–33.

Grillon, C., Krimsky, M., Charney, D., Vytal, K., Ernst, M., & Cornwell, B. (2013). Oxytocin increases anxiety to unpredictable threat. *Molecular Pharmacology*, *18*(9), 985–960.

Gudenas, B. L., Srivastava, A. K., & Wang, L. (2017). Integrative genomic analyses for identification and prioritization of long non-coding RNAs associated with autism. *PLoS ONE*, *12*(5), 1–15.

Guil, S., & Esteller, M. (2012). Cis-acting noncoding RNAs: Friends and foes. *Nature Structural and Molecular Biology*, *19*(11), 1068–1075.

Guttman, M., Amit, I., Graber, M., French, C., Lin, M. F., Feldser, D., Huarte, M., Zuk, O., Carey, B. W., Cassady, J. P., Cabili, M. N., Jaenisch, R., Mikkelsen, T. S., Jacks, T., Hacohen, N., Bernstein, B. E., Kellis, M., Regev, A., Rinn, J. L., & Lander, E. S. (2009). Chromatin signature reveals over a thousand highly conserved large non-coding RNAs in mammals. *Nature*, *458*(7235), 223–227.

Hagena, H., & Manahan-Vaughan, D. (2012). Learning-facilitated long-term depression and long-term potentiation at mossy fiber-CA3 synapses requires activation of β-adrenergic receptors. *Frontiers in Integrative Neuroscience*, *6*(23), 1–11.

Hainer, S. J., Boskovic, A., McCannell, K., Rando, O. J., & Fazzio, T. J. (2019). Profiling of pluripotency factors in individual stem cells and early embryos. *Cell*, *177*(5), 1319–1329.

Hakimah Ab Hakim, N., Majlis, B. Y., Suzuki, H., & Tsukahara, T. (2017). Neuron-specific splicing. *BioScience Trends*, *11*(1), 16–22.

Han, X., Zhu, J., Zhang, X., Song, Q., Ding, J., Lu, M., Sun, S., & Hu, G. (2018). Plin4-dependent lipid droplets hamper neuronal mitophagy in the MPTP/p-induced mouse model of Parkinson's disease. *Frontiers in Neuroscience*, *12*(397), 1–14.

Handley, S. L., & McBlane, J. W. (1993). An assessment of the elevated X-maze for studying anxiety and anxiety-modulating drugs. *Journal of Pharmacological and Toxicological Methods*, *29*(3), 129–138.

He, Y., Luo, Y., Liang, B., Ye, L., Lu, G., He, W., He, Y., Luo, Y., Liang, B., Ye, L., Lu, G., He, W., He, Y., Luo, Y., Liang, B., Ye, L., & He, G. L. and W. (2017). Potential applications of MEG3 in cancer diagnosis and prognosis. *Oncotarget*, *8*(42), 73282–73295.

Heeren, A., Dricot, L., Billieux, J., Philippot, P., Grynberg, D., De Timary, P., & Maurage, P. (2017). Correlates of social exclusion in social anxiety disorder: An fMRI study. *Scientific Reports*, *7*(260), 1–10.

Ho, V. M., Lee, J.-A., & Martin, K. C. (2011). The cell biology of synaptic plasticity. *Science*, *334*(6056), 623–628.

Hocine, S., Singer, R. H., & Grünwald, D. (2010). RNA processing and export. *Cold Spring Harbor Perspectives in Biology*, *2*(12), 1–20.

Hofmann, S. G., Hofmann, S. G., Meuret, A. E., Meuret, A. E., Smits, J. a J., Smits, J. a J., Simon, N. M., Simon, N. M., Pollack, M. H., Pollack, M. H., Eisenmenger, K., Eisenmenger, K., Shiekh, M., Shiekh, M., Otto, M. W., & Otto, M. W. (2006). Augmentation of exposure therapy with D-cycloserine for social anxiety disorders. *Archives of General Psychiatry*, *63*, 289–304.

Horwood, J. M., Dufour, F., Laroche, S., & Davis, S. (2006). Signalling mechanisms mediated by the phosphoinositide 3-kinase/Akt cascade in synaptic plasticity and memory in the rat. *European Journal of Neuroscience*, *23*(12), 3375–3384.

Hsieh, L. S., Wen, J. H., Miyares, L., Lombroso, P. J., & Bordey, A. (2017). Outbred CD1 mice are as suitable as inbred C57BL/6J mice in performing social tasks. *Neuroscience Letters*, *637*, 142–147.

Ioannides, Y., Lokulo-Sodipe, K., Mackay, D. J. G., Davies, J. H., & Temple, I. K. (2014). Temple syndrome: Improving the recognition of an underdiagnosed chromosome 14 imprinting disorder: An analysis of 51 published cases. *Journal of Medical Genetics*, *51*(8), 495–501.

Isosaka, T., Hattori, K., Kida, S., Kohno, T., Nakazawa, T., Yamamoto, T., Yagi, T., & Yuasa, S. (2008). Activation of Fyn tyrosine kinase in the mouse dorsal hippocampus is essential for contextual fear conditioning. *European Journal of Neuroscience*, *28*(5), 973–981.

Iyer, S., Modali, S. D., & Agarwal, S. K. (2017). Long noncoding RNA MEG3 is an epigenetic determinant of oncogenic signaling in functional pancreatic neuroendocrine tumor cells. *Molecular and Cellular Biology*, *37*(22), 1–17.

Jacobs, H. L., & Smith, F. L. (1960). The classification of social stimuli: "Social" and "non-social" distraction in the albino rat. *Animal Behaviour*, *8*(3), 134–140.

Jansen, A., Dieleman, G. C., Smit, A. B., Verhage, M., Verhulst, F. C., Polderman, T. J. C., & Posthuma, D. (2017). Gene-set analysis shows association between FMRP targets and autism spectrum disorder. *European Journal of Human Genetics*, *25*(7), 863–868.

Johnson, R. (2012). Long non-coding RNAs in Huntington's disease neurodegeneration. *Neurobiology of Disease*, *46*(2), 245–254.

Jung, H., Yoon, B. C., & Holt, C. E. (2012). Axonal mRNA localization and local protein synthesis in nervous system assembly, maintenance and repair. *Nature Reviews Neuroscience*, *13*(5), 308–324.

Kagami, M., O'Sullivan, M. J., Green, A. J., Watabe, Y., Arisaka, O., Masawa, N., Matsuoka, K., Fukami, M., Matsubara, K., Kato, F., Ferguson-Smith, A. C., & Ogata, T. (2010). The IG-DMR and the MEG3-DMR at human chromosome 14q32.2: Hierarchical interaction and distinct functional properties as imprinting control centers. *PLoS Genetics*, *6*(6), 1–13.

Kaneko, S., Bonasio, R., Saldaña-Meyer, R., Yoshida, T., Son, J., Nishino, K., Umezawa, A., & Reinberg, D. (2014). Interactions between JARID2 and noncoding RNAs regulate PRC2 recruitment to chromatin. *Molecular Cell*, *53*(2), 290–300.

Katsel, P., Roussos, P., Fam, P., Khan, S., Tan, W., Hirose, T., Nakagawa, S., Pletnikov, M. V., & Haroutunian, V. (2019). The expression of long noncoding RNA NEAT1 is reduced in schizophrenia and modulates oligodendrocytes transcription. *Npj Schizophrenia*, *5*(1), 1–9.

Kessler, R. C., Petukhova, M., Sampson, N. A., Zaslavsky, A. M., & Wittchen, H.-U. (2012). Twelve-month and lifetime prevalence and lifetime morbid risk of anxiety and mood disorders in the United States. *International Journal of Methods in Psychiatric Research*, *21*(3), 169–184.

Khakpai, F., Zarrindast, M. R., Nasehi, M., Haeri-Rohani, A., & Eidi, A. (2013). The role of glutamatergic pathway between septum and hippocampus in the memory formation. *EXCLI Journal*, *12*, 41–51.

Kim, D., Langmead, B., & Salzberg, S. L. (2015). HISAT: a fast spliced aligner with low memory requirements. *Nature Methods*, *12*(4), 357–360.

Klug, A. (1968). Rosalind Franklin and the discovery of the structure of DNA. *Nature*, *219*, 808–844.

Kollack-Walker, S., Watson, S. J., & Akil, H. (1997). Social stress in hamsters: Defeat activates specific neurocircuits within the brain. *Journal of Neuroscience*, *17*(22), 8842–8855.

Kopp, F., & Mendell, J. T. (2018). Functional classification and experimental dissection of long noncoding RNAs. *Cell*, *172*(3), 393–407.

Kubota, H., Noguchi, R., Toyoshima, Y., Ozaki, Y. ichi, Uda, S., Watanabe, K., Ogawa, W., & Kuroda, S. (2012). Temporal coding of insulin action through multiplexing of the AKT pathway. *Molecular Cell*, *46*(6), 820–832.

Kukharsky, M. S., Ninkina, N. N., An, H., Telezhkin, V., Meritens, C. R. De, Cooper-knock, J., Nakagawa, S., Hirose, T., Buchman, V. L., Shelkovnikova, T. A., Building, M., & Kingdom, U. (2019). Long non-coding RNA Neat1 regulates adaptive behavioural response to stress in mice. *BioRxiv*, *44*, 1–61.

Kullmann, D. M., Erdemli, G., & Asztély, F. (1996). LTP of AMPA and NMDA receptor-mediated signals: Evidence for presynaptic expression and extrasynaptic glutamate spill-over. *Neuron*, *17*(3), 461–474.

Kumar, A., Lawrence, J. C., Jung, D. Y., Ko, H. J., Keller, S. R., Kim, J. K., Magnuson, M. A., & Harris, T. E. (2010). Fat cell-specific ablation of rictor in mice impairs insulin-regulated fat cell and whole-body glucose and lipid metabolism. *Diabetes*, *59*(6), 1397–1406.

Labuschagne, I., Phan, K. L., Wood, A., Angstadt, M., Chua, P., Heinrichs, M., Stout, J. C., & Nathan, P. J. (2010). Oxytocin attenuates amygdala reactivity to fear in generalized social anxiety disorder. *Neuropsychopharmacology*, *35*(12), 2403–2413.

Lai, F., & Shiekhattar, R. (2014). Enhancer RNAs: the new molecules of transcription. *Current Opinion in Genetics and Development*, *25*, 38–42.

Lander, E. s. (2001). Erratum: correction: Initial sequencing and analysis of the human genome. *Nature*, *412*(6846), 565–566.

Landt, S. G., Marinov, G. K., Kundaje, A., Kheradpour, P., Pauli, F., Batzoglou, S., Bernstein, B. E., Bickel, P., Brown, J. B., Cayting, P., Chen, Y., DeSalvo, G., Epstein, C., Fisher-Aylor, K. I., Euskirchen, G., Gerstein, M., Gertz, J., Hartemink, A. J., Hoffman, M. M., … Snyder, M. (2012). ChIP-seq guidelines and practices of the ENCODE and modENCODE consortia. *Genome Research*, *22*(9), 1813–1831.

Lang, F., Böhmer, C., Palmada, M., Seebohm, G., Strutz-Seebohm, N., & Vallon, V. (2006). (Patho)physiological significance of the serum- and glucocorticoid-inducible kinase isoforms. *Physiological Reviews*, *86*(4), 1151–1178.

Lang, F., Strutz-seebohm, N., Seebohm, G., & Lang, U. E. (2010). Significance of SGK1 in the regulation of neuronal function. *The Journal of Physiology*, *588*(18), 3349–3354.

Langgartner, D., Füchsl, A. M., Uschold-Schmidt, N., Slattery, D. A., & Reber, S. O. (2015). Chronic subordinate colony housing paradigm: a mouse model to characterize the consequences of insufficient glucocorticoid signaling. *Frontiers in Psychiatry*, *6*(18), 1–18.

Latorre, E., Mesonero, J. E., & Harries, L. W. (2019). Alternative splicing in serotonergic system: Implications in neuropsychiatric disorders. *Journal of Psychopharmacology*, *33*(11), 1352–1363.

Laugesen, A., Højfeldt, J. W., & Helin, K. (2019). Molecular mechanisms directing PRC2 recruitment and H3K27 methylation. *Molecular Cell*, *74*(1), 8–18.

Lee, C. T., Ma, Y. L., & Lee, E. H. Y. (2007). Serum- and glucocorticoid-inducible kinase1 enhances contextual fear memory formation through down-regulation of the expression of Hes5. *Journal of Neurochemistry*, *100*, 1531–1542.

Leichsenring, F., & Leweke, F. (2017). Social anxiety disorder. *New England Journal of Medicine*, *376*(23), 2255–2264.

Li, R., Fang, L., Pu, Q., Bu, H., Zhu, P., Chen, Z., Yu, M., Li, X., Weiland, T., Bansal, A., Ye, S. Q., Wei, Y., Jiang, J., & Wu, M. (2018). MEG3-4 is a miRNA decoy that regulates IL-1β abundance to initiate and then limit inflammation to prevent sepsis during lung infection. *Science Signaling*, *11*(536), 1–14.

Li, W., Notani, D., & Rosenfeld, M. G. (2016). Enhancers as non-coding RNA transcription units: Recent insights and future perspectives. *Nature Reviews Genetics*, *17*(4), 207–223.

Liao, Y., & Hung, M. C. (2010). Physiological regulation of Akt activity and stability. *American Journal of Translational Research*, *2*(1), 19–42.

Ličen, M., Hartmann, F., Repovš, G., & Slapničar, S. (2016). The Impact of Social Pressure and Monetary Incentive on Cognitive Control. *Frontiers in Psychology*, *7*(93), 1–16.

Lin, C. H., Yeh, S. H., Lin, C. H., Lu, K. T., Leu, T. H., Chang, W. C., & Gean, P. W. (2001). A Role for the PI-3 kinase signaling pathway in fear conditioning and synaptic plasticity in the amygdala. *Neuron*, *31*(5), 841–851.

Luo, Z., Lin, C., Woodfin, A. R., Bartom, E. T., Gao, X., Smith, E. R., & Shilatifard, A. (2016). Regulation of the imprinted Dlk1-Dio3 locus by allele-specific enhancer activity. *Genes and Development*, *30*(1), 92–101.

Lyu, Y., Lou, J., Yang, Y., Feng, J., Hao, Y., Huang, S., Yin, L., Xu, J., Huang, D., Ma, B., Zou, D., Wang, Y., Zhang, Y., Zhang, B., Chen, P., Yu, K., Lam, E. W. F., Wang, X., Liu, Q., … Jin, B. (2017). Dysfunction of the WT1-MEG3 signaling promotes AML leukemogenesis via p53-dependent and -independent pathways. *Leukemia*, *31*(12), 2543–2551.

Ma, M., Xiong, W., Hu, F., Deng, M. F., Huang, X., Chen, J. G., Man, H. Y., Lu, Y., Liu, D., & Zhu, L. Q. (2020). A novel pathway regulates social hierarchy via lncRNA AtLAS and postsynaptic synapsin IIb. *Cell Research*, *30*(2), 105–118.

Ma, Y. L., Tsai, M. C., Hsu, W. L., & Lee, E. H. Y. (2006). SGK protein kinase facilitates the expression of long-term potentiation in hippocampal neurons. *Learning and Memory*, *13*(2), 114–118.

Maag, J. L. V., Panja, D., Sporild, I., Patil, S., Kaczorowski, D. C., Bramham, C. R., Dinger, M. E., & Wibrand, K. (2015). Dynamic expression of long noncoding RNAs and repeat elements in synaptic plasticity. *Frontiers in Neuroscience*, *9*(351), 1–16.

Man, H. Y., Wang, Q., Lu, W. Y., Ju, W., Ahmadian, G., Liu, L., D'Souza, S., Wong, T. P., Taghibiglou, C., Lu, J., Becker, L. E., Pei, L., Liu, F., Wymann, M. P., MacDonald, J. F., & Wang, Y. T. (2003). Activation of PI3-kinase is required for AMPA receptor insertion during LTP of mEPSCs in cultured hippocampal neurons. *Neuron*, *38*(4), 611–624.

Manning, B. D., & Toker, A. (2017). AKT/PKB signaling: Navigating the network. *Cell*, *169*(3), 381–405.

McNay, E. C., & Pearson-Leary, J. (2020). GluT4: A central player in hippocampal memory and brain insulin resistance. *Experimental Neurology*, *323*, 1–9.

Menon, R., Grund, T., Zoicas, I., Althammer, F., Fiedler, D., Biermeier, V., Bosch, O. J., Hiraoka, Y., Nishimori, K., Eliava, M., Grinevich, V., & Neumann, I. D. (2018). Oxytocin signaling in the lateral septum prevents social fear during lactation. *Current Biology*, *28*(7), 1066–1078.

Mercer, T. R., Dinger, M. E., Sunkin, S. M., Mehler, M. F., & Mattick, J. S. (2008). Specific expression of long noncoding RNAs in the mouse brain. *Proceedings of the National Academy of Sciences of the United States of America*, *105*(2), 716–721.

Mergenthaler, P., Lindauer, U., Dienel, G., & Meisel, A. (2013). Sugar for the brain: the role of glucose in physiological and pathological brain function. *Trends in Neuroscience*, *36*(10), 587–597.

Miczek, K. A., & Grossman, S. P. (1972). Effects of septal lesions on inter- and intraspecies aggression in rats. *Journal of Comparative and Physiological Psychology*, *79*(1), 37–45.

Mikics, E., Toth, M., Biro, L., Bruzsik, B., Nagy, B., & Haller, J. (2017). The role of GluN2B-containing NMDA receptors in short- and long-term fear recall. *Physiology and Behavior*, *177*, 44–48.

Minichiello, L. (2009). TrkB signalling pathways in LTP and learning. *Nature Reviews Neuroscience*, *10*(12), 850–860.

Minkova, L., Sladky, R., Kranz, G. S., Woletz, M., Geissberger, N., Kraus, C., Lanzenberger, R., & Windischberger, C. (2017). Task-dependent modulation of amygdala connectivity in social anxiety disorder. *Psychiatry Research - Neuroimaging*, *262*, 39–46.

Miyoshi, N., Wagatsuma, H., Wakana, S., Shiroishi, T., Nomura, M., Aisaka, K., Kohda, T., Azim Surani, M., Kaneko-Ishino, T., & Ishino, F. (2000). Identification of an imprinted gene, Meg3/Gtl2 and its human homologue MEG3, first mapped on mouse distal chromosome 12 and human chromosome 14q. *Genes to Cells*, *5*(3), 211–220.

Mondal, T., Subhash, S., Vaid, R., Enroth, S., Uday, S., Reinius, B., Mitra, S., Mohammed, A., James, A. R., Hoberg, E., Moustakas, A., Gyllensten, U., Jones, S. J. M., Gustafsson, C. M., Sims, A. H., Westerlund, F., Gorab, E., & Kanduri, C. (2015). MEG3 long noncoding RNA regulates the TGF-β pathway genes through formation of RNA-DNA triplex structures. *Nature Communications*, *6*(7743), 1–17.

Mongeau, R., Miller, G. A., Chiang, E., & Anderson, D. J. (2003). Neural correlates of competing fear behaviors evoked by an innately aversive stimulus. *Journal of Neuroscience*, *23*(9), 3855–3868.

Montecucco, A., & Biamonti, G. (2013). Pre-mRNA processing factors meet the DNA damage response. *Frontiers in Genetics*, *4*(102), 1–14.

Moradi, M. T., Fallahi, H., & Rahimi, Z. (2018). Interaction of long noncoding RNA MEG3 with miRNAs: A reciprocal regulation. *Journal of Cellular Biochemistry*, *120*(3), 3339–3352.

Morrison, A. S., & Heimberg, R. G. (2013). Social anxiety and social anxiety sisorder. *Annual Review of Clinical Psychology*, *9*(1), 249–274.

Moy, S. S., Nadler, J. J., Perez, A., Barbaro, R. P., Johns, J. M., Magnuson, T. R., Piven, J., & Crawley, J. N. (2004). Sociability and preference for social novelty in five inbred strains: an approach to assess autistic-like behavior in mice. *Genes, Brain and Behavior*, *3*(5), 287–302.

Napoli, I., Mercaldo, V., Boyl, P. P., Eleuteri, B., Zalfa, F., De Rubeis, S., Di Marino, D., Mohr, E., Massimi, M., Falconi, M., Witke, W., Costa-Mattioli, M., Sonenberg, N., Achsel, T., & Bagni, C. (2008). The Fragile X Syndrome protein represses activity-dependent translation through CYFIP1, a new 4E-BP. *Cell*, *134*(6), 1042–1054.

Neumann, I. D., Wegener, G., Homberg, J. R., Cohen, H., Slattery, D. A., Zohar, J., Olivier, J. D. A., & Mathé, A. A. (2011). Animal models of depression and anxiety: What do they tell us about human condition? *Progress in Neuro-Psychopharmacology & Bilogical Psychiatry*, *35*(6), 1357–1375.

Niazi, F., & Valadkhan, S. (2012). Computational analysis of functional long noncoding RNAs reveals lack of peptide-coding capacity and parallels with 3' UTRs. *Cold Spring Harbor Laboratory Press*, *18*(4), 825–843.

Nie, J., Li, T., & Zhang, X. (2019). Roles of non-coding RNAs in normal human brain development, brain tumor, and neuropsychiatric disorders. *MDPI*, *5*(36), 1–17.

Niewiadomska, G., Baksalerska-Pazera, M., & Rieder, G. (2009). The septo-hippocampal system, learning and recovery of function. *Progress in Neuro-Psychopharmacology and Biological Psychiatry*, *33*(5), 791–805.

Nishiyama, Y., Okamoto, Y., Kunisato, Y., Okada, G., Yoshimura, S., Kanai, Y., Yamamura, T., Yoshino, A., Jinnin, R., Takagaki, K., Onoda, K., & Yamawaki, S. (2015). fMRI study of social anxiety during social ostracism with and without emotional support. *PLoS ONE*, *10*(5), 1–14.

Nogueiras, R., Habegger, K. M., Chaudhary, N., Finan, B., Banks, A. S., Dietrich, M. O., Horvath, T. L., Sinclair, D. a, Pfluger, P. T., & Matthias, H. (2013). Sirtuin1 and sirtuin3: physiological modulators of metabolism. *Physiological Reviews*, *92*(3), 1479–1514.

Ogata, T., & Kagami, M. (2016). Kagami-Ogata syndrome: A clinically recognizable upd(14)pat and related disorder affecting the chromosome 14q32.2 imprinted region. *Journal of Human Genetics*, *61*(2), 87–94.

Opazo, P., Watabe, A. M., Grant, S. G. N., & O'Dell, T. J. (2003). Phosphatidylinositol 3-kinase regulates the induction of long-term potentiation through extracellular signal-related kinase-independent mechanisms. *Journal of Neuroscience*, *23*(9), 3679–3688.

Palazzo, A. F., & Lee, E. S. (2015). Non-coding RNA: What is functional and what is junk? *Frontiers in Genetics*, *5*(2), 1–11.

Pang, K., Jiao, X., & Sinha, S. (2011). Damage of GABAergic neurons in the medial septum impairs spatial working memory and extinction of active avoidance: effects on proactive interference. *Hippocampus*, *21*(8), 835–846.

Parikshak, N. N., Swarup, V., Belgard, T. G., Irimia, M., Ramaswami, G., Gandal, M. J., Hartl, C., Leppa, V., Ubieta, L. D. L. T., Huang, J., Lowe, J. K., Blencowe, B. J., Horvath, S., & Geschwind, D. H. (2016). Genome-wide changes in lncRNA, splicing, and regional gene expression patterns in autism. *Nature*, *540*(7633), 423–427.

Pathania, M., Davenport, E. C., Muir, J., Sheehan, D. F., López-Doménech, G., & Kittler, J. T. (2014). The autism and schizophrenia associated gene CYFIP1 is critical for the maintenance of dendritic complexity and the stabilization of mature spines. *Translational Psychiatry*, *4*(3), 1–11.

Paulsen, M., Takada, S., Youngson, N. A., Benchaib, M., Charlier, C., Segers, K., Georges, M., & Ferguson-Smith, A. C. (2001). Comparative sequence analysis of the imprinted Dlk1-Gtl2 locus in three mammalian species reveals highly conserved genomic elements and refines comparison with the Igf2-H19 region. *Genome Research*, *11*(12), 2085–2094.

Paxinos, G., & Franklin, K. (2001). *The mouse brain in stereotaxic coordinates.*

Pertea, M., Kim, D., Pertea, G. M., Leek, J. T., & Salzberg, S. L. (2016). Transcript-level expression analysis of RNA-seq experiments with HISAT, StringTie and Ballgown. *Nature Protocols*, *11*(9), 1650–1667.

Pertea, M., Pertea, G. M., Antonescu, C. M., Chang, T. C., Mendell, J. T., & Salzberg, S. L. (2015). StringTie enables improved reconstruction of a transcriptome from RNA-seq reads. *Nature Biotechnology*, *33*(3), 290–295.

Peters, S., Slattery, D. A., Uschold-schmidt, N., Reber, S. O., & Neumann, I. D. (2014). Dose-dependent effects of chronic central infusion of oxytocin on anxiety , oxytocin receptor binding and stress-related parameters in mice. *Psychoneuroendocrinology*, *42*, 225–236.

Pfaffl, M. W. (2001). A new mathematical model for relative quantification in real-time RT-PCR. *Nucleic Acids Research*, *29*(9), 2002–2007.

Quan, Z., Zheng, D., & Qing, H. (2017). Regulatory roles of long non-coding rnas in the central nervous system and associated neurodegenerative diseases. *Frontiers in Cellular Neuroscience*, *11*(175), 1–14.

Quinn, J. J., & Chang, H. Y. (2016). Unique features of long non-coding RNA biogenesis and function. *Nature Reviews Genetics*, *17*(1), 47–62.

Radulovic, J., Rühmann, A., Liepold, T., & Spiess, J. (1999). Modulation of learning and anxiety by corticotropin-releasing factor (CRF) and stress: Differential roles of CRF receptors 1 and 2. *Journal of Neuroscience*, *19*(12), 5016–5025.

Reddy, A. S., O'Brien, D., Pisat, N., Weichselbaum, C. T., Sakers, K., Lisci, M., Dalal, J. S., & Dougherty, J. D. (2017). A comprehensive analysis of cell type–specific nuclear RNA from neurons and glia of the brain. *Biological Psychiatry*, *81*(3), 252–264.

Redish, A. D., Jensen, S., Johnson, A., & Kurth-Nelson, Z. (2007). Reconciling reinforcement learning models with behavioral extinction and renewal: Implications for addiction, relapse, and problem gambling. *Psychological Review*, *114*(3), 784–805.

Rescorla, R. A., & Heth, D. C. (1975). Reinstatement of fear to an extinguished conditioned stimulus. *Journal of Experimental Psychology: Animal Behavior Processes*, *104*(1), 88–96.

Robinson, L., Kellett, S., & Delgadillo, J. (2019). Dose-response patterns in low and high intensity cognitive behavioral therapy for common mental health problems. *Anxiety and Depression Association of America*, *37*(3), 1–10.

Rodebaugh, T. L., Holaway, R. M., & Heimberg, R. G. (2004). The treatment of social anxiety disorder. *Clinical Psychology Review*, *24*(7), 883–908.

Rom, A., Melamed, L., Gil, N., Goldrich, M. J., Kadir, R., Golan, M., Biton, I., Perry, R. B. T., & Ulitsky, I. (2019). Regulation of CHD2 expression by the Chaserr long noncoding RNA gene is essential for viability. *Nature Communications*, *10*(1), 1–28.

Royer, M., Bludau, A., Meister, G., Neumann, I. D., & Menon, R. (2019). Epigenetic regulation of the social brain. *Trends in Neurosciences*, *42*(7), 1–14.

Ryan, B. C., Young, N. B., Moy, S. S., & Crawley, J. N. (2009). Olfactory cues are sufficient to elicit social approach behaviors but not social transmission of food preference in C57BL/6J mice. *Behavioural Brain Research*, *193*(2), 235–242.

Sahakyan, A., Yang, Y., & Plath, K. (2018). The role of Xist in X-chromosome dosage compensation. *Trends in Cell Biology*, *28*(12), 999–1013.

Sanli, I., Lalevée, S., Cammisa, M., Perrin, A., Rage, F., Llères, D., Riccio, A., Bertrand, E., & Feil, R. (2018). Meg3 non-coding RNA expression controls imprinting by preventing transcriptional upregulation in cis. *Cell Reports*, *23*(2), 337–348.

Sanna, P. Pietro, Cammalleri, M., Berton, F., Simpson, C., Lutjens, R., Bloom, F. E., & Francesconi, W. (2002). Phosphatidylinositol 3-kinase is required for the expression but not for the induction or the maintenance of long-term potentiation in the hippocampal CA1 region. *Journal of Neuroscience*, *22*(23), 3359–3365.

Sarbassov, D. D., Guertin, D. A., Ali, S. M., & Sabatini, D. M. (2005). Phosphorylation and regulation of Akt/PKB by the rictor-mTOR complex. *Science*, *307*(5712), 1098–1101.

Sartori, S. B., Maurer, V., Murphy, C., Schmuckermair, C., Muigg, P., Neumann, I. D., Whittle, N., & Singewald, N. (2016). Combined neuropeptide S and D-cycloserine augmentation prevents the return of fear in extinction-impaired rodents: Advantage of dual versus single drug approaches. *International Journal of Neuropsychopharmacology*, *19*(6), 1–11.

Sathishkumar, C., Prabu, P., Mohan, V., & Balasubramanyam, M. (2018). Linking a role of lncRNAs (long non-coding RNAs) with insulin resistance, accelerated senescence, and inflammation in patients with type 2 diabetes. *Human Genomics*, *12*(41), 1–9.

Savell, K. E., Bach, S. V., Zipperly, M. E., Revanna, J. S., Goska, N. A., Tuscher, J. J., Duke, C. G., Sultan, F. A., Burke, J. N., Williams, D., Ianov, L., & Day, J. J. (2019). A neuron-optimized CRISPR/dCas9 activation system for robust and specific gene regulation. *ENeuro*, *6*(1), 1–17.

Scheid, M. P., Marignani, P. A., & Woodgett, J. R. (2002). Multiple phosphoinositide 3-kinase-dependent steps in activation of protein kinase B. *Molecular and Cellular Biology*, *22*(17), 6247–6260.

Schuster-Gossler, K., Bilinski, P., Sado, T., Ferguson-Smtth, A., & Gossler, A. (1998). The mouse Gtl2 gene is differentially expressed during embryonic development, encodes multiple alternatively spliced transcripts, and may act as an RNA. *Developmental Dynamics*, *212*(2), 214–228.

Seila, A. C., Calabrese, J. M., Levine, S. S., Yeo, G. W., Rahl, P. B., Flynn, R. A., Young, R. A., & Sharp, P. A. (2008). Divergent transcription from active promoters. *Science*, *322*(5909), 1849–1851.

Sheehan, T. P., Chambers, R. A., & Russell, D. S. (2004). Regulation of affect by the lateral septum: Implications for neuropsychiatry. *Brain Research Reviews*, *46*(1), 71–117.

Shemesh, Y., Forkosh, O., Mahn, M., Anpilov, S., Sztainberg, Y., Manashirov, S., Shlapobersky, T., Elliott, E., Tabouy, L., Ezra, G., Adler, E. S., Ben-Efraim, Y. J., Gil, S., Kuperman, Y., Haramati, S., Dine, J., Eder, M., Deussing, J. M., Schneidman, E., … Chen, A. (2016). Ucn3 and CRF-R2 in the medial amygdala regulate complex social dynamics. *Nature Neuroscience*, *19*(11), 1489–1496.

Sherpa, C., Rausch, J. W., & Le Grice, S. F. J. (2018). Structural characterization of maternally expressed gene 3 RNA reveals conserved motifs and potential sites of interaction with polycomb repressive complex 2. *Nucleic Acids Research*, *46*(19), 10432–10447.

Shi, Y., Lv, C., Shi, L., & Tu, G. (2018). MEG3 inhibits proliferation and invasion and promotes apoptosis of human osteosarcoma cells. *Oncology Letters*, *15*(2), 1917–1923.

Skene, P. J., & Henikoff, S. (2017). An efficient targeted nuclease strategy for high-resolution mapping of DNA binding sites. *ELife*, *6*, 1–35.

Slattery, D. A., Neumann, I. D., Flor, P. J., & Zoicas, I. (2017). Pharmacological modulation of metabotropic glutamate receptor subtype 5 and 7 impairs extinction of social fear in a time-point-dependent manner. *Behavioural Brain Research*, *328*, 57–61.

Song, L., & Crawford, G. E. (2010). DNase-seq: a high-resolution technique for mapping active gene regulatory elements across the genome from mammalian cells. *Cold Spring Harbor Protocols*, *2*(1), 1–7.

Spadaro, P. A., Flavell, C. R., Widagdo, J., Ratnu, V. S., Troup, M., Ragan, C., Mattick, J. S., & Bredy, T. W. (2015). Long noncoding RNA-directed epigenetic regulation of gene expression is associated with anxiety-like behavior in mice. *Biological Psychiatry*, *78*(12), 848–859.

Sparks, P. D., & LeDoux, J. E. (1995). Septal lesions potentiate freezing behavior to contextual but not to phasic conditioned stimuli in rats. *Behavioral Neuroscience*, *109*(1), 184–188.

Standart, N., & Weil, D. (2018). P-bodies: Cytosolic droplets for coordinated mRNA storage. *Trends in Genetics*, *34*(8), 612–626.

Stein, D. J., Stein, M. B., Pitts, C. D., Kumar, R., & Hunter, B. (2002). Predictors of response to pharmacotherapy in social anxiety disorder, an analysis of 3 placebo-controlled paroxetine trial. *The Journal of Clinical Psychiatry*, *63*(2), 152–155.

Stevens, D. R., Gallagher, J. P., & Shinnick-Gallagher, P. (1987). In vitro studies of the role of γ-aminobutyric acid in inhibition in the lateral septum of the rat. *Synapse*, *1*(2), 184–190.

Su, C. H., Dhananjaya, D., & Tarn, W. Y. (2018). Alternative splicing in neurogenesis and brain development. *Frontiers in Molecular Biosciences*, *5*(12), 1–9.

Sun, Y., Miao, N., & Sun, T. (2019). Detect accessible chromatin using ATAC-sequencing, from principle to applications. *Hereditas*, *156*(29), 1–9.

Tabak, B. A., McCullough, M. E., Szeto, A., Mendez, A. J., & McCabe, P. M. (2011). Oxytocin indexes relational distress following interpersonal harms in women. *Psychoneuroendocrinology*, *36*(1), 115–122.

Takahashi, N., Okamoto, A., Kobayashi, R., Shirai, M., Obata, Y., Ogawa, H., Sotomaru, Y., & Kono, T. (2009). Deletion of Gtl2, imprinted non-coding RNA, with its differentially methylated region induces lethal parent-origin-dependent defects in mice. *Human Molecular Genetics*, *18*(10), 1879–1888.

Tan, M. C., Widagdo, J., Chau, Y. Q., Zhu, T., Wong, J. J.-L., Cheung, A., & Anggono, V. (2017). The activity-induced long non-coding RNA Meg3 modulates AMPA receptor surface expression in primary cortical neurons. *Frontiers in Cellular Neuroscience*, *11*(124), 1–12.

Terashima, M., Tange, S., Ishimura, A., & Suzuki, T. (2017). MEG3 long noncoding RNA contributes to the epigenetic regulation of epithelial-mesenchymal transition in lung cancer cell lines. *Journal of Biological Chemistry*, *292*(1), 82–99.

Terranova, J. I., Pèrio, A., Worms, P., Le Fur, G., & Soubrié, P. (1994). Social olfactory recognition in rodents: deterioration with age, cerebal ischaemia and septal lesion. *Behavioural Pharmacology*, *5*, 90–98.

Thomas, E., Burock, D., Knudsen, K., Deterding, E., & Yadin, E. (2013). Single unit activity in the lateral septum and central nucleus of the amygdala in the elevated plus-maze: A model of exposure therapy? *Neuroscience Letters*, *548*, 269–274.

Tierling, S., Dalbert, S., Schoppenhorst, S., Tsai, C. E., Oliger, S., Ferguson-Smith, A. C., Paulsen, M., & Walter, J. (2006). High-resolution map and imprinting analysis of the Gtl2-Dnchc1 domain on mouse chromosome 12. *Genomics*, *87*(2), 225–235.

Toth, I., Neumann, I. D., & Slattery, D. A. (2012). Social fear conditioning: a novel and specific animal model to study social anxiety disorder. *Neuropsychopharmacology*, *37*(6), 1433–1443.

Tronson, N. C., Corcoran, K. A., Jovasevic, V., & Radulovic, J. (2013). Fear conditioning and extinction: emotional states encoded by distinct signaling pathways. *Trends in Neuroscience*, *35*(3), 145–155.

Tsai, K. J., Chen, S. K., Ma, Y. L., Hsu, W. L., & Lee, E. H. Y. (2002). Sgk, a primary glucocorticoid-induced gene, facilitates memory consolidation of spatial learning in rats. *Proceedings of the National Academy of Sciences of the United States of America*, *99*(6), 3990–3995.

Tumolo, J. M., Kutlu, M. G., & Gould, T. J. (2018). Chronic nicotine differentially alters spontaneous recovery of contextual fear in male and female mice. *Behavioural Brain Research*, *341*, 176–180.

Ulitsky, I. (2016). Evolution to the rescue: Using comparative genomics to understand long non-coding RNAs. *Nature Reviews Genetics*, *17*(10), 601–614.

Uroda, T., Anastasakou, E., Rossi, A., Teulon, J. M., Pellequer, J. L., Annibale, P., Pessey, O., Inga, A., Chillón, I., & Marcia, M. (2019). Conserved pseudoknots in lncRNA MEG3 are essential for stimulation of the p53 pathway. *Molecular Cell*, *75*(5), 982-995.e9.

von Hertzen, L. S. J. (2005). Memory reconsolidation engages only a subset of immediate-early genes induced during consolidation. *Journal of Neuroscience*, *25*(8), 1935–1942.

Vouimba, R. M., Garcia, R., & Jaffard, R. (1998). Opposite effects of lateral septal LTP and lateral septal lesions on contextual fear conditioning in mice. *Behavioral Neuroscience*, *112*(4), 875–884.

Vuckovich, J. A., Semel, M. F., & Baxter, M. G. (2004). Extensive lesions of cholinergic basal forebrain neurons do not impair spatial working memory. *Learning and Memory*, *11*(1), 87–94.

Wagner, S. (2019). Urocortins and their unfolding role in mammalian social behavior. *Cell and Tissue Research*, *375*(1), 133–142.

Wallace, K. J., & Rosen, J. B. (2001). Neurotoxic lesions of the lateral nucleus of the amygdala decrease conditioned fear but not unconditioned fear of a predator odor: comparison with electrolytic lesions. *Journal of Neuroscience*, *21*(10), 3619–3627.

Wang, K. C., & Chang, H. Y. (2012). Molecular mechanisms of long noncoding RNAs. *Molecular Cell*, *43*(6), 904–914.

Wang, L.-X., Li, P., He, H., Guo, F., Tian, P., Li, C., Cui, L.-B., Xi, Y.-B., & Yin, H. (2019). The prevalence of cavum septum pellucidum in mental disorders revealed by MRI: A meta-analysis. *The Journal of Neuropsychiatry and Clinical Neurosciences*, *7*, 1–10.

Wang, Y., Liu, J., Huang, B., Xu, Y.-M., Li, J., Huang, Li.-F., Lin, J., Zhang, J., Min, Q.-H., Yaang, W.-M., & Wang, X.-Z. (2015a). Mechanism of alternative splicing and its regulation. *Biomedical Reports*, *3*(2), 152–158.

Wang, Y., Xie, Y., Li, L., He, Y., Zheng, D., Yu, P., Yu, L., Tang, L., Wang, Y., & Wang, Z. (2018). EZH2 RIP-seq identifies tissue-specific long non-coding RNAs. *Current Gene Therapy*, *18*(5), 275–285.

Wang, Y., Zhao, X., Ju, W., Flory, M., Zhong, J., Jiang, S., Wang, P., Dong, X., Tao, X., Chen, Q., Shen, C., Zhong, M., Yu, Y., Brown, W. T., & Zhong, N. (2015b). Genome-wide differential expression of synaptic long noncoding RNAs in autism spectrum disorder. *Translational Psychiatry*, *5*(10), 1–10.

Wasylishen, A. R., & Lozano, G. (2016). Attenuating the p53 pathway in human cancers: Many means to the same end. *Cold Spring Harbor Perspectives in Medicine*, *6*(8), 1–20.

Wei, Y., Zhou, J., Yu, H., & Jin, X. (2019). AKT phosphorylation sites of Ser473 and Thr308 regulate AKT degradation. *Bioscience, Biotechnology and Biochemistry*, *83*(3), 429–435.

Wetmore, L., Green-Johnson, J., Gartner, J. G., Sanders, V., & Nance, D. M. (1994). The effect of kainic acid-incuced lesions in the lateral septal area on cell-mediated immune function. *Brain, Behavior, and Immunity*, *8*(4), 341–354.

Whitehead, A., & Crawford, D. L. (2005). Variation in tissue-specific gene expression among natural populations. *Genome Biology*, *6*(2), 1–14.

Willis, D. E., & Twiss, J. L. (2010). Regulation of protein levels in subcellular domains through mRNA transport and localized translation. *Molecular and Cellular Proteomics*, *9*(5), 952–962.

Winter, J., Meyer, M., Berger, I., Peters, S., Royer, M., Langgartner, D., Reber, S. O., Kuffner, K., Schmidtner, A. K., Hübner, K., Bludau, A., Bianchi, M., Stang, S., Bosch, O., Slattery, D. A., Burg, H. Van Den, Inga, D., & Jurek, B. (n.d.). Oxytocin- induced synthesis of soluble CRFR2α triggers anxiety Oxytocin. *In Preparation.*

Wong, L. C., Wang, L., D'Amour, J. A., Yumita, T., Chen, G., Yamaguchi, T., Chang, B. C., Bernstein, H., You, X., Feng, J. E., Froemke, R. C., & Lin, D. (2016). Effective modulation of male aggression through lateral septum to medial hypothalamus projection. *Current Biology*, *26*(5), 593–604.

Wu, P., Zuo, X., Deng, H., Liu, X., Liu, L., & Ji, A. (2013). Roles of long noncoding RNAs in brain development, functional diversification and neurodegenerative diseases. *Brain Research Bulletin*, *97*, 69–80.

Yadin, E., Thomas, E., Grishkat, H. L., & Strickland, C. E. (1993). The role of the lateral septum in anxiolysis. *Physiology and Behavior*, *53*(6), 1077–1083.

Yan, H., Yuan, J., Gao, L., Rao, J., & Hu, J. (2016). Long noncoding RNA MEG3 activation of p53 mediates ischemic neuronal death in stroke. *Neuroscience*, *337*.

Yang, J., Cron, P., Thompson, V., Good, V. M., Hess, D., Hemmings, B. A., & Barford, D. (2002). Molecular mechanism for the regulation of protein kinase B/Akt by hydrophobic motif phosphorylation. *Molecular Cell*, *9*(6), 1227–1240.

Yang, L., Zou, B., Xiong, X., Pascual, C., Xie, J., Malik, A., Xie, J., Sakurai, T., & Xie, X. S. (2013). Hypocretin/orexin neurons contribute to hippocampus-dependent social memory and synaptic plasticity in mice. *Journal of Neuroscience*, *33*(12), 1–23.

Yap, D. B. S., Hsieh, J. K., Chan, F. S. G., & Lu, X. (1999). Mdm2: A bridge over the two tumour suppressors, p53 and Rb. *Oncogene*, *18*(53), 7681–7689.

Yi, J., & Chen, B. (2019). Upregulation of the lncRNA MEG3 improves cognitive impairment , alleviates neuronal damage , and inhibits activation of astrocytes in hippocampus tissues in Alzheimer ' s disease through inactivating the PI3K / Akt signaling pathway. *Journal of Cellular Biochemistry*, *120*(10), 18053–18065.

Yoon, J.-H., Kim, J., & Gorospe, M. (2016). Long noncoding RNA turnover. *Biochimie*, *117*, 1–17.

You, L., Wang, N., Yin, D., Wang, L., Jin, F., Zhu, Y., Yuan, Q., & De, W. (2015). Downregulation of long noncoding RNA Meg3 affects insulin synthesis and secretion in mouse pancreatic beta cells. *Journal of Cellular Physiology*, *231*(4), 852–862.

Yudushkin, I. (2019). Getting the akt together: Guiding intracellular Akt activity by PI3k. *Biomolecules*, *9*(67), 1–14.

Zalfa, F., Giorgi, M., Primerano, B., Moro, A., Di Penta, A., Reis, S., Oostra, B., & Bagni, C. (2003). The Fragile X syndrome protein FMRP associates with BC1 RNA and regulates the translation of specific mRNAs at synapses. *Cell*, *112*(3), 317–327.

Zapata, A., Chefer, V. I., & Shippenberg, T. S. (2009). Microdialysis in rodents. *Current Protocols in Neuroscience*, *4*, 1–15.

Zaret, K. (1999). Micrococcal nuclease analysis of chromatin structure. In *Current Protocols in Molecular Biology*.

Zelikowsky, M., Hui, M., Karigo, T., Choe, A., Yang, B., Blanco, M. R., Beadle, K., Gradinaru, V., Deverman, B. E., & Anderson, D. J. (2018). The neuropeptide Tac2 controls a distributed brain state induced by chronic social isolation stress. *Cell*, *173*(5), 1265–1279.

Zeng, C., Fukunaga, T., & Hamada, M. (2018). Identification and analysis of ribosome-associated lncRNAs using ribosome profiling data. *BMC Genomics*, *19*(414), 1–14.

Zhang, J., Liang, Y., Huang, X., Guo, X., Liu, Y., Zhong, J., & Yuan, J. (2019). STAT3-induced upregulation of lncRNA MEG3 regulates the growth of cardiac hypertrophy through miR-361-5p/HDAC9 axis. *Scientific Reports*, *9*(1), 1–11.

Zhang, L., Liang, X., & Li, Y. (2017). Long non-coding RNA MEG3 inhibits cell growth of gliomas by targeting miR-93 and inactivating PI3K/AKT pathway. *Oncology Reports*, *38*(4), 2408–2416.

Zhang, M., Ergin, V., Lin, L., Stork, C., Chen, L., & Zheng, S. (2019). Axonogenesis is coordinated by neuron-specific alternative splicing programming and splicing regulator PTBP2. *Neuron*, *101*(4), 690–706.

Zhang, X., Gejman, R., Mahta, A., Zhong, Y., Rice, K. A., Zhou, Y., Cheunsuchon, P., Louis, D. N., & Klibanski, A. (2010a). Maternally expressed gene 3, an imprinted non-coding RNA gene, is associated with meningioma pathogenesis and progression. *Cancer Research*, *70*(6), 2350–2358.

Zhang, X., Rice, K., Wang, Y., Chen, W., Zhong, Y., Nakayama, Y., Zhou, Y., & Klibanski, A. (2010b). Maternally expressed gene 3 (MEG3) noncoding ribonucleic acid: Isoform structure, expression, and functions. *Endocrinology*, *151*(3), 939–947.

Zhang, X., Zhou, Y., Mehta, K. R., Danila, D. C., Scolavino, S., Johnson, S. R., & Klibanski, A. (2003). A pituitary-derived Meg3 isoform functions as a growth suppressor in tumor cells. *Journal of Clinical Endocrinology and Metabolism*, *88*(11), 5119–5126.

Zhang, Y., Chen, K., Sloan, S. A., Bennett, M. L., Scholze, A. R., O'Keeffe, S., Phatnani, H. P., Guarnieri, P., Caneda, C., Ruderisch, N., Deng, S., Liddelow, S. A., Zhang, C., Daneman, R., Maniatis, T., Barres, B. A., & Wu, J. Q. (2014). An RNA-sequencing transcriptome and splicing database of glia, neurons, and vascular cells of the cerebral cortex. *Journal of Neuroscience*, *34*(36), 11929–11947.

Zhao, J., Zhang, X., Zhou, Y., Ansell, P. J., & Klibanski, A. (2006). Cyclic AMP stimulates MEG3 gene expression in cells through a cAMP-response element (CRE) in the MEG3 proximal promoter region. *International Journal of Biochemistry and Cell Biology*, *38*(10), 1808–1820.

Zheng, G. X. Y., Do, B. T., Webster, D. E., Khavari, P. A., & Chang, H. Y. (2014). Dicer-microRNA-Myc circuit promotes transcription of hundreds of long noncoding RNAs. *Nature Structural and Molecular Biology*, *21*(7), 585–590.

Zhou, Y., Cheunsuchon, P., Nakayama, Y., Lawlor, M. W., Zhong, Y., Rice, K. A., Zhang, L., Zhang, X., Gordon, F. E., Lidov, H. G. W., Bronson, R. T., & Klibanski, A. (2010). Activation of paternally expressed genes and perinatal death caused by deletion of the Gtl2 gene. *Development*, *137*(16), 2643–2652.

Zhou, Y., Zhang, X., & Klibanski, A. (2012). MEG3 noncoding RNA: a tumor suppressor. *Journal of Molecular Endocrinology*, *48*(3), 1–16.

Zhou, Y., Zhong, Y., Wang, Y., Zhang, X., Batista, D. L., Gejman, R., Ansell, P. J., Zhao, J., Weng, C., & Klibanski, A. (2007). Activation of p53 by MEG3 non-coding RNA. *Journal of Biological Chemistry*, *282*(34), 24731–24742.

Zhu, J., Liu, S., Ye, F., Shen, Y., Tie, Y., Zhu, J., Wei, L., Jin, Y., Fu, H., Wu, Y., & Zheng, X. (2015). Long noncoding RNA MEG3 interacts with p53 protein and regulates partial p53 target genes in hepatoma cells. *PLoS ONE*, *10*(10), 1–15.

Zhu, W., Botticelli, E. M., Kery, R. E., Mao, Y., Wang, X., Yang, A., Wang, X., Zhou, J., Zhang, X., Soberman, R. J., Klibanski, A., & Zhou, Y. (2019). Meg3-DMR, not the Meg3 gene, regulates imprinting of the Dlk1-Dio3 locus. *Developmental Biology*, *455*(1), 10–18.

Zhu, X., Wu, Y. B., Zhou, J., & Kang, D. M. (2016). Upregulation of lncRNA MEG3 promotes hepatic insulin resistance via increasing FoxO1 expression. *Biochemical and Biophysical Research Communications*, *469*(2), 319–325.

Zoicas, I., Menon, R., & Neumann, I. D. (2016). Neuropeptide S reduces fear and avoidance of con-specifics induced by social fear conditioning and social defeat, respectively. *Neuropharmacology*, *108*, 284–291.

Zoicas, I., Slattery, D. A., & Neumann, I. D. (2014). Brain oxytocin in social fear conditioning and its extinction: involvement of the lateral septum. *Neuropsychopharmacology*, *39*(13), 3027–3035.

CURRICULUM VITAE AND

PUBLICATIONS

Curriculum vitae

Education and Degree	

03/2017 – ongoing	Ph.D. in Neurobiology/Biochemistry; University of Regensburg
	DFG GRK2174 "Neurobiology of Emotional Dysfunctions"
	Department of Biochemistry I, Prof. Dr. Gunter Meister/ Department of Behavioural and Molecular Neurobiology, Prof. Dr. Inga Neumann
	Thesis: Septal coding and non-coding RNAs regulated in social fear – The role of lncRNA Meg3 in social fear extinction
10/2019 – 12/2019	Research stay at the Weizmann Institute of Science, Israel
	Department of Biological Regulation, Functions and Modes of Actions of Long RNAs, Dr. Igor Ulitsky
10/2014 – 10/2016	Master of Science, Biology, University of Regensburg
	Master thesis: Institute of Human Genetics, University Hospital Regensburg, Prof. Dr. Bernhard Weber
10/2011 – 09/2014	Bachelor of Science, Biology, University of Regensburg
	Bachelor thesis: Department of Behavioural and Molecular Neurobiology, University of Regensburg, Prof. Dr. Inga Neumann
09/2002 – 04/2011	Johann-Michael-Fischer-Gymnasium, Burglengenfeld

Stipends	

- 2019 – Travel grant by the Financial Incentive System for Equality Promotion for a Research Stay at the Weizmann Institute of Science, Israel

- 2019 – Travel grant by the Financial Incentive System for Equality Promotion for the Keystone symposium "Long non-coding RNAs", Canada

- 2018 – Travel grant by "Freunde der Universität" Regensburg and invited Students Talk at the meeting "Gene epigenome and environment in pathophysiology in brain illness", Italy

References

- Prof. Dr. Gunter Meister, Department of Biochemistry I, University of Regensburg, +49 941 944 2847, Gunter.Meister@ur.de

- Prof. Dr. Inga Neumann, Department of Behavioural and Molecular Neurobiology, University of Regensburg, +49 941 944 3053, Inga.Neumann@ur.de

- Dr. Karolina Plößl, Institute of Human Genetics, University Hospital Regensburg, +49 941 944 5430, Karolina.Ploessl@klinik.uni-regensburg.de

Publications

- **Royer M.**, Bludau A.*, Meister G., Neumann I. D., Menon R. (*joint first authors). "Epigenetic Regulation of the Social Brain". *Trends in Neuroscience*, Review, 2019.

- Plössl K., **Royer M.**, Bernklau S., Tavraz NN., Friedrich T., Wild J., Weber BHF, and Friedrich U. "Retinoschisin Is Linked to Retinal Na/K-ATPase Signaling and Localization". *Molecular Biology of the Cell,* 2017.

- Winter J., Meyer M., Berger I., Peters S., **Royer M.**, Langgartner D., Reber S., Kuffner K., Schmidtner A., Hübner K., Bludau A., Bianchi M., Stang S., Bosch O. J. , Slattery D. A, Erwin van den Burg E., Neumann I. D., Jurek B. "Oxytocin-induced synthesis of soluble CRFR2α triggers anxiety". *In preparation.*

ACKNOWLEDGEMENTS

DANKSAGUNG

Acknowledgements

An erster Stelle möchte ich mich bei meinen beiden Betreuern, Prof. Dr. Gunter Meister und Prof. Dr. Inga Neumann, für die Möglichkeit bedanken meine Doktorarbeit in dieser Form an ihren Lehrstühlen durchzuführen.

Lieber Gunter, vielen Dank, dass du immer ein offenes Ohr hattest und dir Zeit genommen hast, wenn es nötig war. Danke für deine wissenschaftliche Unterstützung, deine konstruktive Kritik und deine ruhige aber bestimmte Art in jeglicher Situation. Vielen Dank auch, dass du meinen Forschungsaufenthalt am Weizmann Institut unterstützt und initiiert hast.

Liebe Inga, vielen, vielen Dank für deine Unterstützung über die gesamte PhD Zeit. Ich konnte immer zu dir kommen und offen mit dir reden. Danke für die konstruktiven Diskussionen und Ratschläge. Du hast mich sowohl auf wissenschaftlicher als auch auf persönlicher Ebene stets gefordert, gefördert und motiviert.

Des Weiteren möchte ich mich auch bei den weiteren Mitgliedern des Prüfungsausschusses bedanken: Dr. Markus Kretz, Prof. Dr. Rudolf Fuchshofer und Prof. Dr. Stephan Schneuwly. Danke auch an meinen dritten Mentor Prof. Dr. Eugen Kerkhoff für die Ratschläge und Diskussionen während meines Projektes, sowie Prof. Dr. Oliver Bosch für die Hilfe und Organisation v.a. rund um veterinär-bezogene Angelegenheiten.

I also would like to thank Dr. Balagopal Pai and Dr. Rohit Menon.
Balu, I do not how to thank you in adequate way. You were always supportive, taking time for me, performing thousands of analyses and comparisons again and again … . Thank you for all the hours of discussing sequencing data and your critical and refreshing view on the behavioural data. Thank you for all your help! I cannot imagine a better supervisor!

Rohit, many thanks to you for introducing me to the world of "social fear conditioning" and supporting me all over the PhD period. Thanks for the funny time and discussions during many hours of tissue punching! Thank you also Anna Bludau for practical support and sample sharing.

Many thanks also to Dr. Igor Ulitsky and his group, here especially Dr. Rotem Ben-Tov Perry. Thank you for the opportunity to come to your lab at the Weizmann Institute and the possibility to learn and perform new methods. It was a great experience and time over there.

Zu guter Letzt, ein großer Dank an meine Familie und Freunde, die immer für mich da waren und mich in bestimmten Momenten aufgefangen haben.

Liebe Mama, Sandra, Oma und Opa. Was habt ihr euch alles anhören müssen. Danke für eure bedingungslose Unterstützung schon mein ganzes Leben lang.

Lieber Philip, auch dir Danke für einfach ALLES. Danke, dass du die stressigen Jahre mit mir ausgehalten hast, mich immer unterstützt und mir aus so mancher Krise herausgeholfen hast.